Tools and Methodologies for The Rapid Determination and Transfer of Thermodynamic Parameters used in the Prediction of Gas Chromatographic and Two Dimensional Comprehensive Gas Chromatographic Retention Times

By Teague M. M^{c}Ginitie

A thesis submitted in partial fulfillment of the requirements for the degree of

Doctor of Philosophy

Department of Chemistry

University of Alberta

Abstract

Three parameter thermodynamic predictive models have been shown previously to provide superior accuracy in the prediction of gas chromatographic retention times in comparison to other forms of modelling such as retention indices. However, these models suffer from the need for extensive experimentation to generate the data required to make their predictions. This then limits the applicability of the method to real world situations. This thesis sets out to explore new methods and techniques that reduce the required experimentation necessary to make thermodynamic based retention time predictions in gas chromatography. Three main ideas are explored in the process of reducing experimentation: the automation of thermodynamic data collection, the adaptation of thermodynamic collection models from isothermal to temperature programmed based experimentation and a method to rapidly transfer thermodynamic data from one chromatographic system to the next. Along with the above stated goals, this research sets out to develop models for the prediction of retention times in two dimensional gas chromatography using three parameter thermodynamic data. Two dimensional separations are also used to validate the methods and concepts mentioned previously.

Preface

(Mandatory due to collaborative works)

Portions of Chapter 1 have been previously published in the Journal of Chromatography A under the title "Comprehensive multidimensional separations for the analysis of petroleum" K.D. Nizio, T.M. McGinitie, J.J. Harynuk. Volume 1255, (2012) SI pages,12-23. In this work I was responsible along with K.D. Nizio for the collection and interpretation of over 200 papers as well as manuscript composition and edits. K.D. Nizio provided the final organization of reference material. J.J. Harynuk was the supervisory author and was involved with concept formation and manuscript composition and editing.

Sections of Chapter 2 have been previously published under the title "Considerations for the automated collection of thermodynamic data in gas chromatography" in the Journal of Separation Science by T.M. McGinitie and J.J. Harynuk. Volume 35, (2012) pages 2228-2232. I was responsible for all experimentation and interpretation of generated data, as well as development of the new methods used; I was also responsible for the manuscript composition. J.J. Harynuk was the supervisory author and was involved with concept formation and manuscript composition and editing.

Chapter 3 and portions of Chapter 5 were previously published in the Journal of Chromatography A under the title "Rapid determination of thermodynamic parameters from one-dimensional programmed-temperature gas chromatography for use in retention time prediction in comprehensive multidimensional chromatography" by T.M. McGinitie, H. Ebrahimi-Najafabadi, J.J. Harynuk. Volume 1325, (2014) pages 204-212. I was responsible for the experimentation and data collection as well as the formation of the original concept as well as the code upon which the model was constructed. I also composed the manuscript. H. Ebrahimi-Najafabadi assisted in data collection as well as the optimization of previously established code and coding of the non-linear optimization algorithms. J.J. Harynuk was the supervisory author and was involved with concept formation and manuscript composition and editing.

Sections of Chapter 4 were previously published under the title "A standardized method for the calibration of thermodynamic data for the prediction of gas chromatographic retention times" in the Journal of Chromatography A by T.M. McGinitie, H. Ebrahimi-Najafabadi, J.J. Harynuk. Volume 1330, (2014) pages 69-73. I was responsible for the experimentation and data collection as well as the formation of the original concept as well as the code upon which the model was constructed. I also composed the manuscript. H. Ebrahimi-Najafabadi assisted in

data collection as well as the optimization of previously established code and coding of the non-linear optimization algorithms. J.J. Harynuk was the supervisory author and was involved with concept formation and manuscript composition and editing.

Portions of Chapter 5 were previously published as “Prediction of retention times in comprehensive two-dimensional gas chromatography using thermodynamic models” in the Journal of Chromatography A. T.M. McGinitie and J.J. Harynuk. Volume 1255, (2012) pages 184-189. I was responsible for all experimentation and interpretation of generated data, as well as development of the new methods used; I was also responsible for the manuscript composition. J.J. Harynuk was the supervisory author and was involved with concept formation and manuscript composition and editing.

Acknowledgments

The work presented within was only possible through the help and support of a host of people, and I thank everyone who helped me through the process of discovering and writing this research.

I would foremost like to thank my supervisor Dr. James Harynuk for his guidance on this project and for all the opportunities he has provided me with during the last five years to share this work with the chemistry community. I would like to thank all of the members of the Harynuk group for their support and help over the years. In particular I would like to thank Bryan Karolat for his close friendship and for the work he performed in the study of thermodynamic predictions which made this study possible. I would also like to thank Nikolai Sinkov for his help and support both in the lab and as a friend. As well I would like to thank Katie Nizio for her help and for all the hard work she put into the review, which I didn't think would ever get finished.

I want to thank Brenda Crickmore, Richard Paproski and Monica Morphy along with everyone else at Syncrude for their help and guidance throughout the course of this work. As well I would like to thank Syncrude Canada Ltd. for the support provided to me through the NSERC IPS scholarship.

I'd like to thank Dr. Alessandro Casilli, Jack Cochran, Dr. Jean-Marie Dimandja, Dr. Frank Dorman, and Dr. Philip Marriott and their students for their hard work in generating a significant amount of the data for the round robin project and for their help in showcasing thermodynamic methods. Thanks again to Jack for his support through the Restek Corporation.

I would also like to thank Al Chilton for his help on all things electronic over the years and would like to thank Jing Zheng for her assistance with work conducted in the mass spec laboratory.

To all my friends (you already know who you are), thank you all for the awesome times we shared over the last five years. Brent and Greg, I'm not sure if you helped or hindered the whole process but I'm grateful for all the lunch breaks either way.

To Mom and Eric thank you for all your love and support, without you I wouldn't be here today. To Dad, thank you for your support despite the troubles we had over the years. To the rest of my family thank you so much for your love and encouragement. I love you all.

To Liz, I love you more every day, thank you for being by my side throughout this whole process and for getting me through all the rough patches. I'm not a smart man, but I know what love is.

PS To the Midnight Hobo's, thanks for helping me become Dr. Starmonkey, from WotLK to Pandaria, from "here come the pretzels" to "Docking Dad" you guys were a great distraction from the realities of this thesis. Special shoutout to Robble, Povray, Teg, Buttnasty, Hellsjudge Punchizzle, and Dr. Fatty.

"The Sciences, each straining in its own direction, have hitherto harmed us little; but some day the piecing together of dissociated knowledge will open up such terrifying vistas of reality, and of our frightful position therein, that we shall either go mad from the revelation or flee from the deadly light into the peace and safety of a new dark age" – H.P Lovecraft

Table of Contents

List of Tables

List of Figures

List of Abbreviations

CI	-	Chemical Ionization
EI	-	Electron Impact
FAME	-	Fatty acid methyl ester
FID	-	Flame ionization detector
GC	-	Gas Chromatograph
GC×GC	-	Comprehensive multidimensional gas chromatography
GC-GC	-	Multidimensional gas chromatography
LRI	-	Linear retention index
LTPRI	-	Linear temperature programmed retention indices
m/z	-	Mass to charge
MS	-	Mass Spectrometry
NIST	-	National Institute of Standards and Technology
PAH	-	Polyaromatic hydrocarbon
QSRR	-	Quantitative structure retention relationship
RI	-	Retention index
RMSEP	-	Root mean square error of prediction
SEM	-	Scanning electron microscope
TPGC	-	Temperature programmed gas chromatography
WCOT	-	Wall coated open tubular

List of Symbols

μ_o	-	Carrier gas velocity at column outlet
c	-	Stationary phase concentration
c_m	-	Concentration mobile phase
c_s	-	Concentration stationary phase
d_c	-	Column inner diameter
d_f	-	Diameter film thickness
I	-	Retention index number
K	-	Partition coefficient
k	-	Retention factor
L	-	Length
n	-	Precceding alkane in RI measurement
N	-	Trailing alkane in RI measurement
P	-	Inlet to outlet pressure ratio
P_o	-	Column outlet pressure
R	-	Universal gas constant
r_c	-	Column radius
T	-	Temperature
T_0	-	Reference temperature
t_m	-	Void time
t_r	-	Retention time
t_r'	-	Adjusted retention time
$t_r'(j)$	-	Retention time unknown analyte
$t_r'(n)$	-	Retention time preceding alkane

$t_r'(N)$	-	Retention time trailing alkane
u_x	-	Carrier gas velocity at position x
β	-	Phase ratio
ΔC_p	-	Molar heat capacity
ΔG	-	Gibbs free energy of phase transition
ΔH	-	Enthalpy of stationary phase transition
$\Delta H(T_0)$	-	Enthalpy of stationary phase transition at reference temperature
ΔS	-	Entropy of stationary phase transition
$\Delta S(T_0)$	-	Entropy of stationary phase transition at reference temperature
η	-	Dynamic viscosity

Chapter 1: Introduction[1]

1.1 General Introduction

Nearly every physical object found in nature exists as a mixture of chemical components; rarely is anything composed of a single element or compound. As such, if we want to better understand the materials and environment around us we require a means of separating mixtures into their individual components. One form of separation science that is used to study mixtures is chromatography. The first demonstration of chromatography was the separation of plant pigments on an adsorption column performed by Mikhail Tsvet in 1901[1] and it was from this separation of colour compounds that the name 'chromatography' arose. Today, a variety of chromatographic techniques exist, including thin layer, gel, liquid, and gas chromatography. The particular form of chromatography used in a study depends on the chemical properties of the analyte, the matrix that the analyte is found in, as well as the analytical problem in question. In this thesis the field of gas chromatography is discussed exclusively.

Gas chromatography (GC) at its most basic is a technique that allows for the separation of molecules while they exist in a gaseous state. To accomplish this, the modern gas chromatograph flows an inert carrier gas (typically helium or hydrogen) through a capillary column made of fused silica, the walls of which are coated with a liquid-like polymeric stationary phase. The degree to which a particular molecule interacts with the stationary phase dictates the time it will take

[1] Sections of this chapter have been previously published as K.D. Nizio, T.M. McGinitie, J.J. Harynuk. *J. Chromatogr. A.* 1255, (2012) SI p12-23.

for that molecule to elute from the column, and thus a complex mixture composed of many analytes may be separated based upon their specific interaction with the stationary phase. The high efficiency of gas chromatographic separations and the relative low cost of the technique makes it a common choice for the analysis of volatile and semi-volatile analytes. Since its introduction by Martin and James in 1952,[2] gas chromatography has become a mainstay in fields such as petroleum, food and fragrances as well as pharmaceutical research. The original focus for many gas chromatographic techniques was the determination of bulk properties of mixtures, such as boiling point distributions or the compositional make up of a sample by group type. A classic example of a group-type analysis is the PIONA analysis used to profile the hydrocarbon content of petroleum samples according to the concentrations of paraffins, isoparaffins, olefins, naphthenes, and aromatics to provide an overview of its composition.[3,4]

Gas chromatography can also be useful in the investigation of individual analytes within a mixture. Where a complete separation is possible, individual components can easily be determined through the use of standards or through detection methods such as mass spectrometry (MS). However, given the sheer number of components within many of the mixtures examined by gas chromatography, a complete separation of all analytes is often impossible or prohibitively time consuming. In order to separate petroleum and other complex samples (e.g. biological or environmental) researchers have turned to the development of multidimensional separation techniques. In gas chromatography, there are two basic forms of two dimensional separations; the first is heart-cutting

where a fraction of the effluent from the primary column is directed to a secondary column where a second separation is carried out. This form of separation is commonly denoted within the literature by a hyphen (i.e. GC-GC). The second method is a comprehensive two dimensional separation, which has been established from the following criteria:[5,6]

1. At a minimum, a representative fraction of all sample components must be displaced by two or more separation techniques, where each technique provides different selectivity and demonstrates a distinct retention profile (i.e., there is some degree of orthogonality between dimensions).

2. Components separated by any single separation must not be recombined in any further separation dimension (i.e., the sampling/fractionation rate of material entering a separation dimension is sufficiently high to maintain the profiles of compounds eluting from the separation that immediately precedes it).

Comprehensive two dimensional gas chromatography methods are denoted within the literature as GC×GC.[7] The theory pertaining to comprehensive multidimensional separations was developed largely by Giddings and co-workers in the 1980s and 1990s,[5,8,9] with the first GC×GC separation being performed by Liu and Phillips in 1991.[10] GC×GC is a two dimensional separation technique where the separation of complex mixtures is achieved through the use of two orthogonal retention mechanisms. In GC×GC a primary separation is performed, followed by a secondary separation, the fashion in which GC×GC separations are

carried out ensures that the separation achieved in the primary dimension is retained through the secondary dimension. The use of two separation dimensions allows for the separation of complex mixtures that could not have been separated by traditional gas chromatographic means. The vastly increased resolution that is obtained by GC×GC thus enables the separation and identification of specific target analytes within even the most complex of sample matrices.

The increase in resolving power provided by GC×GC techniques comes at a price. The numerous separation conditions that can be altered makes finding an optimal set of conditions difficult, and this optimal set of conditions is often never realized. Even within a traditional one-dimensional separation there are a variety of conditions that can be altered to optimize the separation. For example, the stationary phase, column dimensions, carrier gas flow rate, inlet conditions, and temperature program can all be altered to change the final separation. In GC×GC, the conditions that can be altered are multiplied, as changes made in either dimension will affect the outcome of the separation in the other. Even for experienced practitioners of GC×GC, many methods are often developed through intuitive guesswork. Given the large number of variables that must be optimized the use of predictive modelling could prove to be an extremely beneficial tool in the development of both comprehensive gas chromatographic techniques as well as traditional one-dimensional separations. In an ideal case an analyst would simply pick the analytes of interest that are present in the sample and then software would find the optimal separation conditions for that set of molecules saving the need for extensive experimentation.

Predictive modelling can also be useful in the identification of unknown peaks within chromatographic separations, particularly when used in conjunction with mass spectrometry. The use of retention parameters could be utilized as another layer of information to help distinguish structural isomers that would otherwise be difficult or outright impossible to distinguish by mass spectrometry alone. Given the nature of many of the complex samples analyzed by GC×GC, the situations where retention information is required to supplement mass spectral information are common and additional tools to resolve these issues would be beneficial.

Although it may be self-evident, to perform successful predictions of separation conditions and to predict compound identities one must first be able to accurately model a separation. The work presented within this thesis focuses on the development of effective models for the prediction of GC separations. Considerations made during the generation of data used in these predictive models are also extensively investigated. Finally, the success of the both the separation models and data generation are evaluated as well.

1.1.1 Basics of Gas Chromatography

A gas chromatograph (GC) consists of three basic modules: an inlet, the chromatographic column, and a detector. The inlet serves to first volatilize the sample into the gas phase and introduce the sample onto the chromatographic column. Depending on the requirements of the analysis, a wide variety of specialized techniques can be employed to tailor the manner in which the sample is introduced onto the column. The most common injection technique is split

injection, whereby a liquid sample is volatilized and a small fraction of the total sample is passed onto the column. For the specifics of split injection and other injection techniques the reader is directed to Grob and Barry's *Modern Practice of Gas Chromatography*.[11]

At the other end of the column is the detector. A variety of detectors exists, and are chosen based on the needs of the chromatographer. For a more complete list of detectors and the method of their operation, the reader is again directed to Grob and Barry's *Modern Practice of Gas Chromatography*.[11] The flame ionization detector (FID) is ubiquitous to GC and is the detector of choice for the majority work herein. A FID operates through the combustion of hydrocarbons eluting from the column in a hydrogen/air flame. The ions produced by this combustion interact with a collector electrode and the subsequent electronic signal is interpreted as a chromatogram. The response of the detector is subject to the mass of analyte encountering the detector per unit time, and obviously is destructive in its measurement. The FID is widespread due to its robustness, near universal response factor, high sensitivity and broad dynamic range.

The other detector used in these studies was a quadrupole mass spectrometer. A mass spectrometer is a multivariate detector that separates molecules that have been ionized based upon their mass to charge ratios. In the case of GC-MS the column effluent is directed into the MS detector and ionized using chemical ionization (CI) or electron impact (EI). CI generally yields a simpler spectrum and a molecular ion peak, while EI highly fragments a molecule

creating a complex fragmentation pattern, which may be used for identification. The generated ions are separated on the basis of their mass to charge ratio (m/z) and then collected by the detector to obtain a mass spectrum of the material eluting from the column at a specific instant of time. For further reading on the subject of MS ionization and instrumentation, the reader is directed to Jürgen Gross' *Mass Spectrometry*.[12]

The central component of any gas chromatographic system is the column. The first columns used in gas chromatography consisted of stainless steel or glass tubing with a diameter that was sufficiently large to permit their packing with particles coated in stationary phase, similar to those used in liquid chromatographic columns. Typical packed columns have a length of around 2 m and an inner diameter of 1/8". Packed columns are now rarely used in the field of gas chromatography having been replaced by fused silica capillary columns. Capillary columns offer several advantages over packed columns including increased inertness, increased thermal stability, and higher chromatographic efficiencies.[13] Open tubular capillary columns consist of a fused silica capillary to which an immobilized liquid stationary phase is coated on the inside, and are more commonly referred to as wall-coated open tubular (WCOT) columns. A standard size for most columns is a capillary length of 30 m and an internal diameter of 0.25 mm. The stationary phase film thickness is typically 250 nm. A variety of lengths, inner diameters, film thicknesses and film chemistries are commercially available.

1.1.2 Multidimensional Gas Chromatography

In the last 20 years, significant technological advances in areas such as column and column-coupling technology, mobile phase flow control, and detector design have been combined with improvements in electronics and computers resulting in the proliferation of multidimensional separation techniques. One key development that allowed for the proliferation of GC×GC is the development of modulation techniques. The role of the modulator is to trap/collect effluent from the primary column and then periodically introduce the collected fraction to the secondary column as a narrow pulse. The modulator is ideally operated such that three or four fractions are taken per peak.[14,15] While the second-dimension column is operated such that its separation of one fraction is finished before the subsequent fraction is introduced. The first column is typically of similar dimensions to that used in a conventional one-dimensional separation (10–30 m × 0.18–0.25 mm i.d.) while the second-dimension column is typically shorter and narrower (0.5–2 m × 0.1–0.18 mm i.d.). Two main classes of modulator exist, thermal and pneumatic. Thermal modulators are more widely used than pneumatic modulators and are further subdivided into two basic categories: heated modulators which can trap analytes using above ambient temperatures and cryogen based modulators which use sub-ambient temperatures to trap analytes on the column. While a wide variety of both classes of thermal modulators exist[16] for simplicity a generic example of a dual-stage modulated system is described below. Effluent from the primary column is sent directly onto the secondary column; at the head of the secondary column is the first modulation stage. The

analyte is slowed and sorbed to the column stationary phase through the action of the thermal modulator. After a timed portion of effluent is collected, the thermal effect on the segment of column where the analyte(s) are trapped is reversed which remobilizes the trapped analytes into the carrier gas stream. The analytes travel a few cm down the column where they encounter the second stage of the thermal modulator. This second stage exists to prevent break-through of column effluent into the previously modulated portion. Thermal modulators are popular due to the ease of which they can be tuned to provide different modulation periods, and their ability to trap all but the most volatile analytes. Thermally modulated systems also confer the advantage of refocusing the collected analyte bands before transferring them onto the secondary dimension. Furthermore, the flow rates of carrier gas permit easy coupling with mass spectrometers. The downside associated with thermal modulators is the requirement for cryogens or cryogenic systems and extra heaters to modulate the temperatures at specific points on the capillaries. Important to this research is the fact that thermal modulators rely on chromatographic phenomena and thus one must account for additional zones of chromatographic behavior that must be modeled as well.

While thermal modulators are the most prevalent in the field of GC×GC, pneumatics can also be used to modulate the separation. Early studies into pneumatic modulators focused on valve-based systems for modulation. These systems showed that while it was possible, the rapid switching and high temperatures required to perform a separation limited the use of these modulators which were prone to mechanical failure, leakage, and suffered from issues with

inertness. The solution to this issue of requiring valves for flow modulation was introduced by Deans in 1965.[17] Deans' device was originally designed to allow for the back flushing of column effluent to avoid undesirable analytes from travelling down the length of the column, while allowing the analytes already on the column to continue travelling down a length of column to the detector. It consisted of three valves that could be opened or closed outside the GC oven to direct the flow either entirely down the two column segments or to direct flow down the second column segment while back flushing the contents of the first segment out of a vent. The idea was then expanded to enable heart-cutting GC-GC.[18]

The Deans' switch removes all valves from inside the GC oven and sample flow path, replacing them with a solenoid valve outside of the GC oven. Doing so removes the problems associated with previous mechanical switching devices and increases the usefulness of pneumatic switching devices. The basic premise behind flow-modulated systems is that pressure can be applied to different channels to change the route that a gas will follow through a network of flow paths. This general approach was of limited popularity in the field of GC×GC until the early 2000's, which was when improved column coupling technologies, gas flow technologies, and computerized automation evolved to the point that the routine construction and operation of these devices was feasible. The first use of a valveless flow-modulated system as a GC×GC modulator was performed by Beuno and Seeley in 2004,[19] The design used a solenoid valve to alternate flow down two sample loops to accomplish the modulation of the

primary column effluent. Seeley et al. later replaced this with a single channel device.[20] This basic design was then integrated into a microfabricated chip containing all the Deans switch components with ports for the primary and secondary columns.[21] The use of micro-channel devices helps to prevent diffusion within the modulator. However the fixed channel dimensions limits the total sampling time to that set by the primary column flow. Because of this there is a limited range of modulation periods that can be used. Other commercially available devices incorporate both micro channels and ports that allow for an adjustable sample loop that increases the modulation period range.[22]

A typical Deans' switch for use as a modulator in GC×GC is illustrated below. The Deans' switch lies between the outlet of column one and the inlet of column two. The modulation cycle for flow-modulated systems consists of two states, a sampling state and a flush state. To achieve the desired separation both the flows to and from the columns along with the solenoid channel flows must be carefully calculated and balanced. In the load state the flow is directed by the modulation valve into channel 1 (Figure 1.1). In this state the majority of the flow is directed down the second dimension column (there is minimal flow down the restrictor channel). The primary column effluent continues to flow into the collection channel, however before the primary column effluent fills the entire collection loop the modulation valve switches to channel 2 and the flow flushes the collected sample in the collection channel onto the secondary column leaving

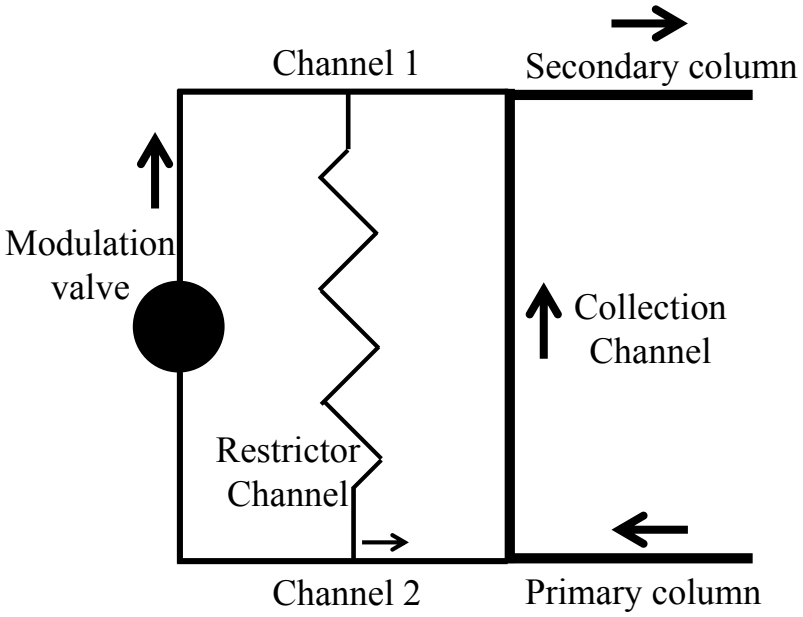

Figure 1.1 Diagram of a Deans' switch pneumatic modulator in the load state. Effluent from primary column fills collection channel. Flow from modulation valve is directed down channel 1 proceeds directly onto the secondary column. A small amount of flow travels from channel 1 down the restrictor channel to prevent primary column effluent from entering channel 2.

the collection channel 'empty'. (Figure 1.2). The time required to flush the sample loop is generally a fraction of the total modulation period (i.e., the time required to complete one modulation cycle). A restrictor channel runs parallel with the collection channel; this restrictor ensures a small amount of flow into both channel 1 and 2, regardless of the modulation valve position, which ensures column effluent is not flushed into either of these channels.

With differential flow pneumatic modulators, it is often advantageous to use a narrow-bore column in the first dimension (0.1 mm) and a wider diameter in the second dimension (0.25 mm).[23] This is because the primary dimension in flow-modulated systems is typically operated at a very low flow rate (<1 $mL \cdot min^{-1}$) and the second dimension is operated at a much higher flow rate (15–20

mL·min^{-1}). Such a setup allows for longer sampling times, prevents analyte breakthrough and ensures the separation remains comprehensive.

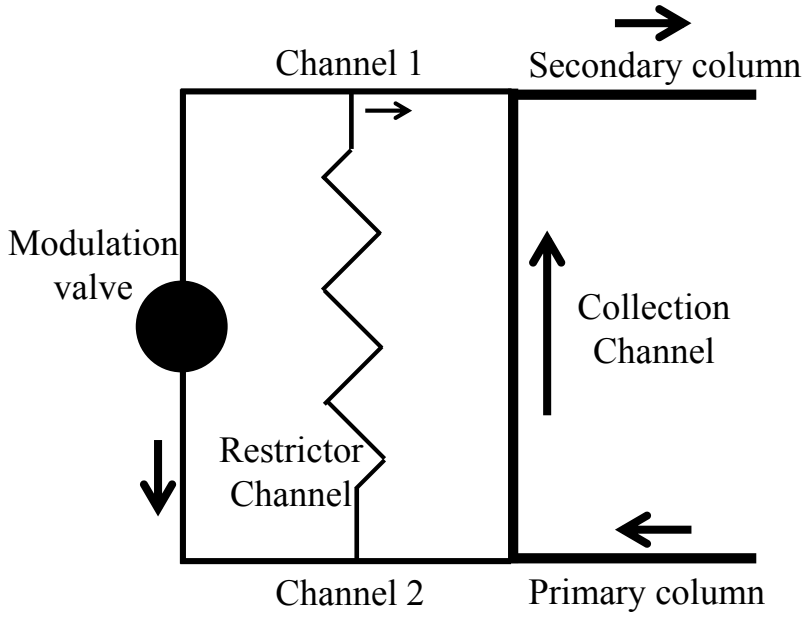

Figure 1.2 Diagram of pneumatic modulator in flush state. Effluent from the primary column is rapidly flushed from the collection channel using a short pulse of flow from Channel 2. Some flow is directed down the restrictor to prevent collection channel effluent from entering channel 1.

As mentioned previously, when making retention time predictions for GC×GC, the use of thermal modulation complicates these predictions by the need to model the chromatography occurring within the modulator. With pneumatic switching there is no chromatography occurring in the modulator, as there is no temperature change and the sample loop typically consists of deactivated silica, or in the case of a micro channel plate, a deactivated metal surface; thus there is no stationary phase. As such, the use of pneumatic modulators simplifies the calculations required to make accurate predictions. For this reason, pneumatic

modulation was used exclusively for the GC×GC experiments throughout this work.

1.2 Basics of Chromatographic Modelling

There are several key formulae that are critical to the explanation of chromatographic processes. These terms describe the basic interactions that occur during the chromatographic process and provide mathematical relationships for certain physical properties important to gas chromatography. As such, they are the foundation for many models of chromatographic behaviour including the ones discussed within this work.

1.2.1 Partition Coefficient

The partition coefficient is a fundamental descriptor of the retention process that occurs within a GC column. As an analyte travels down the column it moves towards a thermodynamic equilibrium between the mobile phase (the inert carrier gas) and the stationary phase. The temperature dependant equilibrium constant for this interaction is known as the partition coefficient K, which relates directly to the concentration of the analyte in the mobile and stationary phase through Equation 1.1. K is defined as the ratio of the concentration of the analyte in the stationary phase c_s to its concentration in the mobile phase c_m, and is the product of the retention factor k and phase ratio β.

$$K = \frac{c_s}{c_m} = k\beta \qquad (1.1)$$

This equilibrium is important as it dictates the time required for an analyte to elute from the column. As K increases, the longer it will take an analyte to elute. Experimentally it is difficult to directly measure the concentration of the analyte

in each phase as it moves down the column and so the partition coefficient can be related to two separate terms, retention factor and phase ratio.

1.2.2 Retention Factor

The retention factor (k) relates the time the analyte spends in the stationary phase compared to if it was entirely unretained. To obtain the retention factor of a specific analyte the void time of the column t_m (the time it takes an unretained compound to travel the length of the column) is subtracted from the retention time of the analyte t_r to give the adjusted retention time t_r'. This is then divided by the void time to give the retention factor k as shown in Equation 1.2

$$k = \frac{t_r'}{t_m} \tag{1.2}$$

1.2.3 Phase Ratio

Along with the retention factor k, the phase ratio β is required to determine the partition coefficient K for an analyte. The phase ratio describes the ratio between the volume of the mobile phase to the volume of the stationary phase. The most common formula used for approximating the phase ratio is that shown below in Equation 1.3:

$$\beta = \frac{r_c}{2d_f} \tag{1.3}$$

where r_c is the internal radius of the column and d_f is the stationary phase film thickness. These nominal values are generally obtained directly from the column manufacturer.

1.3 Predictive Modelling

Over the last 60 years many independent models have been developed to predict retention behaviour of analytes and to model separations without the need for physical experimentation. A well-constructed predictive model has the potential to save time in the laboratory by helping researchers identify optimal conditions that balance the length of the separation against the resolution needed. Predictive models can also be useful in conjunction with other sources of data such as mass spectrometry to assist in the determination of unknown analytes. Most models link some physical characteristic of an analyte to a specific retention parameter such as retention index (RI), relative retention, or retention time. The simplest forms of predictive modeling link a singular physical property to a retention parameter. As an example, the boiling points of analytes may be used to predict retention on non-polar stationary phases in GC. This works well due to the widespread availability of boiling point data within the literature and because the boiling point for most analyte classes corresponds directly to retention on non-polar stationary phases. A wide range of compound classes have been used in these predictions including halogenated hydrocarbons,[24] methylbenzenes,[25] alkylbenzenes,[26,27] halobenzenes and nitrophenols.[28]

1.3.1 Quantitative Structure-Retention Relationships

Arguably the form of predictive modeling invoked the most is that of the quantitative structure-retention relationship or QSRR. Quantitative structure-retention relationships describe a class of modeling techniques that take molecular descriptors and use them to predict retention parameters through the use of

multiple linear regressions, partial least squares, or artificial neural networks. The molecular descriptors used in these models can be any individual characteristic of a molecule, from simple descriptors such as the number of carbon atoms present, to more complex descriptors such as the total number of vibrational states within the molecule. These descriptors are often subdivided into a variety of classes such as physicochemical, topological, or quantum to name a few. Commercial software packages such as Dragon are available which are designed to calculate descriptors for a given molecule based off of a provided structure, making the generation of QSRR data easy and accessible. Often many researchers will develop new descriptors to suit the analyte class they are investigating. A common use of QSRRs is to predict the RI value of an analyte that does not have empirical data available and a quick search brings up over 300 results for QSRR models in gas chromatography. QSRR studies that estimate RI values published within the last few years have focused on polyaromatic hydrocarbons,[29] polybrominated diphenyl ethers,[30] amino acids,[31] target compounds in essential oils,[32] and various other volatile organic compounds.[33,34] QSRR models have also recently been used to predict retention times for samples such as petroleum alkanes,[35] opiates,[36] and fatty acid methyl esters (FAMEs).[37] A more extensive list of QSRR applications is covered by two recent reviews by Kaliszan[38] and Heberger.[39]

1.3.2 Retention Index

Retention indices, due to their simplicity and close use with QSRR models make them one of the most used retention parameters in the modelling of GC separations. One of the early challenges in the field of GC was that due to the

heterogeneity of individual columns methods that allowed for the transfer of relevant chromatographic data between laboratories was required. One of the most popular solutions to the problem of data transfer at the time was the Kováts retention index.[40] In this model the logarithm of the adjusted retention time t_r' for an isothermal separation of *n*-alkanes provides a linear scale to which all other compounds within the separation can be related (Equation 1.4).

$$I = \left[100 \cdot \mathrm{n} + (N - \mathrm{n}) \left(\frac{\log(t'_{r(j)}) - \log(t'_{r(n)})}{\log(t'_{r(N)}) - \log(t'_{r(n)})}\right)\right] \qquad (1.4)$$

The retention index number *I* is given by comparing t_r' of an analyte *j* against the alkanes that elutes before (*n)* and after (*N)* the analyte. This then provides the retention index (RI) for the analyte. While the Kováts retention index applies only to isothermal separations, the same method can be applied to temperature ramped separations using Equation 1.5.

$$I = \left[100 \cdot \mathrm{n} + (N - \mathrm{n}) \left(\frac{(t_{r(j)} - t_{r(n)})}{t_{r(N)} - t_{r(n)}}\right)\right] \qquad (1.5)$$

This form of the Kováts retention index is referred to as the linear temperature-programmed retention index (LTPRI) or LRI for short.[41] The simplicity of the method and near universal applicability has made the Kováts retention index and LTPRI the two most popular methods for modeling retention behavior. Retention indices are popular in retention modelling techniques due to the ease of which data can be collected and used.[42] LRI is more commonly used than the Kováts retention index as data for many compounds can be easily collected in a single temperature programmed run. As such the LRI is often

offered as supporting data when identifying unknown compounds, with the current version of the NIST mass spectral library offering values for 70,835 compounds.[43] The tentative identification of compounds within a separation remains one of the main uses for RI data.[44] By looking at RI data for analytes of interest one is able to estimate the elution order and if peaks are likely to elute at or around the same time. While this is more of an interpolation of data rather than a true prediction, it is useful in modelling nonetheless. However, in combination with QSRR techniques the vast amount of RI data available makes retention indices an attractive option when developing predictive models.

While RI data is fast and easy to use, RI values are also dependant on experimental conditions which leads to variation in the reported RI values for both intra and inter laboratory operations.[45] For the 70,835 compounds with listed RI values in the current NIST database there are 346,757 RI values listed for those compounds and all of these values in the current database exist only for non-polar or slightly polar columns.[46] If retention data are to be used to identify structurally similar compounds, any variation in RI values could lead to inconclusive results or prove useful only for a select set of experimental conditions. As well, while RI are straightforward for traditional GC separations obtaining RI data in GC×GC must be accomplished through the generation of isovolatility curves which remains technically difficult on most instruments and is time consuming.[47] Furthermore, it can be argued that the use of alkanes as retention index standards is not necessarily appropriate for the second dimension separation in GC×GC where highly polar stationary phases are used.[48] Despite these limitations for

GC×GC, the popularity of RI models remains high, with several new studies conducted within the last few years.[49,50] A recent review by von Mühlen and Marriott covers the topic extensively.[42]

1.3.3 Thermodynamics in GC

An alternative strategy that is gaining in popularity for modelling gas chromatographic behaviour is the direct use of an analyte's thermodynamic interaction between the mobile and stationary phase within the chromatographic column. Before discussing the specific usage of these models the basic theory behind thermodynamics in gas chromatography is examined. As mentioned previously, an analyte within a gas chromatographic column will establish a thermodynamic equilibrium between the mobile and stationary phases provided it is at or near infinite dilution. The partitioning process can be referred to in terms of thermodynamic parameters. The most widespread thermodynamic model used to describe the equilibrium in gas chromatography is the van't Hoff equation; Equation 1.6.

$$-RTln(K) = \Delta G = \Delta H - T\Delta S \qquad (1.6)$$

In this equation the change in enthalpy (ΔH) and change in entropy (ΔS) at a specific temperature (T) are related to the Gibbs free energy change (ΔG). This can be related to the partition coefficient through the universal gas constant (R) in the manner shown above. Typically the calculation of these parameters involves the measurement of K across a range of temperatures, and the construction of a van't Hoff plot. The assumption here is that both the change in enthalpy (ΔH) and

change in entropy (ΔS) are independent of temperature. In GC, this assumption holds true only for a very narrow temperature range. While this assumption makes the estimation of ΔH and ΔS simple to perform experimentally, the thermodynamic parameters calculated are not valid across the entire range of temperatures typically experienced in gas chromatography and so limits the accuracy of the thermodynamic data collected from such experiments.[51,52] This limited accuracy in turn affects the quality of models based upon such data. Convenience in this case outweighs the loss in accuracy, and to date most gas chromatographic thermodynamic studies have been performed using the van't Hoff equation. Specific examples are discussed later in this chapter.

A more suitable approach to the estimation of thermodynamic parameters via gas chromatography is the use of a three-parameter linearized equation. In this equation the natural logarithm of the partition coefficient at a specific temperature is regressed against the inverse of temperature and natural logarithm of that temperature according to Equation 1.7;

$$\ln(K) = A + \frac{1}{T} \cdot B + \ln(T) \cdot C \qquad (1.7)$$

The three terms A, B, and C in Equation 1.7 can then be related to the entropy $\Delta S(T_0)$, enthalpy $\Delta H(T_0)$ and isobaric molar heat capacity ΔC_p of the analyte during its transition between mobile and stationary phases through the use of Equations 1.8 – 1.10.

$$A = \frac{\Delta S(T_0) - \Delta C_p \cdot lnT_0 - \Delta C_p}{R} \qquad (1.8)$$

$$B = -\frac{\Delta H(T_0) - \Delta C_p \cdot T_0}{R} \quad (1.9)$$

$$C = \frac{\Delta C_p}{R} \quad (1.10)$$

In the three-parameter model both the entropic and enthalpic terms are temperature dependant. However within these equations they are related to a specific reference temperature (T_0). This reference temperature is arbitrary, and within this work all values of $\Delta S(T_0)$, and $\Delta H(T_0)$ are in reference to 90 °C. The three-parameter model does assume that ΔC_p remains constant, while in reality ΔC_p is a temperature-dependant term though its relatively small contribution in the determination of the partition coefficient makes this discrepancy of minimal importance. The three-parameter model above is based on Clarke and Glew's treatment of thermodynamic equations for the calculation of equilibrium constants.[53] These equations were adapted for use in gas chromatography by Castells[54] for use in the investigation of the thermodynamics of benzene on squalene, triethylene glycol, and tetraethylene glycol stationary phases.

A variety of other two-, three-, and four-parameter equations for the calculation of thermodynamic parameters from GC retention exist and include both linear and non-linear models. The accuracy and precision of these models has been exhaustively compared previously.[52] The three-parameter linearized equation listed above was chosen for use in predictive modelling due to its superior accuracy and precision. Other models also exist. However, these have seen little practical usage and are generally limited to use in a specific compound class.[55-58]

Thermodynamic parameters in GC provide an advantage over retention indices in that they are independent of separation conditions. With retention indices, changing separation conditions such as the temperature ramp rate also affects the reported RI value. As well, RI values can shift if conditions such as isothermal holds are placed throughout the separation. Thermodynamic parameters, on the other hand are dependent only upon the chemistry of the stationary phase and the carrier gas. Therefore regardless of separation conditions such as the temperature profile, ramp rate, physical column dimensions, or carrier gas flows as long as the stationary phase and carrier gas remain unchanged the thermodynamic estimations performed will remain the same, making them ideal for the prediction of separation conditions. As mentioned previously, RIs are difficult to obtain in the second-dimension of a GC×GC separation. However thermodynamic data can easily be applied. The advantage provided by being independent of separation conditions and the increase in GC×GC separations have led to an increase in the usage of thermodynamic estimations within gas chromatography over the last decade.

1.3.4 Examples of Thermodynamic Modelling

While implemented less often than RI data, thermodynamic data has also been used in the modelling and prediction of GC separations. The majority of these thermodynamic predictive models are based upon the van't Hoff equation, using isothermal separations to estimate ΔH and ΔS. Dose modelled nitroaromatic temperature programmed separations using a two-parameter thermodynamic model.[59] Dolan et al. examined phenols using a similar method.[60] Vessani et al.

investigated a variety of compounds using a two-parameter model including alkanes, linear alcohols,[61] and substituted aromatic compounds.[62,63] Aldaeus et al. investigated both polyaromatic hydrocarbons (PAHs)[64] and the Grob standard mix[65,66] using a two-parameter model. Aldaeus then expanded this work to use a three-parameter model for a variety of test molecules.[67] Recent work also includes two separate investigations of volatile organic compounds.[68,69] Within the Harynuk group both an additive thermodynamic model[70] as well as the prediction of alkyl phosphate[71] retention times have been investigated.

1.4 Scope of Thesis

This thesis discusses in detail the development of methods that allow for the collection of thermodynamic data for use in predictive modeling, and the validation of that data in predictive models for both GC×GC and GC. This thesis is divided into four chapters. The first covers the development of automated techniques for thermodynamic data collection. The second outlines the development and validation of a new method for the rapid determination of thermodynamic parameters for use in predictive modelling in GC. The third section outlines procedures for the calibration of column parameters for the transfer of thermodynamic data from instrument-to-instrument and lab-to-lab is validated and discussed. In the final section of this thesis, practical applications of thermodynamic predictions are demonstrated and the success of predictions based upon thermodynamics is descussed for GC×GC.

Chapter 2: Automation in Thermodynamic Data Collection[2]

2.1 Introduction

One of the major obstacles preventing the proliferation of thermodynamic predictive models is the lack of thermodynamic data available to researchers. A main reason for this lack of data is the significant time required for the collection of accurate thermodynamic data; this currently involves manually injected isothermal separations. As an example, to obtain accurate thermodynamic data for a single analyte, isothermal separations should be performed across a range of temperatures to allow for the appropriate collection of partition coefficients. To ensure accuracy, typical methods[70,54,64] include a minimum of six isothermal separations to ensure a suitable range of partition coefficients. Furthermore to ensure the precision of these measurements each isothermal separation should be repeated in triplicate which increases the minimum number of runs to eighteen. For a variety of reasons that shall be explained later in this chapter, previous thermodynamic studies required manual injections to ensure a high level of accuracy and precision in the collected thermodynamic data. Manual injections require an inordinate amount of operator time, thus making the collection of thermodynamic data a slow and labour intensive process. This discourages users from adopting thermodynamic predictive models in favour of systems such as retention index. To increase the practicality of thermodynamic modeling, I set out to develop a system where data can be collected by automated methods without

[2] Sections of this chapter have been previously published as T.M. McGinitie, J.J. Harynuk. *J. Sep. Sci*. 35 (2012) 2228-2232.

operator input while maintaining the accuracy and precision offered by the manual injection approach.

As described in the Chapter 1, due to the direct relationship of both the phase ratio and retention factor in the estimation of $\Delta S(T_0)$, $\Delta H(T_0)$ and ΔC_p both k and β must be precisely and accurately determined to obtain accurate predictions. Alterations in the method used to obtain thermodynamic data such as the addition of an autosampler or the use of multiple instruments must be carefully examined to determine the effect that these changes have upon the determination of k and β. This chapter shall focus on several methods that enable the automatic collection of thermodynamic data, mainly the implementation of autosamplers and the use of void time surrogate markers such that the determination of k remains unchanged from that of manual injection techniques. Also included in this chapter is an investigation into the effect the range of k has upon on the determination of thermodynamic parameters of small molecules.

A fundamental requirement for the accurate estimation of thermodynamic parameters in GC is an accurate and consistent calculation of the retention factor, k. Determination of k in turn requires an accurate and precise measurement of the void time of the column, t_m (Equation 2.1).

$$k = \frac{t_r - t_m}{t_m} \qquad (2.1)$$

Both t_r and t_m must be precisely known to obtain an accurate value for k. While t_r is simply a time measurement several methods exist for the determination of t_m. Theoretically, t_m can be calculated directly from the Hagen-Poiseulle (Equation 2.2). Here η is the viscosity of the carrier gas at a given temperature, d_c is the

column inner diameter, p_o is the outlet pressure of the column, and P is the ratio between the inlet and outlet pressures (p_i / p_o).

$$t_m = \frac{128\eta}{3p_o} \cdot \left(\frac{L}{d_c}\right) \cdot \left(\frac{P^3-1}{(P^2-1)^2}\right) \qquad (2.2)$$

In theory the Hagen-Poiseulle equation should provide an accurate estimate for the void time of the column. However as stated previously the slight variations of column inner diameter along the length of the column make obtaining t_m through this method difficult. Techniques such as scanning electron microscopy[72] can provide a closer estimate for d_c. However such methods are expensive, time consuming, and unless the column is sacrificed to allow for multiple measurements along the column length, cannot provide an accurate estimate due to the random variability of d_c along the column. Literature has also shown that the use of the Hagen-Poiseulle equation will consistently over-estimate the void time of the column.[73]

Regression-based methods are also available for the calculation of the void time on a specific column.[74,75] By regressing the natural logarithm of K for a series of *n*-alkanes, a theoretical value of K for a molecule of carbon length 0 can be estimated and from this the void time calculated. The basis for this calculation is that for a homologous series of alkanes there will be a near-linear relationship to K between alkanes. This relationship tends to deviate from linearity with alkanes that elute early in the chromatographic run due to a lack of retention.[76] Consequently, if these alkanes are used in the regression a bias may occur which can result in an erroneous void time estimate. Similar errors can be induced when using column geometries that have thin stationary phase films or if the column is

short, as is the second dimension column of a two-dimensional separation. Practically speaking, it is not always desirable to have a series of alkanes present in the sample as they may overlap with analytes of interest, and extra sample preparation is often required to introduce these compounds. For these reasons this method was avoided.

A final method for determining the void time of the column is to perform a co-injection of an unretained compound with the sample being studied. When using mass spectrometry for detection, this unretained compound is typically air. However for FID detection methane is used as an unretained marker[70]. This method has the advantage of requiring no calculations and no sample preparation is required. A slight bias in retention can be present as even methane is slightly retained on some phases, especially if the stationary phase film is thick.[73] However, given the ease with which this method can be implemented and the fact that previous studies[70,64,65] have shown success using this method, its use was continued for this study. Unfortunately, it is not always possible to use a co-injection of methane to determine the void time of the column; either due to coelutions of methane with the solvent or from limitations that are imposed by equipment such as auto-samplers. Special methods were developed within this work to overcome such limitations.

The largest problem facing the automation of isothermal thermodynamic data collection is that the current practice of co-injection of methane to determine t_m is impractical with conventional automatic liquid sample injectors. With the large number of experiments necessary to collect precise thermodynamic data and

the relatively short analysis times for each run, a disproportionate amount of operator time must be devoted to sample injection and data collection. Options for automation include the use of more advanced sample handling equipment, which is prohibitively expensive for many laboratories, or solvating methane in the injection solvent and using a conventional injection system.

Initial experimentation using solvated methane and an autosampler resulted in thermodynamic parameters that were incompatible with those collected using manual injection techniques. Two sets of experiments were carried out for this research. The first set was to determine the reason for (and a means to correct) the discrepancy observed in the thermodynamics collected using automated and manual injections. Subsequently, a series of experiments were performed to establish a replacement for methane as a void time marker and thus increase the ease with which autosamplers could be used in the collection of thermodynamic data.

In conjunction with the experiments into autosampler use and the resulting effect on the determined *k*, additional investigations into the effect of *k* on the calculated thermodynamic parameters were carried out. Specifically, previous investigations[70] found that the collected thermodynamic parameters for early eluting compounds were less precise than the same parameters for larger molecular weight compounds. It was hypothesized that this increased variance was due to the collection of thermodynamic parameters under temperatures that did not provide a significant change in *k*. The previously mentioned studies on the effects of autosamplers on *k* provided an opportunity to revisit this hypothesis and

investigate whether using temperature conditions that provided a larger range in the determined values for k would result in an increase in the precision of the thermodynamic values estimated for these early eluting compounds. In this case a cryogen-cooled gas chromatograph was used to enable a range of temperatures that provided a more suitable range of retention factors and a comparison of the two sets of thermodynamic data were made.

2.2 Experimental

2.2.1 Autosampler experiments

Experiments were carried out on an Agilent 6890 GC (firmware version A.08.03; Agilent Technologies, Mississauga, ON) networked to the controlling PC via an ethernet cable. Agilent Chemstation version A.03.08 running on a PC (Windows XP Service Pack 2 OS; Microsoft, Redmond, WA) was used to control the instrument, autosampler, and data acquisition. The GC was equipped with a split/splitless injector and FID. The injector was operated in split mode with a split ratio of 50:1 and a temperature of 250 °C. The flame ionization detector was set at a temperature of 250 °C. The GC was equipped with a 7683 Series autosampler (firmware version G2613A.10.05; Agilent). All runs were conducted isothermally using constant pressure mode where the pressure was set to obtain a measured average linear velocity of 30 $cm \cdot s^{-1}$ at the oven temperature. The column was a 30 m × 0.25 mm i.d. × 0.25 μm SLB5ms column (95% methyl – 5% phenyl siloxane equivalent; Supelco, Oakville, ON). All injections used an injection volume of 1 μL of standard.

A solution of undecane, dodecane, tridecane, and tetradecane (Sigma–Aldrich, Oakville, ON) prepared in CS_2 (Fisher Scientific, Ottawa, ON) at a concentration of 1000 $\mu g \cdot mL^{-1}$ was used as a test mixture. To ensure an accurate comparison of void times using manual and automated injection, a GC vial containing CS_2 was placed in a beaker of dry ice. Methane was solvated in the CS_2 by bubbling it through the sample solution, via a stainless steel cannula. The solvated methane in the CS_2 provided a void time marker compatible with the autosampler and similar to the manual co-injection of methane gas with a liquid sample as used in prior research.[52]

2.2.2 Cryogenic-oven GC work

This work was conducted on an Agilent 6890 with an FID detector set at 280 ^{0}C. The injector was a split/splitless injector operated in split mode with a split ratio of 50:1 and a temperature of 250 ^{0}C. The 6890 was equipped with a standard Agilent CO_2 cryocooled GC oven. All runs were conducted isothermally and in triplicate. The column used was a Supelco 30m × 0.25 mm i.d. × 0.25 μm SLB5ms column (95% methyl – 5% phenyl siloxane equivalent). All injections were performed by manual injection of 1 μL of standard. Chemical standards used in this experiment consisted of 2,4-dimethylpentane, 2,2-dimethylpentane, n-heptane, and 2-methylhexane. The standards were prepared in toluene at a concentration of 1000 ppm.

2.3 Results and Discussion

2.3.1 Autosampler Correction

A shift in the dead time was observed when comparing manual and automated injections of the same sample under otherwise identical conditions. It was observed that the GC run time began slightly before the actual injection of the sample. The result being that for identical operating conditions the apparent void time of the column changed, causing a small, but significant error in the thermodynamic parameters estimated via the two different injection approaches. The end result was an error in the predicted retention times if manually-collected data were used to predict an automated injection or vice-versa shown in the last two columns of Table 2.1. To explore this phenomenon, five replicate manual injections of the test mixture were performed at 30 °C intervals ranging from 40-200 °C. The experiment was then repeated with automated injection. In both cases, methane was solvated in the sample solution. It was found that there was a constant delay of 2.4 ± 0.15 s regardless of temperature. Careful observation of the sequence of events on the instrument suggests that the delay arises as follows: Initially, the autosampler syringe sits prepared with its tip submerged in the GC vial of the autosampler, waiting for the instrument to signal that it is ready. The instrument then starts its analysis and signals the autosampler to inject. This is when data starts recording. The syringe must then withdraw from the vial, the turret must rotate, and then the syringe can inject into the injection port. Due to a lack of resources it was not investigated whether this delay is the same for all

Table 2.1. A comparison of the estimated thermodynamic data based upon the method used to inject the sample. The last two columns show the RMSEP against the actual retention times for manual and autosampler injected samples, respectively.

Compound	Thermodynamics Collected From:	ΔC_p ($J \cdot mol^{-1} \cdot K^{-1}$)	ΔH T(o) ($KJ \cdot mol^{-1}$)	ΔS T(o) ($J \cdot mol^{-1} \cdot K^{-1}$)	RMSEP vs Actual Manual tr (s)	RMSEP vs Actual Autosampler tr (s)
Undecane	Manual	92.59	-47.09	-73.11	0.1	3.1
	error (absolute)	0.46	0.06	0.42		
	Autosampler	81.96	-46.87	-72.68	3.0	0.1
	error (absolute)	0.18	0.02	0.16		
	Autosampler corrected	82.15	-46.82	-72.37	0.4	N/A
	error (absolute)	0.18	0.02	0.16		
Dodecane	Manual	94.05	-51.30	-78.98	0.2	5.7
	error (absolute)	0.31	0.04	0.28		
	Autosampler	86.04	-51.12	-78.66	5.5	0.1
	error (absolute)	0.12	0.02	0.11		
	Autosampler corrected	86.23	-51.08	-78.35	0.3	N/A
	error (absolute)	0.12	0.02	0.11		
Tridecane	Manual	96.87	-55.52	-84.89	0.3	10.6
	error (absolute)	0.23	0.03	0.20		
	Autosampler	90.96	-55.37	-84.65	10.4	0.2
	error (absolute)	0.11	0.01	0.10		
	Autosampler corrected	91.14	-55.33	-84.34	0.3	N/A
	error (absolute)	0.11	0.01	0.10		
Tetradecane	Manual	104.05	-59.87	-91.15	0.2	5.6
	error (absolute)	0.19	0.02	0.17		
	Autosampler	86.51	-59.11	-89.33	5.5	0.2
	error (absolute)	0.55	0.07	0.49		
	Autosampler corrected	86.66	-59.06	-89.02	0.3	N/A
	error (absolute)	0.55	0.07	0.49		

6890/7890 Agilent systems and whether other vendors' equipment exhibit similar delays or not. Thermodynamic parameters were then estimated for the test set of alkanes using both the manual and autosampler data without any correction for the initial delay. The parameters from the two approaches were similar in value (Table 2.1); however, the differences were statistically significant at a 95%

confidence level. Moreover, while the predictions of retention times for manual injections using manually collected data and the predictions of retention times for automated injections using autosampler-collected data (without corrections) were both very precise (average root mean square error of prediction (RMSEP) of 0.21 s and 0.12 s, respectively), when the predictions of retention time made based on the thermodynamic parameters collected using the autosampler without any corrections were compared to the manual-injection retention times, the average RMSEP was substantially higher (6.25 s). Application of the correction for the initial delay of the autosampler resulted in predictions which were in much closer agreement with the manually collected data (average RMSEP of 0.31 s) (Table 2.1).

2.3.2 Surrogate dead time markers

The second goal of this research was to investigate the possibility of using a surrogate dead time marker for the estimation of thermodynamic properties as the use of methane is impractical with conventional liquid injection systems for GC. The approach taken here was to calibrate the relationship between k_{CS2} and temperature over the temperature range of interest. This would then allow the back-calculation of the theoretical retention time of methane from the retention time of the CS_2 peak. Though presented here are calculations using CS_2, this approach should, in principle, work for any other poorly retained, highly volatile solvent (e.g. pentane, CH_2Cl_2, etc…).

In this set of experiments, the test mixture was injected both manually and

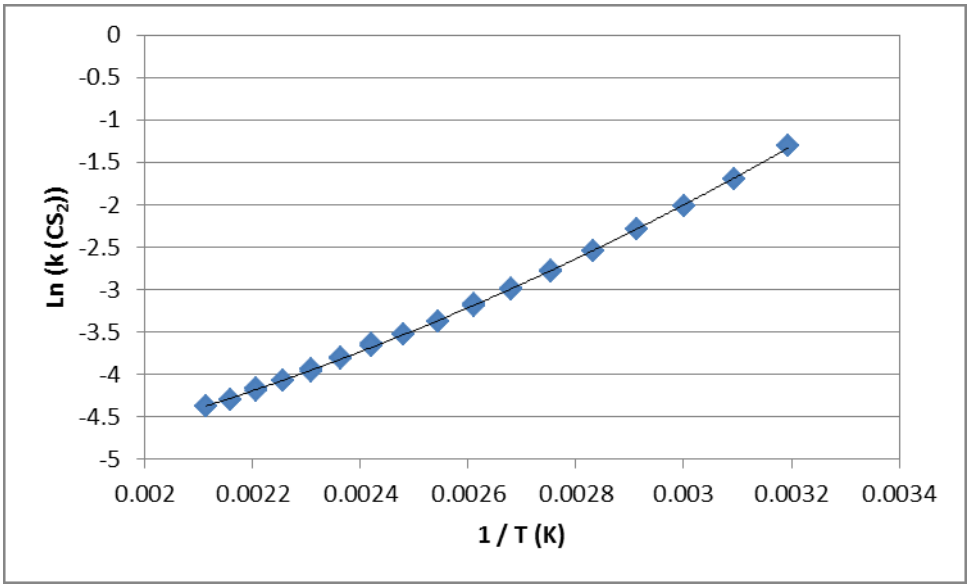

Figure 2.1. ln(k) for CS_2 vs. 1/T (K^{-1}). Three replicate measurments for each point are shown. The injection source was an autosampler.

using the autosampler over the temperature range that was being used to estimate the thermodynamic properties of the alkanes under study (100-160 °C in 10 °C intervals). Methane was co-injected or solvated in the CS_2 for every run to verify the void time. A plot of ln(k_{CS_2}) vs. 1/T (K^{-1}) was generated. As expected[52,77] the relationship follows a second-order polynomial (Figure 2.1). From this relationship, t_m can be calculated from k_{CS_2} and the measured retention time for CS_2 at any temperature within the operating range (50 – 200 °C) based on Equations 2.3 and 2.4.

$$\ln(k) = 7.276 \cdot 10^6 \cdot (1/T)^2 - 1.045 \cdot 10^3 \cdot (1/T) - 5.417 \qquad (2.3)$$

$$t_m = \frac{t_{rCS_2}}{(k+1)} \qquad (2.4)$$

It was found that using this fit provided a RMSEP of 0.1 s across the temperature range of 50 – 200 °C. Injections of CS_2 containing dissolved methane were used to verify the accuracy of t_m predicted on the basis of the CS_2 retention (Table 2.2). A second calibration curve was created for manual injections to ensure any error that was present in the predictive model was a result of using CS_2 as a dead time surrogate and not from deviations caused by the autosampler. Finally, thermodynamic parameters were determined for a series of alkanes on the basis of both manual and automated liquid injections (with the autosampler timing delay correction) and using CS_2 to estimate t_m. The values for k_{alkane} as a function of temperature were then used to estimate the thermodynamic parameters. The values of these parameters were then compared (Table 2.2). By using CS_2 as a surrogate there is a slight drop in the precision of the predictions; comparing the results of manually collected thermodynamics that either use methane or the CS_2 surrogate we see an increase in the RMSEP from 0.2s to 0.5 s. Most likely this increase in error is due to the inaccuracy of manual injections in both the measurement and from using manual injections in the calibration curve. From Table 2.2 it is apparent that application of both the injection delay correction and the estimation of t_m from the retention of CS_2 generated estimates of thermodynamic parameters and predictions of retention times that correlated well with manually collected data with a RMSEP of 0.7 s compared to the uncorrected autosampler values of 6.9 s.

Table 2.2. Estimated thermodynamic parameters using CS_2 dead time surrogate for various injection methods and corresponding RMSEP to the actual manually injected and autosampler (delay corrected) retention times.

Compound	Thermodynamic Collection Source	ΔCp $J \cdot mol^{-1} \cdot K^{-1}$	$\Delta H\ (T(o))$ $kJ \cdot mol^{-1}$	$\Delta S\ (To)$ $J \cdot mol^{-1} \cdot K^{-1}$	RMSEP vs Actual Manual *tr* (s)	RMSEP vs Actual Auto corr *tr* (s)
Undecane	Manual	92.59	-47.09	-73.11	0.1	0.4
	error (absolute)	0.46	0.06	0.42		
	Autosampler CS_2 t_m	88.44	-47.13	-73.39	3.2	2.9
	error (absolute)	0.44	0.06	0.40		
	Autosampler corrected +CS_2 t_m	90.26	-47.18	-73.36	0.4	0.2
	error (absolute)	0.44	0.06	0.40		
Dodecane	Manual	94.05	-51.30	-78.98	0.2	0.5
	error (absolute)	0.31	0.04	0.28		
	Autosampler CS_2 t_m	91.04	-51.31	-79.19	5.9	5.5
	error (absolute)	0.31	0.04	0.28		
	Autosampler corrected +CS_2 t_m	91.06	-51.31	-79.02	0.5	0.2
	error (absolute)	0.31	0.04	0.28		
Tridecane	Manual	96.87	-55.52	-84.89	0.3	0.9
	error (absolute)	0.23	0.03	0.20		
	Autosampler CS_2 t_m	95.13	-55.53	-85.08	10.9	10.2
	error (absolute)	0.25	0.03	0.22		
	Autosampler corrected +CS_2 t_m	95.15	-55.53	-84.91	0.8	0.4
	error (absolute)	0.25	0.03	0.23		
Tetradecane	Manual	104.05	-59.87	-91.15	0.3	0.9
	error (absolute)	0.19	0.02	0.17		
	Autosampler CS_2 t_m	107.86	-60.10	-91.93	7.4	6.6
	error (absolute)	0.79	0.08	0.72		
	Autosampler corrected +CS_2 t_m	108.03	-60.11	-91.78	0.9	0.3
	error (absolute)	0.79	0.08	0.72		

Even slight variations in injection conditions and the measurement of retention and void time can have a significant impact on the validity of thermodynamic models of GC retention, leading to significant errors in predictions based on these models. This is a significant challenge in the development of thermodynamic models which can be transferred between laboratories, or even between instruments within a laboratory. Demonstrated here

is a manner by which thermodynamic parameters may be automatically collected and used to make predictions which agree with manual injections. This bodes well for cross-platform compatibility of the predictions observed in our work.

It is important to note that I have not ascertained if the injection delay observed in the autosampler used in this work is constant for a given make/model of instrumentation or if it varies from one instrument to another (of the same make/model). However, it certainly will vary from manufacturer-to-manufacturer. Consequently, it is prudent to investigate and if necessary calibrate each instrument-autosampler combination prior to use when collecting thermodynamic data via isothermal methods. Subsequent chapters will discuss methods that replace the need for many of the considerations for autosampler corrections. Furthermore, it is worth noting that the estimation of accurate thermodynamic parameters depends on an accurate measurement of the phase ratio, β. In this work we have used only the nominal value for β. Errors introduced by assuming the nominal value is accurate are not a concern in this work as all experiments were performed with a single column, canceling out these errors. However, accounting for these differences in β is important and will be discussed in Chapter 4.

2.3.3 Cryo-cooled GC Studies

Previous work by B. Karolat[52] had shown that small molecules suffered from lower accuracy in their predictions for retention time when compared to larger molecules. It was hypothesised that due to the low retention of small

molecules on phenyl substituted polydimethylsiloxane columns, an inadequate range of retention factors was obtained to estimate the thermodynamic parameters of these molecules. It was assumed that lightly retained molecules would be more susceptible to minor variations present within the GC system and thus have lower precision. It was also hypothesised that the range of temperatures used in the previous study was close to the operational limit of that particular GC system and that errors in temperature control may have contributed to the lower precision. A cryogen-equipped gas chromatograph designed to operate at lower temperatures was used in this study to expand the temperature range over which retention data could be collected. The thermodynamic estimations from this low temperature experiment were then compared to the thermodynamic data that were collected previously. Four compounds were chosen from the selection of molecules used in the previous studies,[70] 2,4-dimethylpentane, 2,2-dimethylpentane, n-heptane, and 2-methylhexane. These four were chosen due to their low molecular weights and their limited retention on a 5% phenyl substituted PDMS column.

The previous estimation of the thermodynamics for these small molecules was accomplished by looking at a temperature range of 40 – 100 °C. Across this range the average change in the retention factor Δk was only 0.74. For the thermodynamics collected on the cryogen system an average Δk of 4.27 was found for the four probe molecules. The new range of collected retention factors is typical of what would be observed in larger molecules used in previous studies. When comparing the standard deviation found in the high temperature thermodynamic parameters with the standard deviation of the low temperature

thermodynamic parameters all three parameters $\Delta S(T_0)$, $\Delta H(T_0)$, and ΔC_p have a variance that was statistically identical at a 95% confidence level (Table 2.3).

Table 2.3 Collected thermodynamic data and the associated absolute error in their measurements under two temperature ranges.

Compound	Collection Range	$\Delta S\ (T_0)$ $J \cdot mol^{-1} \cdot K^{-1}$	$\Delta H\ (T_0)$ $KJ \cdot mol^{-1}$	ΔCp $J \cdot mol^{-1} \cdot K^{-1}$
2,4-Dimethylpentane	40 - 100 C	-44.94	-26.92	58.09
	error (absolute)	0.16	0.03	0.18
	0 - 60 C	-44.79	-26.82	53.34
	error (absolute)	0.17	0.04	0.19
2,2-Diethylpentane	40 - 100 C	-44.28	-27.43	56.82
	error (absolute)	0.13	0.03	0.14
	0 - 60 C	-44.05	-27.30	51.38
	error (absolute)	0.27	0.07	0.31
n-Heptane	40 - 100 C	-50.01	-30.27	58.37
	error (absolute)	0.23	0.05	0.26
	0 - 60 C	-48.91	-29.84	59.28
	error (absolute)	0.21	0.05	0.24
2-Methylhexane	40 - 100 C	-48.42	-29.01	45.72
	error (absolute)	0.45	0.13	0.52
	10 - 60 C	-45.58	-27.95	65.15
	error (absolute)	0.16	0.03	0.18

This result supports the conclusion that regardless of the range of retention values used to estimate thermodynamic parameters the precision of the estimation remains the same. As a result it is unlikely that the lower accuracy that was observed in predictions using these molecules was a result of the conditions used for the estimation of the thermodynamics. Given this fact it is most likely that these molecules are inherently more susceptible to subtle variations within the separation and thus harder to predict accurately. The focus of this thesis was directed at larger molecular weight molecules and so no further investigation into

the cause of the lower accuracy of small molecules was carried out.

2.4 Conclusions

The use of an autosampler when collecting isothermal retention data used in the estimation of thermodynamic parameters requires special attention to detail to obtain the same thermodynamics as manual injections. However, so long as the differences between the two techniques are accounted for the two methods are able to provide compatible thermodynamic values. Furthermore, the use of void time surrogates is a useful way of removing the need for methane which is often incompatible with autosamplers. The problems that arise when switching between manual and autosampler injection highlight the caution that must be taken when collecting thermodynamic values to ensure consistency within the generated parameters.

The techniques presented within this chapter enabled the collection of some of the thermodynamic information that is presented and used within Chapter 5. Specifically all thermodynamic information that pertains to polyaromatic hydrocarbons was collected using the automated techniques highlighted here. The implementation of these techniques was instrumental in the creation of a small library of thermodynamic information for 23 PAHs on five stationary phases (Appendix A). Even with automation, the creation of this library required several months of instrument time. Without the implementation of these techniques the same library would have taken more than half a year to complete under the careful watch of an operator. Despite the huge reduction in operator input, automation alone is not enough to make predictive models based upon thermodynamic data

an attractive alternative to RI methods. The following chapter shall discuss further improvement to the collection of thermodynamics that are able to rival that of RI methods.

Chapter 3: Rapid Determination of Thermodynamic Parameters[3]

3.1 Introduction

Despite the refinements mentioned in the previous chapter, the collection of thermodynamic data via isothermal separations remains a time consuming endeavor. Using our previous approach, a minimum of 18 isothermal separations is required to obtain accurate thermodynamic parameters for a single compound. While it is possible to run a solution that contains a mixture of several analytes of interest, the nature of isothermal chromatography limits the utility of this approach. While the speed of data collection for the determination of thermodynamic predictions can be increased by reducing the number of data points, doing so would have the undesirable effect of reducing the accuracy and precision of the obtained thermodynamic values. The ideal solution would be something akin to that used for RI determinations, a single temperature-programmed run that would allow for the simultaneous estimation of thermodynamic parameters for as many compounds as can be separated. To accomplish this, a method relating the thermodynamic parameters $\Delta S(T_0)$, $\Delta H(T_0)$, and ΔC_p to the retention times of analytes in temperature-programmed separations is required.

A wide variety of models exist to describe the chromatographic behavior of analytes in temperature-programmed GC. While many variations exist, the vast

[3] Sections of this chapter have been previously published as T.M. McGinitie, H. Ebrahimi-Najafabadi, J.J. Harynuk. *J. Chromatogr. A*. 1325 (2014) p. 204-212.

majority of these models function in the same basic manner; instrument parameters affecting the separation are calculated as a function of time and are broken into finite segments that assume these instrument parameters are constant for the duration of the interval. The calculated parameters are then used in conjunction with boiling point, LRI, or thermodynamic parameters to calculate retention time. One of the first instances of using thermodynamic data to model temperature-programmed separations was performed by Dose in 1987, who introduced the use of (ΔH) and (ΔS) in conjunction with the finite element method to predict analyte retention times.[59] Snijders et al.[78] refined this finite element method and much of the recent work done towards the modelling of programmed temperature separations is based upon their work. Snijder et al. broke the finite element model of the separation down into discrete time segments (typically 0.01s). However there exist other finite element models that use discrete distances rather than time to perform their calculations. One such model is McGuigan and Sacks'[77] band trajectory model which uses the time it takes an analyte band to travel finite distances, to predict retention times from van't Hoff plots. Previous work within our group had focused on adapting this band trajectory model from a two-parameter thermodynamic model to a three-parameter thermodynamic model based upon $\Delta S(T_0)$, $\Delta H(T_0)$, and ΔC_p.[52] While this work was for the most part successful, the use of distance rather than time as the discrete interval introduced errors as highly retained compounds could take significant time to travel the interval distances. Under temperature-programmed conditions the assumption that

instrumental conditions remain constant over the interval is violated. As such the use of the McGuigan Sacks model was avoided in this work.

Another finite element method that has been used for thermodynamic predictions was developed by Aldaeus, Thewalim, and Colmsjö.[64,65,67] From their model they investigate both the use of two-parameter and three-parameter thermodynamic data sets for the prediction of retention time in TPGC. Later work by Colmsjö[79,66] focuses again on the use of the two-parameter model, and attempts to reduce the number of data points needed to estimate thermodynamic data used in predictions. The model used within this thesis was adapted directly from the McGuigan, Sacks equations. However, it is similar to that developed by Colmsjö in its use of thermodynamics and time as a discrete interval. Apart from the models mentioned here a large number of variations to the finite element model exist. However as the list of these models is extensive, the reader is directed to Castello, Moretti, and Vezzani's[80] recent review of programmed-temperature GC models for further information.

All thermodynamic based models published so far (with the exception of a study by Dorman)[81] rely on isothermal data collection to obtain estimates for the thermodynamic parameters used within the various predictive models. Ignoring the loss of accuracy that occurs from using a minimal set of data points, the use of isothermal methods is still flawed in comparison to LRI methods as isothermal separations limit the number of analytes that can be separated in the same time frame. As well, the use of isothermal separations to gather thermodynamic data

can be tedious as a wide range of temperatures must be experimented with to find appropriate retention factors for each analyte.

The use of temperature-programmed separations has several advantages. First a wide range of analytes can be investigated simultaneously. At the same time, the nature of TPGC ensures that if starting from a sufficiently low temperature all analytes will have a high initial retention factor and as the temperature increases each analyte will experience essentially the same migration down the column. This ensures an internal consistency in the manner in which thermodynamic data are collected which is difficult to obtain from isothermal separations.

The above models have demonstrated that it is possible to generate models that accurately depict a temperature-programmed separation, and by extension are able to accurately predict analyte retention times. It therefore stands to reason that such a model could be made to work in reverse and generate accurate thermodynamic values from precise retention data. Presented in this chapter is the adaptation of a finite element model for the modelling of TPGC separations for use with three-parameter thermodynamic methods. The adaptation of the model to provide a novel method for the determination of thermodynamic parameters from temperature-programmed retention data is also discussed.

3.1.1 Basic Components of a GC separation Model

There are several basic components to a GC separation that must be accounted for if the separation is to be modelled accurately. The first and simplest is the temperature of the column during the separation. Given the small thermal mass of a fused silica column the assumption is made that the column temperature matches exactly with the programmed oven temperature. Modern gas chromatographs are able to tightly control the oven temperature, both during isothermal operation and during temperature programming. While there have been some suggestions that slight deviations of oven temperature control exist[82,83] within this work any such deviations were minor and ignored. As such the temperature of the column was simply calculated as a function of time to match the oven program.

The second major component of the separation that must be modelled is the velocity of the carrier gas as it travels down the length of the column. This is important as due to the compressibility of the gas, the velocity of the gas increases as it travels down the length of the column. Therefore to obtain an accurate retention time for an analyte, the velocity at every point in the column must be known. In the case of GC several assumptions are made; the column is represented as a tube with a uniform cross section along its length; the carrier gas is an ideal compressible fluid; the flow through the column is laminar; and finally the inlet mass flow equals the outlet mass flow, i.e. no gas is lost through the capillary walls. With these assumptions, Poiseuille's equation for compressible

fluid flow (Equation 3.1) can be used to solve for the outlet velocity of the column u_o (cm·s^{-1}).

$$u_o = \frac{{d_c}^2}{32}\frac{P^2-1}{2\eta L}P_o \tag{3.1}$$

Here a capillary column having a length L (cm), and a diameter d_c (cm) can be combined with the viscosity of the carrier gas η (poise (g·cm^{-1}·s^{-1})) at the oven temperature, along with P which is a dimensionless inlet-to-outlet pressure ratio, and P_o (dynes·g·(cm^2)$^{-1}$) which is the pressure at the outlet of the column. To account for the increase of viscosity with the temperature program, Equation 3.2 was used when using helium as a carrier gas and Equation 3.3 for hydrogen. Here T is the temperature in Kelvin.

$$\eta = -2.151^{-10} \cdot T^2 + 5.954^{-7} \cdot T + 3.923^{-5} \tag{3.2}$$

$$\eta = -1.089^{-10} \cdot T^2 + 2.780^{-7} \cdot T + 1.950^{-5} \tag{3.3}$$

From the calculated outlet velocity the linear velocity at every segment of the column u_x (cm·s^{-1}) can be calculated through Equation 3.4 where x is the position in cm from the front of the column.[77]

$$u_x = \frac{u_o}{\sqrt{P^2-\left(\frac{x}{L}\right)(P^2-1)}} \tag{3.4}$$

Once the carrier gas velocities are known along the length of the column the distance Δx (cm) that an analyte will travel in a finite interval of time Δt (s) is given by Equation 3.5, where the retention factor, k, is calculated based on the thermodynamically predicted partition coefficient for the analyte at the current

temperature and for the given phase ratio for the column (β) through the use of Equation 3.6.

$$\Delta x = u_x \frac{1}{(1+k)} \Delta t \tag{3.5}$$

$$k = \frac{K}{\beta} \tag{3.6}$$

After the distance the analyte has travelled is calculated, the carrier gas velocity is recalculated using the new temperature and viscosity for that particular time step and at the new distance along the column. The total distance traveled by the compound over the calculated iterations is evaluated and compared to the length of the column. When the inequality in Equation 3.7 is satisfied, then the retention time is calculated by summing the number of time steps needed to reach the total length of the column as per Equation 3.8 where x_i is the distance travelled in the i^{th} time interval and n is equal to the number of iterations required for the molecule to exit the column.

$$L \leq \sum_{i=1}^{n} \Delta x_i \tag{3.7}$$

$$t_r = n \, \Delta \, t \tag{3.8}$$

The accurate modelling of separation conditions as described above is key to the development of a method that can estimate thermodynamic parameters from temperature-programmed separations rather than a series of isothermal separations. In this chapter, basic validation of the predictive model will be discussed along with the development of a nonlinear optimization technique for the estimation of thermodynamic parameters. The obtained thermodynamic

parameters from this method are compared with the previous isothermal method and the advantages of the new method are discussed.

3.2 Experimental

3.2.1 Chemicals

A single standard mixture comprised of alkanes, alcohols and ketones was used in all experiments. *n*-Alkanes ranging from undecane to tetradecane were obtained from Sigma-Aldrich (Oakville, ON). 2-Undecanone, 2-dodecanone, and 2-tridecanone were purchased from Alfa-Aesar (Ward Hill, MA). Primary alcohol standards ranging from 1-undecanol to 1-tetradecanol were also purchased from Sigma-Aldrich. The standard mixture was prepared at a concentration of 1000 ppm in toluene (Sigma-Aldrich). Methane from the laboratory natural gas supply was used as a dead time marker when needed.

3.2.2 Instrumental

A 7890A gas chromatograph (Agilent Technologies, Mississauga, ON) equipped with a split/splitless injector, and flame ionization detector was used for all experiments. Injections were performed in split mode with a split ratio of 100:1 and an inlet temperature of 280 °C. The flame ionization detector was maintained at a temperature of 250 °C with a data sampling rate of 200 Hz. 99.999 % Hydrogen (Praxair, Edmonton, AB) was used as carrier gas. One-dimensional separations were carried out on a Supelco SLB5ms (30 m × 0.25 mm i.d. × 0.25 μm); 5% phenyl substituted polydimethylsiloxane, Supelco SPB50 column (30 m × 0.25 mm i.d. × 0.25 μm); 50% phenyl substituted

polydimethylsiloxane) (30 m × 0.25 mm i.d. × 0.25 μm), and Supelcowax (30 m × 0.25 mm i.d. × 0.25 μm), polyethylene glycol).

All separations were performed under constant flow conditions at 1.1 $mL \cdot min^{-1}$. The separations were initialized at 30 °C, with the oven temperature programmed at ramp rates of 3, 5, 8, 10, 12, 16, and 20 $°C \cdot min^{-1}$ to 230 °C, with a hold time of one minute at the beginning and end of the run. Thermodynamic estimations and retention time predictions were calculated using custom scripts written in MATLAB.

3.3 Rapid Determination Method

As mentioned, if an accurate model of a temperature-programmed separation and estimates for the analytes' thermodynamic parameters of $\Delta S(T_0)$, $\Delta H(T_0)$, and ΔC_P are able to accurately predict retention time, then the reverse should also be possible, i.e. accurate thermodynamic values should be obtainable from retention data. In this study, a nonlinear optimization procedure is used to estimate the thermodynamic parameters that would be required for an analyte to exhibit the retention times observed in a series of temperature-programmed separations. Here the previously used time summation model is combined with the Nelder-Mead simplex algorithm.[84] However, any other optimization technique such as genetic algorithms, particle swarm optimization, or Quasi-Newton techniques could be used to minimize the error values of the predicted retention times. The Nelder-Mead simplex was chosen because it is simple, fast, and has high reproducibility. The simplex starts with four vertices as there are three thermodynamic parameters and then it sequentially moves through the

experimental domain by a reflection, an expansion, or a contraction to eventually solve the optimal values of $\Delta S(T_0)$, $\Delta H(T_0)$, and ΔC_P.[85]

The entire thermodynamic estimation process proceeds as follows; a series of temperature-programmed separations are carried out. The absolute retention times for the analytes of interest are recorded for each temperature program and input into the script. Instrumental parameters including the column dimensions, inlet and outlet pressures at each hold temperature, the initial and final oven temperatures, isothermal hold times, oven temperature ramp rates, and carrier gas type are also input into the script. The time step used in the script's calculations is also set at this time, along with the reference temperature of the output thermodynamic parameters. To obtain the thermodynamic estimates for $\Delta S(T_0)$, $\Delta H(T_0)$, and ΔC_P, data from a minimum of three temperature ramps is required. However the use of more ramps helps ensure the accuracy and robustness of the approach and any number of ramps could be used. For every analyte, the script generates an initial guess j for $\Delta S(T_0)$, $\Delta H(T_0)$, and ΔC_P. The script determines the number of temperature programs used, N and initializes using the first ramp i. The i^{th} ramp is excluded and the initial guess j for the thermodynamic parameters is combined with the retention data from the remaining ramps. The Nelder-Mead simplex alters the values of $\Delta S(T_0)$, $\Delta H(T_0)$, and ΔC_P to obtain a minimum error between the experimental retention times and predicted retention times for the remaining temperature ramps (the set with the i^{th} ramp removed). The algorithm terminates after falling below a predetermined threshold for the sum of square error (SSE) for each ramp. To increase the likelihood of finding the optimal

solution, the procedure is then repeated M times with new set of random guesses of j for each iteration. The estimate that provides the minimal SSE from M number of optimizations is retained from that ramp and the script proceeds to the $(i + 1)^{th}$ ramp. Once the script has reached N number of ramps the retained values for the thermodynamic parameters obtained for each i are averaged and these values are stored within a library to be used in subsequent predictions. The entire procedure is outlined in Figure 3.1 below.

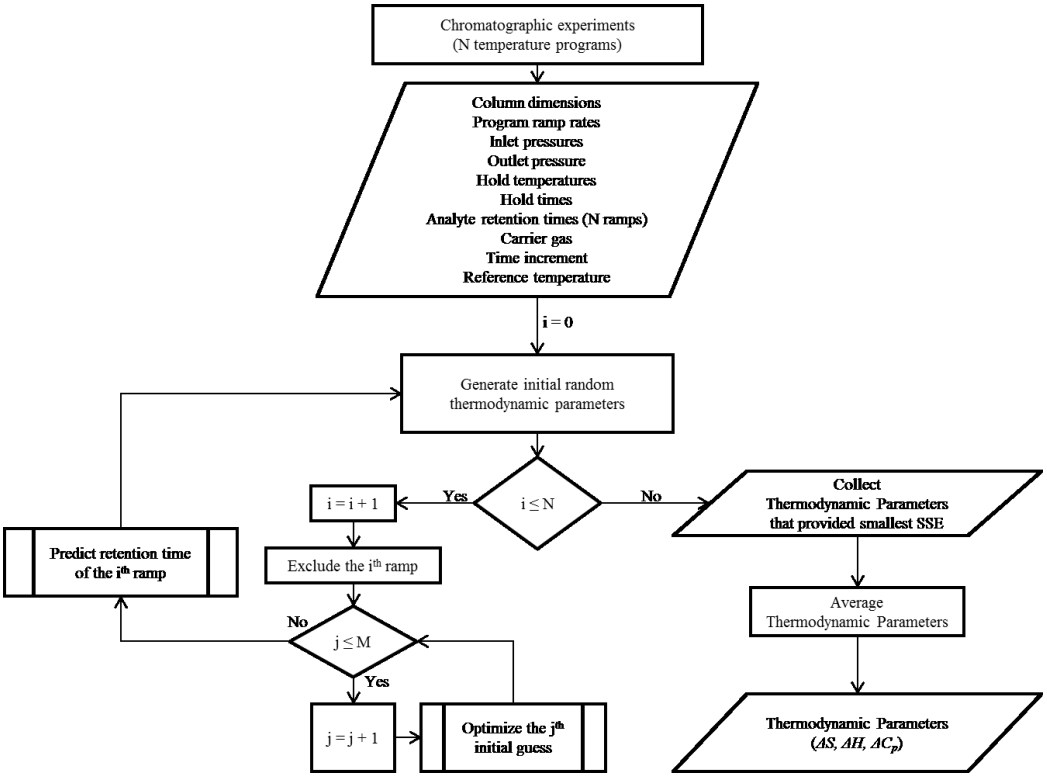

Figure 3.1 Flowchart outlining the estimation of thermodynamic parameters $\Delta S(T_0)$, $\Delta H(T_0)$, and ΔC_P from temperature programmed retention data.

3.3.1 Method Validation

Validation of the method was carried out via several independent checks. The thermodynamic optimization method was first validated through the use of the leave-one-out (LOO) methodology. The input data set consisted of the collected retention times for the test mixture using 3, 5, 12, and 20 °C·min^{-1} temperature-programmed runs (N = 4). For each analyte, the iterative process described above was used to obtain estimates for $\Delta S(T_0)$, $\Delta H(T_0)$, and ΔC_P. This process was repeated ten times (M = 10) for each temperature ramp and the average of the four optimization solutions were used as the final thermodynamic values for $\Delta S(T_0)$, $\Delta H(T_0)$, and ΔC_P. Table 3.1 provides an example of the estimated thermodynamic parameters using the training sets for dodecane, dodecanone and dodecanol along with the comparison of the experimental and predicted retention times for the ramp that was left out for all three stationary phases investigated.

Similar data for the remaining analytes is provided in Appendix A. The average absolute error in the predicted retention times for all analytes using the LOO validation on the 5 % phenyl, 50 % phenyl and wax column were 0.17 s, 0.81 s, and 0.30 s respectively; with the largest error across all analytes and columns being 3.60 s. For all three columns there was no significant difference in the errors of prediction between fast or slow ramp rates. Nor was there any relationship between the time an analyte spends in the column and the accuracy of the prediction.

Table 3.1 Thermodynamic estimates for $\Delta S(T_0)$, $\Delta H(T_0)$, and ΔC_P, as estimated from the LOO methodology. Each listed ramp rate is the i^{th} ramp rate which was left out of the calculation.

Compound		LOO Ramp	Estimated $\Delta H(T_o)$ (kJ·Mol-1)	Estimated $\Delta S(T_o)$ (J·K-1·Mol-1)	Estimated ΔCp (J·K-1·Mol-1)	Experimental Retention Time (min)	Predicted Retention Time (min)	Error (s)
Dodecane	5 % Phenyl Column (SLB5ms)	3	-51.59	-80.15	87.45	25.039	25.043	-0.3
		5	-51.56	-80.07	86.80	17.748	17.745	0.2
		12	-51.56	-80.05	87.86	10.014	10.015	-0.1
		20	-51.56	-80.05	87.86	7.337	7.338	-0.1
		Average Value	-51.57	-80.08	87.49			0.1
	50 % Phenyl Column (SPB50)	3	-44.31	-63.81	199.88	21.780	21.792	-0.7
		5	-44.28	-63.73	195.71	15.873	15.867	0.4
		12	-44.26	-63.65	197.56	9.362	9.363	-0.1
		20	-44.27	-63.69	195.43	7.033	7.033	0.0
		Average Value	-44.28	-63.72	197.14			
	Wax Column (Supelco Wax)	3	-42.34	-69.22	32.02	13.231	13.230	0.1
		5	-42.36	-69.25	31.23	10.405	10.407	-0.1
		12	-42.36	-69.26	31.96	6.812	6.808	0.2
		20	-41.90	-67.96	49.16	5.371	5.377	-0.3
		Average Value	-42.24	-68.93	36.09			0.2
1-Dodecanol	5 % Phenyl Column (SLB5ms)	3	-63.88	-98.21	126.12	36.743	36.752	-0.5
		5	-62.14	-93.63	89.83	24.865	24.877	-0.7
		12	-63.90	-98.26	128.02	13.043	13.042	0.1
		20	-63.89	-98.26	129.38	9.172	9.175	-0.2
		Average Value	-63.45	-97.09	118.34			0.4
	50 % Phenyl Column (SPB50)	3	-61.90	-92.13	180.80	37.777	37.757	1.2
		5	-59.41	-85.55	129.07	25.642	25.678	-2.2
		12	-62.23	-92.95	183.88	13.537	13.538	-0.1
		20	-62.27	-93.07	183.24	9.565	9.553	0.7
		Average Value	-61.45	-90.93	169.25			
	Wax Column (Supelco Wax)	3	-65.12	-94.19	70.15	42.413	42.403	0.6
		5	-65.30	-94.64	71.98	28.357	28.360	-0.2
		12	-65.38	-94.84	72.74	14.548	14.547	0.1
		20	-65.86	-96.10	81.38	10.082	10.083	-0.1
		Average Value	-65.41	-94.94	74.06			0.1
2-Dodecone	5 % Phenyl Column (SLB5ms)	3	-59.34	-90.05	84.94	33.761	33.750	0.7
		5	-59.33	-90.00	83.13	23.053	23.062	-0.5
		12	-59.37	-90.13	83.63	12.268	12.268	0.0
		20	-59.38	-90.15	82.80	8.700	8.695	0.3
		Average Value	-59.36	-90.08	83.62			
	50 % Phenyl Column (SPB50)	3	-58.50	-86.52	170.57	35.056	35.030	1.6
		5	-58.49	-86.43	166.89	23.982	23.997	-0.9
		12	-58.61	-86.76	171.27	12.827	12.835	-0.5
		20	-58.65	-86.88	168.07	9.133	9.118	0.9
		Average Value	-58.56	-86.65	169.20			
	Wax Column (Supelco Wax)	3	-54.63	-78.03	47.07	33.366	33.362	0.3
		5	-54.93	-78.83	55.07	22.936	22.935	0.1
		12	-54.95	-78.89	54.96	12.304	12.302	0.1
		20	-55.00	-79.02	57.89	8.745	8.748	-0.2
		Average Value	-54.88	-78.69	53.75			

A second validation was performed by using the thermodynamic parameters estimated using the LOO approach. In this validation the previously collected thermodynamic parameters were used to predict the retention times of analytes using three additional temperature ramps (8, 10, and 16 °C·min^{-1}). This validation was performed to ensure the success of the predictions outside of the training set as the leave one out method incorporates data from the validation set when determining the average thermodynamic parameters. Again for all columns studied there was an excellent agreement between the predicted and experimental values for the three ramps, with the average error for all analytes being 0.07 s, 0.31 s, and 0.35 s for the 5 % phenyl, 50 % phenyl and wax columns, respectively. Using the parameters that were estimated in this work, the average error in retention time for all predictions of all analytes across all temperature ramps used was 0.07 s (5 % phenyl), 0.30 s (50 % phenyl), and 0.20 s (wax). Table 3.2 shows a representative sample of the results using dodecane, dodecanone and dodecanol for all retention time predictions made for these one dimensional separations. All other compounds may be found in appendix A.

The thermodynamic data collected using this new method was compared to data collected previously using the older isothermal approach as another validation of the results. This comparison is shown for the 5 % phenyl and wax columns in Table 3.3. The 5 % phenyl column shows excellent agreement between the two methods with the average relative error for $\Delta H(T_0)$, and $\Delta S(T_0)$ being 0.67 % and 1.22 % respectively. For the wax column there is a slightly higher deviation between the two methods with an average error of 2.82 % and

Table 3.2 Comparison of the experimentally determined and predicted retention times using the average of the determined thermodynamics $\Delta H(T_0)$, $\Delta S(T_0)$, and ΔC_P from each LOO analysis.

Compund	Column	Temperature Ramp °C·min^{-1}	Experimental tr (min)	Predicted tr (min)	Difference (s)
dodecane	5 % Phenyl Column (SLB5ms)	3	25.039	25.040	-0.1
		5	17.748	17.747	0.1
		12	10.014	10.013	0.0
		20	7.337	7.337	0.0
		8	12.997	12.995	0.1
		10	11.246	11.245	0.1
		16	8.381	8.382	0.0
	50 % Phenyl Column (SPB50)	3	21.780	21.783	-0.2
		5	15.873	15.868	0.3
		12	9.362	9.363	-0.1
		20	7.033	7.033	0.0
		8	11.907	11.905	0.1
		10	10.419	10.420	-0.1
		16	7.947	7.948	-0.1
	Wax Column (Supelco Wax)	3	13.231	13.232	0.0
		5	10.405	10.405	0.0
		12	6.812	6.810	0.1
		20	5.371	5.372	0.0
		8	8.280	8.283	-0.2
		10	7.402	7.433	-1.9
		16	5.948	5.947	0.1
dodecanol	5 % Phenyl Column (SLB5ms)	3	36.743	36.747	-0.2
		5	24.865	24.867	-0.1
		12	13.043	13.043	0.0
		20	9.172	9.172	0.0
		8	17.498	17.498	0.0
		10	14.866	14.867	0.0
		16	10.666	10.667	-0.1
	50 % Phenyl Column (SPB50)	3	37.777	37.770	0.4
		5	25.642	25.653	-0.7
		12	13.537	13.542	-0.3
		20	9.565	9.555	0.6
		8	18.101	18.113	-0.7
		10	15.405	15.415	-0.6
		16	11.099	11.097	0.1
	Wax Column (Supelco Wax)	3	42.413	42.410	0.2
		5	28.357	28.358	-0.1
		12	14.548	14.548	0.0
		20	10.082	10.082	0.0
		8	19.721	19.725	-0.2
		10	16.667	16.662	0.3
		16	11.801	11.802	0.0
dodecanone	5 % Phenyl Column (SLB5ms)	3	33.761	33.757	0.3
		5	23.053	23.057	-0.2
		12	12.268	12.268	0.0
		20	8.700	8.697	0.2
		8	16.350	16.352	-0.1
		10	13.942	13.943	-0.1
		16	10.080	10.078	0.1
	50 % Phenyl Column (SPB50)	3	35.056	35.047	0.6
		5	23.982	23.992	-0.6
		12	12.827	12.832	-0.3
		20	9.133	9.125	0.5
		8	17.048	17.060	-0.7
		10	14.557	14.567	-0.6
		16	10.562	10.560	0.1
	Wax Column (Supelco Wax)	3	33.366	33.365	0.1
		5	22.936	22.935	0.1
		12	12.304	12.303	0.0
		20	8.745	8.747	-0.1
		8	16.342	16.343	-0.1
		10	13.967	13.962	0.3
		16	10.123	10.125	-0.1

Table 3.3 Comparison of thermodynamic parameters estimated using isothermal method and temperature-programmed methods.

		5% Phenyl Column			Wax Column		
	Estimation Method	Estimated $\Delta H(T_o)$ (kJ·Mol-1)	Estimated $\Delta S(T_o)$ (J·K-1·Mol-1)	Estimated ΔCp (J·K-1·Mol-1)	Estimated $\Delta H(T_o)$ (kJ·Mol-1)	Estimated $\Delta S(T_o)$ (J·K-1·Mol-1)	Estimated ΔCp (J·K-1·Mol-1)
undecane	isothermal	-47.34	-73.41	83.80	-36.71	-56.75	75.94
	temperature programmed	-47.30	-74.11	81.41	-37.80	-61.81	70.33
	relative error	0.1	-1.0	2.9	-3.0	-8.9	7.4
dodecane	isothermal	-51.87	-80.03	92.58	-40.40	-61.92	81.59
	temperature programmed	-51.57	-80.08	87.49	-42.24	-68.93	36.09
	relative error	0.6	-0.1	5.5	-4.5	-11.3	55.8
tridecane	isothermal	-56.18	-86.12	98.56	-44.10	-67.10	87.42
	temperature programmed	-55.73	-85.77	91.90	-45.41	-72.46	31.92
	relative error	0.8	0.4	6.8	-3.0	-8.0	63.5
tetradecane	isothermal	-60.42	-92.08	104.00	-47.78	-72.27	92.83
	temperature programmed	-59.31	-90.33	101.77	-48.48	-75.89	63.92
	relative error	1.8	1.9	2.1	-1.5	-5.0	31.1
undecanone	isothermal	-55.28	-84.20	94.33	-52.27	-75.03	83.26
	temperature programmed	-55.24	-84.87	99.80	-51.62	-74.60	41.83
	relative error	0.1	-0.8	-5.8	1.2	0.6	49.8
dodecanone	isothermal	-59.55	-90.18	100.07	-55.82	-79.86	86.90
	temperature programmed	-59.36	-90.08	83.62	-54.88	-78.69	53.75
	relative error	0.3	0.1	16.4	1.7	1.5	38.2
tridecanone	isothermal	-63.76	-96.06	105.30	-59.29	-84.56	91.65
	temperature programmed	-63.63	-96.55	110.93	-57.77	-81.87	54.84
	relative error	0.2	-0.5	-5.3	2.6	3.2	40.2
undecanol	isothermal	-58.70	-89.04	98.38	-64.33	-95.05	110.57
	temperature programmed	-59.05	-90.73	108.95	-62.01	-90.38	62.92
	relative error	-0.6	-1.9	-10.7	3.6	4.9	43.1
dodecanol	isothermal	-62.94	-94.95	103.67	-67.81	-99.73	114.57
	temperature programmed	-63.45	-97.09	118.34	-65.41	-94.94	74.06
	relative error	-0.8	-2.3	-14.1	3.5	4.8	35.4
tridecanol	isothermal	-67.31	-101.03	110.92	-71.20	-104.60	119.20
	temperature programmed	-68.22	-104.32	133.31	-68.62	-99.03	80.96
	relative error	-1.4	-3.3	-20.2	3.6	5.3	32.1
tetradecanol	isothermal				-75.42	-110.49	130.14
	temperature programmed	-71.94	-109.01	130.32	-71.90	-103.36	88.75
	relative error				4.7	6.5	31.8

5.35 % for $\Delta H(T_0)$, and $\Delta S(T_0)$. In both cases ΔC_P exhibits a larger error between the two methods. However, due to the relatively small contribution of ΔC_P and the assumption that it is constant when using this approach, this is expected and not critical to the performance of the approach. Additionally, the use of this new method was able to significantly reduce the required analysis time necessary for the determination of the thermodynamic parameters $\Delta S(T_0)$, $\Delta H(T_0)$, and ΔC_P. By taking the sum of the retention times used to estimate the thermodynamics for each analyte in our previous study,[86] it was determined that on average 250 minutes of instrument run time are required per analyte, for a total analysis time of 41.6 hours. In comparison using the same ten analytes and the new temperature-programmed method of thermodynamic estimation a total run time of only 2 hours was required to obtain all necessary data. It is also important to note that in the case of the temperature-programmed method, each additional analyte that can be fit within the separation space represents an additional 250 minutes of saved analysis time. With this reduction in analysis time this new method for determining thermodynamic parameters for use in GC provides thermodynamic-based techniques that are competitive with established RI methods as far as raw analysis time and overall more accurate in their predictions.

3.4 Conclusions

The close agreement with the isothermally collected thermodynamics and the ability to accurately predict retention times for temperature programmed separations that were outside of the training data highlights the validity of this new method. The reduction in analysis time and the ability to determine the

thermodynamics for large numbers of compounds within a series of temperature-programmed runs makes this new method a potential replacement for RI data. The ability to generate data without alkane standards and on a wide range of columns is advantageous. The methods used here enabled the techniques that shall be discussed in the subsequent chapters. Chapter 4 discusses the use of the technique in the normalization of data between columns and laboratories while Chapter 5 discusses practical uses of this technique.

Chapter 4: Compensating for Column Geometry Effects[4]

4.1 Introduction

The impact of column geometry on both the calculated phase ratio β and flow calculations used in retention time predictions means that even the most carefully collected thermodynamics will not necessarily provide accurate predictions on a column of the same phase and nominal geometry in another laboratory. Column manufacturers are able to make highly reproducible columns but are unable to completely eliminate variance in the inner diameter and film thickness between columns. Simply put, the vendor-provided nominal column dimensions are not precise enough to allow the transfer of thermodynamic data from column to column.

Obviously this hampers the practicality of thermodynamic methods, as such a method to normalize thermodynamic data and account for variation in column geometry in order to obtain accurate predictions across multiple columns was required. To be practically useful, the method must fulfill several requirements: the experimentation required to calibrate the column must be rapid and compatible with standard commercial GC equipment. Secondly, the chemicals required should also be both universally available and inexpensive.

Fused silica capillaries are formed by drawing a preform piece of fused silica through a heated furnace. Most producers of fused silica tubing have

[4] Sections of this chapter have been previously published: T.M. McGinitie, H. Ebrahimi-Najafabadi, J.J. Harynuk. *J. Chromatogr. A.* 1330, (2014) p. 69-73.

proprietary methods for the manufacture of their capillaries, and literature in the field is limited. The information on column production presented here is based upon the work of Dorman and Dawes in Chapter 3 of *Gas Chromatography*[87] and from early literature on fiber optic production techniques which parallel the production of fused silica tubing.[88] Precision manufacturing of the fused silica capillary is critical as variations during this process can affect the reproducibility of column dimensions. Critical to the process of producing columns is the use of a high quality fused silica preform as slight variations in the dimensions of this preform or impurities can manifest themselves as defects in the finished column. To ensure quality, preforms are cleaned and the manufacture process is carried out in a clean room to prevent dust from causing defects in the column. The preform is heated using an inductive furnace and is then drawn out to form the column. The final dimensions of the column are controlled by two aspects. One is the ratio of the inner and outer diameter of the silica preform, as this ratio remains unchanged as the column is drawn out. The second variable is the ratio between the speed the column is drawn to the speed of the column feed. This relationship between draw and feed speeds is otherwise known as the draw ratio. By tightly controlling both the temperature of the draw furnace and the draw ratio, columns can be reproducibly manufactured. The exact column dimensions are measured using laser scattering measurements,[89] which are then used in a feedback mechanism to precisely adjust the draw ratio to keep the column dimensions within specification.

As soon as the column is drawn a protective polyimide layer is coated on the outside of the capillary. This coating is used to protect the column from damage as even minute scratches can cause the capillary to shatter. Contaminants as small as dust can cause damage and so the coating is applied immediately after drawing, with subsequent layers of imide applied along the feeding of the column. Once the imide coating is applied the column is quite robust and can be handled without risk of severe damage.

Once the fused silica capillary is manufactured, a stationary phase must be applied to the capillary. Before coating the capillary in the stationary phase, the capillary is often treated to remove active sites. However, given the many ways deactivation can be accomplished and the proprietary nature of such deactivation, it is sufficient for this discussion to know that such a step occurs. The two methods commonly used for the coating of WCOT stationary phases are dynamic and static coating. Dynamic coating is a rapid method for coating columns. However it leads to non-uniform stationary phase thicknesses. Consequently it is typically only used in the development of experimental columns. In dynamic coating a high concentration solution (typically 5-25% wt/vol) of stationary phase is dissolved in a solvent along with an immobilization agent and is pushed through the capillary under high pressure. This method while rapid, results in a stationary phase that deceases in thickness along the length of the capillary. This non-uniformity results in a column that is non-ideal for high efficiency separations.

To achieve a stationary phase with a uniform film thickness, static coating procedures must be used. Static coating procedures employ a low concentration solution (0.1-1% wt/vol) of stationary phase dissolved in solvent. The required concentration is determined from the relationship between film thickness (d_f), the column inner diameter (d_c) and % concentration of the stationary phase solution (c) as described by Equation 4.1.[90]

$$d_f = 2.5 \cdot d_c\,(mm) \cdot c \qquad (4.1)$$

The capillary is filled with this solution and then one end of the capillary is sealed. Vacuum is then applied to the other end to evaporate the solvent and leave a film of stationary phase behind. Given the relationship between d_f and d_c as described by Equation 4.1 static coatings are able to theoretically provide a column of equal phase ratio.

Despite the tight controls that manufacturers have for the production of columns, slight variances exist in the inner diameter and the average film thickness between columns. A study performed by Polymicro Technologies highlights the typical variance in modern manufactured columns. For a column with a nominal value of 250 µm d_c, the standard deviation was 1.62 µm.[91] These variances while small were found to have a profound effect on the accuracy of the thermodynamic models discussed in this thesis.

Discussed within this chapter are two methods of column calibration that were employed throughout this work. The discussed calibration techniques were

developed in parallel with the isothermal thermodynamic collection method discussed previously in the introduction and the temperature programmed thermodynamic method discussed in the previous chapter. In both cases a calibration procedure was developed to address the loss of accuracy in the prediction of retention times when using thermodynamic data across multiple columns.

4.2 Experimental

4.2.1 Isothermal Calibration

A mixture comprised of alkanes, alcohols and ketones was used for the validation of the calibration procedure. n-Alkanes ranging from undecane to tetradecane were obtained from Sigma-Aldrich (Oakville, ON). 2-Undecanone, 2-dodecanone, and 2-tridecanone were purchased from Alfa-Aesar (Ward Hill, MA). Primary alcohol standards 1-undecanol, 1-dodecanol and 1-tridecanol were also purchased from Sigma-Aldrich. The standard mixture was prepared at a concentration of 1000 ppm in isooctane (Sigma-Aldrich). Methane from the laboratory natural gas supply was used as a dead time marker.

All experiments were carried out on a Varian 3800 GC (Varian Inc., Mississauga, ON) equipped with a flame ionization detector and a split/splitless injector. Both the injector and detector were maintained at 230 ^{o}C. Injections consisted of 1 μL of standard injected manually at a split ratio of 50:1. All standard solutions were co-injected with methane which served as a void time marker. All separations were conducted under isothermal conditions using

constant pressure to ensure an average linear velocity of 30 $cm \cdot s^{-1}$. A set of three Rtx®-5 (polydimethylsiloxane with 5% phenyl substitution) columns were used. The three columns of nominal geometries of (30m x 0.25 mm i.d. × 0.25µm) were obtained from Restek with sequential serial numbers, ensuring they were from the same batch and should theoretically be as identical as possible.

4.2.2 Scanning Electron Microscopy

Scanning electron microscopy SEM was used to determine the actual column diameter and film thickness for select sections of the columns. Images were taken using a JEOL 6301F field emission scanning electron microscope with a Si diode detector. Samples were prepared by mounting each section vertically on a custom designed SEM slide. A layer of colloidal silver was painted on the base of the slide and up the sides of the column sections to near the top. After 24 hours of drying a layer of chromium was deposited on the SEM slide. Images were taken using an accelerating voltage of 5.0 kV with a working distance of 14.0 mm. 200× magnification was used for inner diameter images while the stationary phase images were taken at 20,000× magnification. Using the program ImageJ[92] the inner diameter was measured by taking three diameter measurements. Stationary phase thickness was determined by taking six images equally spaced around the circle. Then on each image three measurements were taken and an average calculated.

4.2.3 Nonlinear Optimization Calibration

A Grob mix (Sigma-Aldrich #47304; Oakville, ON) consisting of 2,3-butanediol, decane, dicyclohexylamine, 2,6-dimethylaniline, 2,6-dimethylphenol, 2-ethylhexanoic acid, methyl decanoate, methyl laurate, methyl undecanoate, nonanal, 1-octanol, and undecane was used to normalize the column geometry. The compounds are of varying concentration ranging from 290 – 530 μg/mL (Sigma-Aldrich).

A second mixture comprised of alkanes, alcohols and ketones was used for the validation of the calibration procedure. n-Alkanes ranging from undecane to tetradecane were obtained from Sigma-Aldrich (Oakville, ON). 2-Undecanone, 2-dodecanone, and 2-tridecanone were purchased from Alfa-Aesar (Ward Hill, MA). Primary alcohol standards 1-undecanol, 1-dodecanol and 1-tridecanol were also purchased from Sigma-Aldrich. The standard mixture was prepared at a concentration of 1000 ppm in toluene (Sigma-Aldrich). Methane from the laboratory natural gas supply was used as a dead time marker.

4.2.4 Instrumental

A Bruker 461 GC (Bruker, Milton, ON) equipped with a split/splitless injector and flame ionization detector was used for all experiments. Injections were performed in split mode with a split ratio of 100:1 and an inlet temperature of 280 °C. The flame ionization detector was maintained at a temperature of 250 °C with a data sampling rate of 100 Hz. 99.999 % Helium (Praxair, Edmonton, AB) was used as a carrier gas. All columns used for the study were of

a 5 % phenyl substituted polydimethylsiloxane stationary phase, specifically SLB5ms (Supleco, Bellefonte, PA). The dimensions of each column used are listed in Table 4.1.

Table 4.1 Nominal and experimentally determined dimensions for the four columns used within the intralab normalization experiment. All columns were SLB5ms (5% phenyl substituted polydimethylsiloxane).

Column	Determined Length (m)	Determined Inner Diameter (mm)	Estimated Average Film Thickness (µm)
30 m × 0.25 mm × 0.25 µm (reference)	29.99	0.248	0.250
30 m × 0.25 mm × 0.50 µm	31.66	0.244	0.567
15 m × 0.1 mm × 0.1 µm	16.40	0.103	0.121
30 m × 0.25 mm × 0.25 µm (3 year conditioned)	29.10	0.254	0.253

Except where mentioned, all separations were performed under constant flow conditions. For all 0.25 mm i.d. columns, the carrier gas flow was 1.0 $mL \cdot min^{-1}$ and for the 0.1 mm i.d. column, the carrier gas flow rate was 0.29 $mL \cdot min^{-1}$. The separations were initialized at 50 °C, with the oven temperature programmed at ramp rates of 5, 8, 10, 12, 16, and 20 $°C \cdot min^{-1}$ to 250 °C. The column inner diameter, column film thickness, thermodynamic estimations, and GC retention time predictions were calculated using custom scripts written in MATLAB 7.10.0 (The Mathworks, Natick, MA).

4.2.5 Round Robin

The inter-lab study was carried out with the assistance of three other research groups, Dr. Alessandro Cassili's (Universidade Federal do Rio de Janeiro), Jack Cochran's (Restek Corporation), and Dr. Phillip Marriott's (Monash University). Columns were obtained from Restek (Bellefonte, PA), all columns were of the nominal dimensions (30 m × 0.25 mm i.d. × 0.25 μm) the stationary phases used were Rxi®-1ms (100% dimethyl polysiloxane), Rxi®-17Sil ms (50% diphenyl substituted, dimethyl polysiloxane), Stabilwax® (polyethylene glycol), and Rtx®-200 (6% trifluoropropylmethyl polysiloxane). Two columns from three separate production batches were used in this study with, a single set of columns going to each lab group involved in the study. The production of these columns was spaced across six months.

Standards for the study were also provided by Restek, a Grob standard (Restek, 35000) was the standard mix used to calibrate the column stationary phase film thickness. A total of 89 distinct molecules were studied from six separate test mixtures, WA VPH Standard (Restek, 30451), SV Calibration Mix #5 (Restek, 31011), Marine Oil Test Mix (Restek, 35249), Diesel Range Organics Mix (Restek, 31064), 8270 Calibration Mix #2 (Restek, 31619), and 8270 Calibration Mix #1 (Restek, 31618). These standards were chosen to provide a representative sampling of molecular classes including alkanes, phenols, amines, anilines, methyl esters, alkyl monoaromatics and polyaromatic hydrocarbons. The use of commercial standard mixes ensured all labs had access to the test set and prevented misidentification from contamination or structural isomers.

The instrument used for the experimentation varied lab from lab. All GCs used in the round robin study were equipped with split/splitless injectors set at 250 °C. The split ratio varied between 20-50:1 depending on the exact instrument used. All detectors were FIDs set at 250 °C, flow rates were set as per the standard operating flows for each instrument. A data rate of 200 Hz was set for all instruments. Our lab used an Agilent 6890 (Agilent, ON) for all round robin experimentation. The instruments used by the other labs were as follows: Casilli Agilent 6890N, Cochran Agilent 7890, and Marriott Agilent 6850.

4.3 Results and Discussion

4.3.1 Isothermal Calibration

The methods discussed here were developed prior to the TPGC method of data collection discussed in Chapter 3. As such data collection was carried out as per the method discussed in Chapter 1. Retention data were collected for every standard using two columns of a sequentially produced set of three. To obtain an exact measurement of the retention factor k for each analyte, all standards were co-injected with gaseous methane, which provided an accurate measure of column void time. Retention data were collected for all compounds using a series of isothermal runs in 10 ^{o}C intervals over a span of 80 ^{o}C. The total length of each column was first accurately measured by unwinding before use. Thermodynamics were then estimated from retention data collected using the entire length of column. Each column was then cut into a 10 m section and 20 m section. These two sections of column were then used to obtain thermodynamics for each analyte. Finally the 20 m section of column was cut in half and thermodynamics

were then obtained from each 10 m half of the column. This procedure resulted in ten sets of retention data for each analyte (five from each column) from which thermodynamic parameters could be estimated. From each end of every column segment created, two 6 mm pieces of column were cut for analysis by SEM.

After retention data were obtained for the first two columns in the manner described above; two methods were used to estimate $\Delta S(T_0)$, $\Delta H(T_0)$, and ΔC_p for each analyte. In the first method the column's phase ratio β was calculated from the manufacturer's listed column inner diameter and film thickness (Equation 4.2) where r is column radius and d_f is the film thickness.

$$\beta = \frac{r}{2d_f} \tag{4.2}$$

Using the manufacturer's provided β along with k, the partition coefficient K can be determined through the use of Equation 4.3.

$$\beta \cdot k = K \tag{4.3}$$

A linear regression of K against both the inverse of temperature and the natural logarithm of temperature can be used to determine the factors A, B, and C in Equation 4.4 where A, B, C relate to the three thermodynamic parameters $\Delta S(\mathrm{T_o})$, $\Delta H(\mathrm{T_o})$, ΔC_p for each analyte as discussed previously in Chapter 1.[54] These three parameters then relate back to an analyte's retention through the use of Equations 4.2 and 4.3.

$$\ln(K) = A + B \cdot \frac{1}{T} + C \cdot \ln(T) \tag{4.4}$$

This information can then be used to predict analyte retention under either isothermal or temperature-programmed conditions. However validation in this case was carried out using isothermal separations only.

After estimating the three thermodynamic parameters for each segment of column, an average value for $\Delta S(T_0)$, $\Delta H(T_0)$, and ΔC_p was determined. The thermodynamics estimated from all segments of columns one and two were then averaged to provide thermodynamic parameters for each analyte. Once this was accomplished retention data were gathered for dodecane, dodecanol, and 2-dodecanone on the third column. Using these three analytes as probes on the third column along with known retention data and the thermodynamic data from the original two columns, the phase ratio for the third column was estimated through the equations listed above. Using this new phase ratio and the previously collected thermodynamics for tridecane, tridecanol and 2-tridecanone, the retention times of these three analytes were then predicted across a range of isothermal separations and the root mean square error of prediction RMSEP was used to determine the success of the calibration (Table 4.2). The RMSEP values obtained using the nominal phase ratio was used to contrast these results (Table 4.2).

Table 4.2 Average RMSEP when using the nominal, normalized, and SEM determined phase ratio for isothermal predictions.

Analyte	Nominal β *RMSEP (s)*	Normalized β *RMSEP (s)*	SEM β *RMSEP (s)*	Calculated β Normalized	Calculated β SEM
Tridecanol	0.9	0.3	0.3	256.4	225.3
Tridecane	0.3	0.3	0.3	252.4	221.9
Tridecanone	0.5	0.4	0.4	251.5	221.0
Average	0.6	0.4	0.3	253.4	222.7

While the predicted phase ratio of the third column differed by only 1.26% from the nominal value, accounting for this difference did in fact increase the accuracy of predictions. Using the previously collected thermodynamic data for tridecane, tridecanol and 2-tridecanone along with the nominal phase ratio of the column, the root mean square error of prediction RMSEP for each compound was 0.3 s, 0.9 s and 0.5 s respectively. However, using the above method to account for the small variation in phase ratio, the RMSEP was reduced to 0.1 s, 0.6 s, and the ketone's RMSEP remained at 0.5 s. While the above example may at first appear insignificant it is important to remember that these columns were as near to identical as possible, having been produced sequentially. Despite this, discrepancies in the phase ratio were present. Furthermore, statistical analysis of the data by t-test using the relative percent error of prediction for each temperature investigated results in a significant reduction in error at the 99% confidence error (excluding the ketone which was significant at 90%). The above example points to the fact that even when predictions are made on 'identical' columns, accounting for the inter-column differences in phase ratio when attempting to make retention time predictions will improve retention time predictions.

In the aforementioned method, the β used for the third column to predict retention times is not the 'true' β of the column but rather a normalized value which enables the use of previously collected thermodynamics for the accurate prediction of retention time. In an attempt to find the 'true' β for any new column a similar method which employed SEM data was used. As mentioned previously

for every segment of column two 6 mm sections were cut off of the ends and run using SEM analysis. The true dimensions of the columns varied slightly from the manufacturer's listed values. Table 4.3 highlights the difference between the nominal values (250 μm × 250 nm) for film thickness and column diameter as well as the average values determined by SEM along each segment of column 1 and 2. The results also show high variability in both the determined stationary phase film thickness with a relative standard deviation of 27 % for column 1 and 23 % in column 2 (Table 4.3). This is from a total of 166 and 117 measurements of the film thickness for columns 1 and 2 respectively. This high variability comes from the non-uniformity of the stationary phase on the column, both longitudinally along the column and radially around a specific cross sectional plane. Figures 4.1 (a,b, and c) demonstrate the high variablity that is present in a single cross section of column. This variablity necessitates a high number of measurments to obtain an accurate value for d_f along the length of the column.

Using the average of the average film thickness and inner diameter measurements across the length of the column a new value of β was determined for both columns 1 and 2. This new value for β was then used along with the previously collected retention data to obtain the estimated values of $\Delta S(T_0)$, $\Delta H(T_0)$, and ΔC_p for all test analytes. Using these new thermodynamic values the phase ratio of the third column was estimated using the same C_{12} probe molecules as before. SEM images of the third column were taken and the thermodynamically determined value for β was compared with the β determined from these images were within 0.9% of the experimentally determined value.

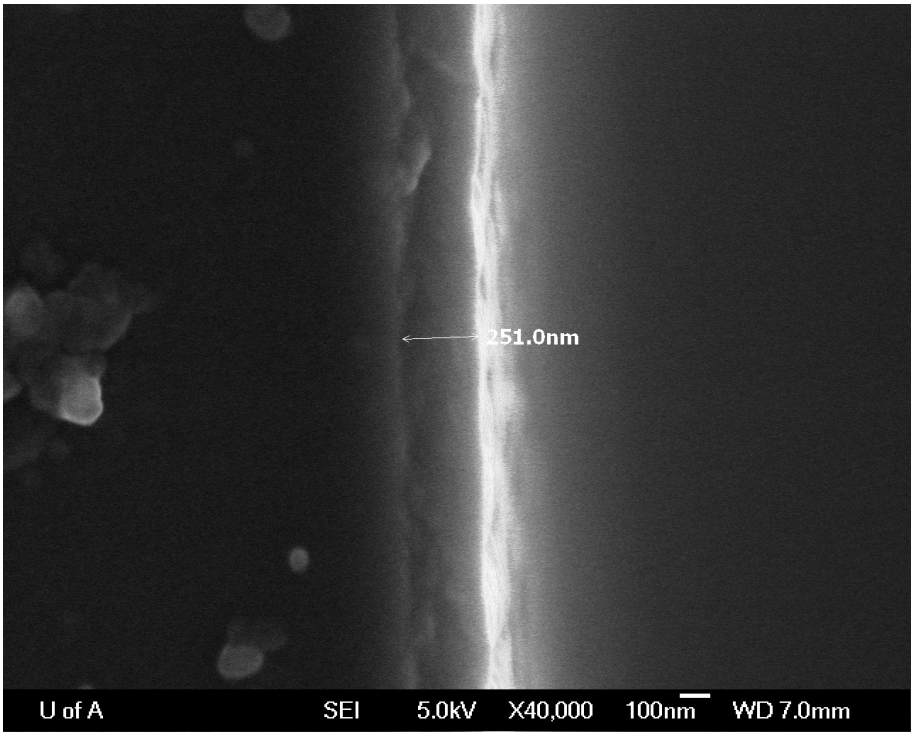

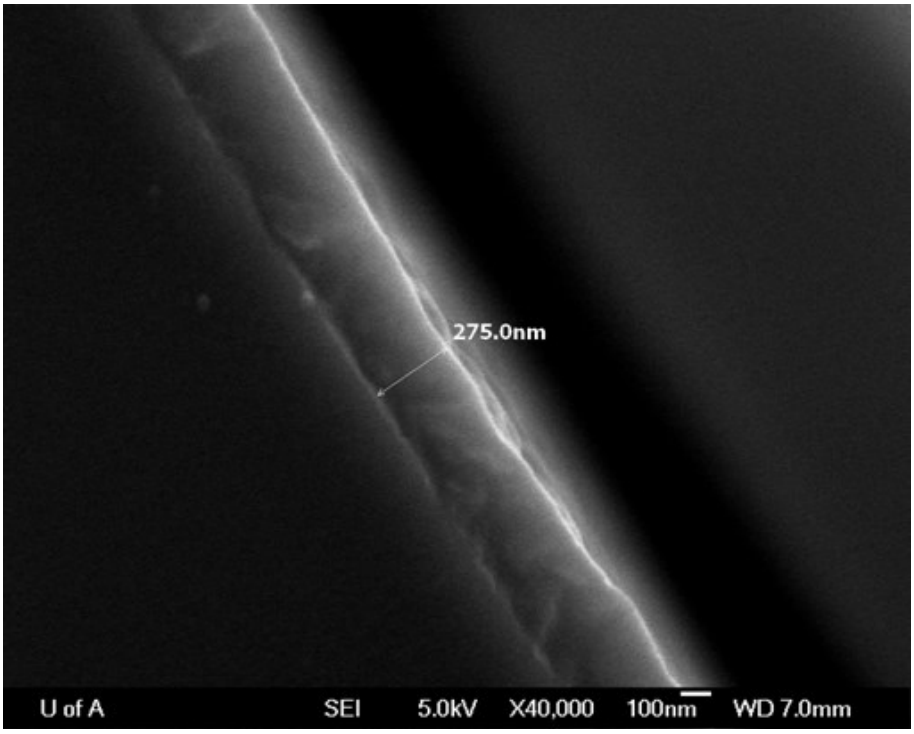

Figure 4.1(a,b) SEM image of 5% phenyl substituted polydimethylsiloxane column of nominal dimensions 30m × 0.25 mm i.d. × 0.25 µm. Subsequent figures are of same cross section.

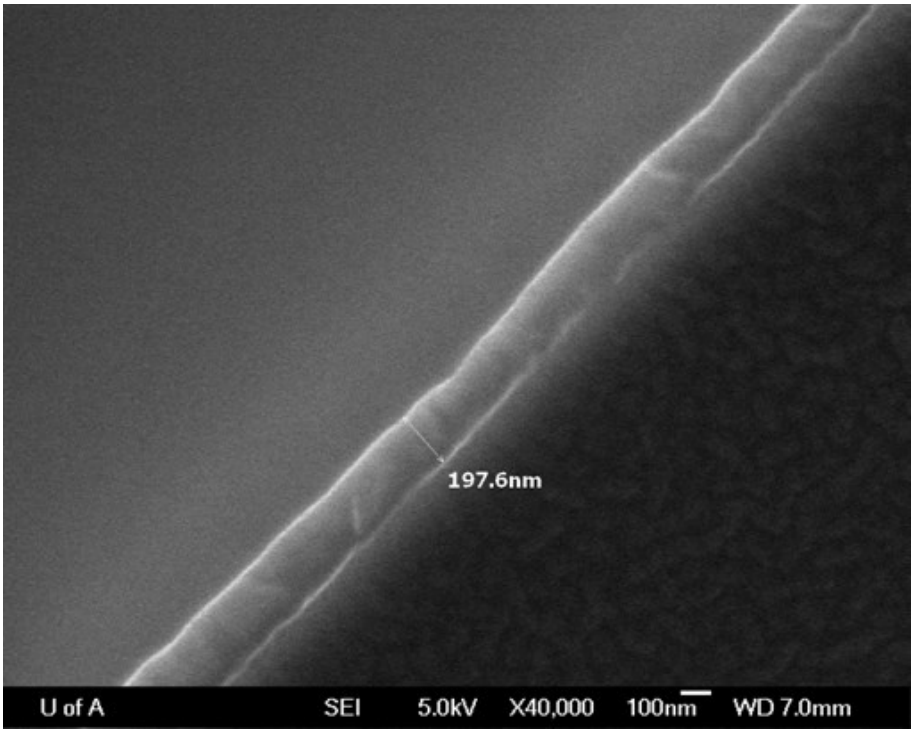

Figure 4.1(c) Third and final image of stationary phase film thickness for 5% phenyl substituted PDMS column of nominal dimensions 30 m × 0.25 mm i.d. × 0.25 µm.

Using this new value of β to predict retention times for tridecane, tridecanol and 2-tridecanone on the third column again showed exceptional results with a RMSEP of 0.2, 0.3 and 0.9 s respectively (Table 4.2). It is important to note that while both the nominal and SEM methods are able to provide accurate predictions of retention times, if an analytes' thermodynamics are estimated using either the nominal or SEM method it is not possible to use those thermodynamics with the other methods determined β as the two values will not agree with each other.

Table 4.3 Average SEM determined column inner diameter and stationary phase film thickness for reference columns 1 and 2. Values calculated using ImageJ.

		Position on Column (m)				Average Value
		0	10	20	30	
Column 1	Average Film Thickness (nm)	301	272	282	273	282
	Rel % Std Dev	28	32	33	15	27
	Average Inner Diameter (μm)	248	234	233	239	239
	Rel % Std Dev	1	7	11	7	6
Column 2	Average Film Thickness (nm)	269	278	284	314	286
	Rel % Std Dev	18	12	32	28	23
	Average Inner Diameter (μm)	250	251	243	269	253
	Rel % Std Dev	1	1	2	0	1

Of the two calibration methods, the nominal phase ratio method is preferred to the SEM method. Both methods provided an equal RMSEP. However obtaining SEM data were difficult and inconsistent. Often the stationary phase film thickness was unable to be measured and many measurements were needed to obtain a suitable average. While it could be argued from a fundamental standpoint that it is better to reference the phase ratio to a 'true' value of d_c and d_f, there is no practical benefit in terms of accuracy of predictions, and the costs in terms of time, effort, equipment, and the sacrificing of a column to use the SEM method cannot be justified.

4.3.2 Nonlinear Calibration Techniques

Concurrent with the nonlinear optimization techniques discussed in Chapter 3, a new method was developed for the rapid calibration of the column dimensions to allow for the transfer of data from column-to-column. Nonlinear calibration of the column is carried out in three steps: first the column length must be determined; followed by the determination of the column inner diameter; and

finally the estimation for the stationary phase film thickness. A 30 m × 0.25 mm; 0.25 μm film column was chosen to serve as a reference column for this study. This column was chosen as the reference column due to historical usage of this size of column within our previous thermodynamic studies and because these dimensions are among the most popular commercially.

4.3.3 Column Length

To determine column length, the reference column was unwound from the column cage and measured to the nearest cm. This was done to ensure accurate measurement of the internal diameter as the calculation of internal diameter is dependent upon the column length (Equation 4.5). Subsequent column lengths were estimated by measuring the diameter of the column coil and counting loops on the column cage. This estimation if performed on a well-wound column is typically able to provide estimates with an error of ±10 cm. If greater precision is required, then a new column can be unwound and measured directly.

4.3.4 Estimation of Inner Diameter

The column inner diameter is estimated based on fluid dynamics equations for a compressible fluid where the radius of the column, *r* (cm) is given by Equation 4.5[93]

$$r = \sqrt{\frac{32UF\eta L}{3}\frac{(P_i^3 - P_o^3)}{(P_i^2 - P_o^2)^2}} \qquad (4.5)$$

where *U* is the experimental average carrier gas velocity in cm·s^{-1} determined by the taking the length of the column *L* and dividing by the retention time of

methane, η is the viscosity in poise ($g \cdot cm^{-1} \cdot s^{-1}$) of the carrier gas at the experimental temperature T, in degrees Kelvin (K) (Equation 4.6 for He and Equation 4.7 for H_2).[94] P_i and P_o are the pressures in dynes ($g \cdot cm \cdot s^{-1}$) at the column inlet and outlet, respectively.

$$\eta = -2.151^{-10} \cdot T^{o2} + 5.954^{-7} \cdot T^{o2} + 3.923^{-5} \qquad (4.6)$$

$$\eta = -1.089^{-10} \cdot T^{o2} + 2.780^{-7} \cdot T^{o2} + 1.950^{-5} \qquad (4.7)$$

The column radius was estimated based on triplicate injections of methane at each of three temperatures: 50 °C, 100 °C, and 150 °C. For each temperature the instrument flow was set to an average linear velocity of ~30 $cm \cdot s^{-1}$. The average result from these nine estimates of inner diameter was then used as the actual internal diameter for this column.

4.3.5 Stationary Phase Film Thickness

Obtaining an accurate value for the stationary phase film thickness is difficult to accomplish experimentally. The physical thickness of the stationary phase can be measured via scanning electron microscopy. However, even the best-manufactured column is subject to non-uniformity in the film thickness along its length. As was observed previously the film thickness will change even over a few cm along the column, and in a given segment of column, the thickness can vary depending on the position around the cross section of the column.[95] Thus estimation of the film thickness by SEM requires multiple measurements along the length of the column and the ultimate destruction of the column. Obviously the need to sacrifice a column and the extensive time required to perform SEM

measurements makes this a poor method to determine the stationary phase film thickness in practice.

In this approach, a series of probe molecules is used to compare the film thickness of a new column to a 'reference column'. While this technique does not result in the true physical dimension of the film thickness of a particular column, it provides a relative comparison that permits normalization of thermodynamic data between columns. A similar concept which compared the elution temperatures of a probe molecule to determine the film thickness of different columns was originally proposed by Grob.[96] It is fitting then that the probe molecules chosen here for calibrating the film thickness are the Grob Mix compounds. They are widely available as a ready-made, inexpensive mixture covering a range of chemistries, and thus should perform well across a range of column chemistries.

To determine the film thickness, a series of temperature-programmed separations with ramp rates of 5, 8, 10, 12, 16 and 20 °C·min^{-1} were performed using the Grob standard. 2,3-Butanediol, 2-Ethylhexanoic acid, and dicyclohexylamine were omitted from subsequent calculations due to their poor chromatographic performance on the 5% phenyl stationary phase. The identities of all compounds were verified via mass spectrometry. The thermodynamic parameters for all components of the Grob Mix on the reference column were obtained using the non-linear optimization techniques described previously.[97] In these thermodynamic calculations the length and inner diameter of the column were determined as per the above protocols while the nominal value was assumed

for the stationary phase film thickness. The resulting thermodynamic estimations for the nine test compounds are shown in Table 4.4.

Table 4.4 Estimated thermodynamic parameters for Grob test mixture used in the determination of column film thickness.

Compound Name	Estimated $\Delta H(T^o)$ ($kJ \cdot mol^{-1}$)	Estimated $\Delta S(T^o)$ ($J \cdot K^{-1} \cdot mol^{-1}$)	Estimated ΔCp ($J \cdot K^{-1} \cdot mol^{-1}$)
Decane	-43.94	-69.57	11.51
1-Octanol	-47.69	-75.66	31.99
Undecane	-48.02	-74.90	26.22
Nonanal	-47.69	-73.70	23.39
2,6-Dimethylphenol	-47.53	-73.17	109.60
2-Ethylhexanoic acid	-49.83	-79.17	5.97
2,6-Dimethylaniline	-47.40	-69.35	39.46
C10 acid methyl ester	-57.35	-87.61	58.77
Dicyclohexylamine	-56.09	-79.39	45.16
C11 acid methyl ester	-59.97	-89.28	41.88
C12 acid methyl ester	-65.36	-98.18	74.80

Subsequent determinations of the stationary phase film thickness for a particular column rely on the thermodynamic values determined for the Grob Mix using the 'reference column'. To determine the film thickness of the three other columns, the Grob Mix was run on the remaining three columns using the same set of temperature programs as the reference column and the absolute retention times for each analyte were collected.

The retention data for the Grob Mix on the new column are then used in conjunction with the previously estimated thermodynamic parameters for the compounds on the 'reference column' and the chromatographic conditions to calculate the average effective film thickness the column. This was performed by a custom-written script in Matlab that relies on the Nelder-Mead simplex

algorithm to estimate a value for the film thickness that is consistent with both the collected experimental data and the previously estimated thermodynamic parameters.

The script begins by using the nominal value for the film thickness and the estimated thermodynamic values to predict the retention time for each analyte under every temperature ramp using the time summation model presented in Chapter 3. The algorithm proceeds to change the film thickness to minimize the error between the predicted and experimental retention times for all compounds simultaneously, thus providing an estimate for the column stationary phase film thickness. In this case the model functions nearly identical to the situation described in the previous chapter. However, it optimizes for film thickness rather than thermodynamics.

The columns for the study were chosen to span a range of geometries and demonstrate that the calibration method was effective regardless of the geometry or age of the column. A new, unused (30 m × 0.25 mm; 0.25 μm) column was chosen as the reference column to avoid effects due to column degradation. A column of nominal length (30 m × 0.25 mm; 0.5 μm) was chosen to evaluate the effect of film thickness on the calibration and another new (15 m × 0.1 mm; 0.1 μm) column was used to investigate if the calibration would be effective for a column of radically different dimensions but of the same stationary phase. Finally a column of the same stationary phase and dimensions as the reference column (30 m × 0.25 mm i.d. × 0.25 μm) that had been used extensively over a period of

three years was used to investigate the use of the calibration method to recalibrate an aged, partially degraded column.

Each column was normalized to the reference column using the method described above. The experimentally determined column diameter and film thicknesses for each column are listed in Table 4.1. The experimentally determined column inner diameters agree closely with the nominal values with an average error of 2.0 %. The stationary phase film thickness shows a larger discrepancy between the nominal and experimentally determined values with an average error of 11.8 %. However, both the error in the column inner diameter and film thickness are typical of the variation observed when using SEM to observe the column directly.[91,95]

To validate the results of the calibration, a test mixture of alkanes, ketones and alcohols was prepared and the thermodynamic parameters $\Delta S(T_0)$, $\Delta H(T_0)$, and ΔC_p were gathered for each analyte based on experimental data obtained using the reference column. Subsequently, the test mixture was separated on each of the other columns using temperature programs of 5, 8, 10, 12, 16, and 20 °C·min^{-1}. The retention times for each analyte were predicted using the thermodynamic prediction model described previously[97] and the predicted and experimental results compared. Table 4.5 presents the absolute error between the predicted and experimental results of each test compound across all four columns. The retention times for all compounds were predicted on the reference column to compare the relative success of the calibration on the other columns. The largest absolute error for the reference column was 1.49 s while the average absolute error for all

compounds on the reference column was 0.36 s. In comparison the, 30 m × 0.25 mm; 0.5 μm film column had an average error of 2.1 s, the 15 m × 0.1 mm; 0.1 μm film column 1.5 s, and the old 30 m × 0.25 mm; 0.25 μm film column had an average error of 1.1 s. The largest error across all compounds and columns was for tridecanol on the 15 m column at 6.4 s.

Table 4.5 Average absolute error for each analyte across 5, 8, 10, 12, 16, and 20 °C·min^{-1} temperature ramps on each column.

Compound	Average Absolute Error (s) (master column)	Average Absolute Error (s) (30 × 0.25 × 0.5)	Average Absolute Error (s) (15 × 0.10 × 0.10)	Average Absolute Error (s) (30 × 0.25 × 0.25)
undecane	0.4	1.9	1.2	1.1
dodecane	0.3	2.3	1.3	1.1
tridecane	0.6	2.3	1.1	1.1
tetradecane	0.2	2.0	0.8	1.1
2-undecanone	0.2	2.2	0.7	1.2
2-dodecanone	0.2	2.1	0.6	1.1
2-tridecanone	0.3	2.0	2.4	1.1
1-undecanol	0.8	2.3	0.4	1.0
1-dodecanol	0.3	2.0	2.1	1.1
1-tridecanol	0.2	1.6	4.7	1.2

Using undecanone as an example we can compare these results to those found using LRI. The LRI value reported for undecanone using flavornet is 1296,[98] however other sources place the LRI value at 1294.[99] This variation is typical when using LRI and so for this comparison we will assume that a 'true' LRI value any experimental value would optimistically fall within ±2 LRI units of the measured value. Furthermore between our 5 °C·min^{-1} and 20 °C·min^{-1} experiments we found a difference of 3 RI units (1293-1296). If we convert each LRI unit into a measure of time, the associated error for all columns given ± 2 RI values would be ± 3.2 s, an order of magnitude larger than the error of our

reference column, and larger than any of the errors observed for this molecule across all of the columns in the study.

To demonstrate the need for column calibration, the retention time predictions were also made using the nominal column inner diameters and film thicknesses. Without the calibration the average error for the each column (30 m, 15 m, and 30 m old) increased to 34.1, 9.9, and 7.9 s, respectively. The large increase in errors when using the nominal dimensions highlights the importance of column calibration if attempting to make retention time predictions based on thermodynamic models.

4.3.6 Round Robin Investigation

To test both the temperature programmed thermodynamic collection method and nonlinear calibration method further an inter-lab investigation was conducted to study the practicality and real world success of these new thermodynamic techniques. If these techniques are to be used as a universal method for collecting and sharing thermodynamic data they should first be extensively validated. This investigation expanded the scope of the study from the original investigation that was conducted in our lab to include a wider range of molecules and a variety of stationary phases. As well columns for the study were taken from several different production batches to study the effect of inter and intra batch stationary phase variance on the outcome of thermodynamic determinations and predictions. Thermodynamics have long been touted as being independent of operating conditions. While this had been demonstrated previously by our intra-lab studies the use of multiple instruments and operators allows for more rigorous testing of

this claim. Presented here are the preliminary findings from the inter-lab study, as at present not all labs have submitted their data for analysis. However, the data available provides a representative example of the successes and failures of the current calibration procedure.

Each lab was instructed to carry out the column calibration in the manner described in the previous section, with each lab first calculating the length of the column from the mentioned geometry method. The column inner diameter was then determined as described previously via three isothermal injections of 5 μL of methane performed in triplicate at 50, 100, and 150 °C. For each of these experiments the user set an inlet pressure that provided 1 $mL \cdot min^{-1}$ the inlet pressure and outlet pressure were accurately recorded at all three temperatures.

Film thickness determinations and temperature programmed thermodynamic information were collected in the following fashion. Five temperature programmed runs that had a ramp rate of 5, 8, 10, 12, 16 $°C \cdot min^{-1}$ were used to separate all test mixtures. The separations initiated at a temperature of 50 °C and ramped to the minimum bleed temperature of each column; for some mixes an isothermal hold of the final temperature was used to allow for the elution of highly retained compounds. In all cases constant flow mode was used to obtain a flow of 1 $mL \cdot min^{-1}$, and the inlet pressure was accurately determined for both the initial and final temperature of the ramp. 1 μL of each sample mixture was injected for each temperature program.

Before collecting the relevant retention data for the six test mixtures the column were conditioned per the manufacturer's instructions to ensure excess stationary phase was removed. Each lab first determined the column length and inner diameter via the established procedures before proceeding to collect retention data. The Grob standard mix was used to calibrate the thermodynamic data between laboratories, and to act as a standard to ensure no abnormalities occurred over the course of data collection. The Grob test mixture was run before every two sample mixtures, i.e. the five temperature programmed separations were carried out for the Grob standard mix, then mixture 1, and then mixture 2. The Grob mix was then reanalysed and another two samples run until all 6 standard mixes were completed for a column. After the collection of retention data were finished the raw retention information was sent to me for processing. Jack Cochran's laboratory provided tentative identification for all analytes via GC-MS analysis.

For the preliminary study our columns were used as the standard reference columns for the four groups, i.e. the thermodynamics parameter for each analyte were determined using our lab's retention data. The thermodynamic parameters for the Grob standard mixture were determined using the Harynuk lab retention data. The film thicknesses for all other columns were then determined using these thermodynamic parameters and each lab's collected retention values via the non-linear calibration method. The column used for this preliminary investigation was a Restek rxi®-1ms (100% polydimethylsiloxane). The determined dimensions for each lab's column are listed in Table 4.6.

Table 4.6 Experimentally determined length, d_c, and d_f for rxi®-1ms columns.

Dimension	Group 1	Group 2	Group 3	Group 4
Column Length (m)	29.89	29.6	30.04	30.36
Column Inner Diameter (mm)	0.229	0.242	0.258	0.265
Stationary Phase Film Thickness (μm)	0.25	0.266	0.295	0.376

The determined inner diameters showed slightly higher variance from nominal values over those obtained from previous studies with an average relative error of 5.2 %. The deviation from the nominal value for the stationary phase film thickness was 6.4 % for group 2, 18.0 % for group 3 and 50.4 % for group 4. The exceptionally high deviation in group 4 could be attributed to the use of incorrect pressure settings which resulted in a flow of only 0.56 $mL \cdot min^{-1}$ rather than the procedure's recommended 1.0 $mL \cdot min^{-1}$. This resulted in longer than normal retention times and sub optimal chromatography which may have impacted the accuracy of the calculations.

Once each column was calibrated for use with the thermodynamic data generated from the Harynuk lab, the retention times for each analyte were predicted and the absolute error in prediction for each compound was determined. The average error across all compounds in each mixture was determined and summarized in Table 4.7.

Table 4.7 Average absolute error in prediction for each test mixture across all four groups on the rxi®-1ms column.

	Average Absolute Error (s)			
Mixture	Group 1	Group 2	Group 3	Group 4
31618	0.8	3.7	3.8	8.9
31619	0.9	5.5	5.7	8.9
30451	0.6	4.0	3.4	9.8
31064	0.7	8.0	7.9	9.8
35249	0.8	9.7	10.1	13.0
31011	0.9	9.8	9.0	9.6

Group 1 in Table 4.7 is the Harynuk lab, the results show an average error that is comparable to the error determined in the previous intra-lab study for a single column. However, the error in predictions for the other three labs is an order of magnitude greater than for the intra-lab predictions. This error is comparable across all three laboratories and sample mixtures suggesting no bias in the accuracy of predictions across compounds or locations. While inter-lab experiments often experience higher variance than within lab results, considering the success of the intra lab experiments the increase in the average absolute error was greater than expected. Looking at the error between the predicted retention times and experimental retention times for all analytes certain biases in the predictions become apparent. Table 4.8 shows the absolute error in prediction for all analytes as determined by Group 2 for an rxi®-17ms column (50 % phenyl substituted polydimethylsiloxane).

Table 4.8 Absolute error for all analytes across 5 temperature programs on rxi®17ms column (30 m × 0.25 mm × 0.25 µm).

Mixture #	Compound Name	Absolute Error in Prediction				
		5 °C·Min^{-1}	8 °C·Min^{-1}	10 °C·Min^{-1}	16 °C·Min^{-1}	20 °C·Min^{-1}
31618	Phenol	-7.3	-7.0	-6.8	-6.7	-6.7
	2-Chlorophenol	-7.6	-6.6	-6.3	-6.3	-6.4
	2-Methylphenol	-1.0	-4.1	-4.8	-5.6	-5.7
	4-Methyphenol	-2.2	-3.8	-4.1	-4.6	-4.8
	3-Methylphenol	-2.3	-3.7	-4.1	-4.7	-4.9
	2,4-Dimethyphenol	0.6	-1.3	-2.0	-3.1	-3.5
	2-Nitrophenol	-0.1	-1.7	-2.3	-3.2	-3.6
	Benzoic acid	0.4	-0.5	-1.0	-2.5	-3.2
	2,4-Dichlorophenol	1.1	-0.2	-0.7	-2.3	-3.0
	2,6-Dichlorophenol	3.5	1.3	0.5	-1.4	-2.2
	4-Chloro-3-methylphenol	7.8	3.4	2.1	-0.2	-1.1
	2,4,6-Trichlorophenol	10.5	5.2	3.8	1.0	-0.1
	2,4,5-Trichlorophenol	8.7	5.6	4.1	1.2	-0.1
	2,3,4,6-Tetrachlorophenol	17.0	10.7	8.4	4.0	2.3
	4-Nitrophenol	17.6	11.2	8.5	3.9	2.4
	2,4-Dinitrophenol	19.1	10.4	8.0	3.9	2.5
	4,6-Dinitro-2-methylphenol	20.3	12.2	9.5	4.8	3.0
	Pentachlorophenol	22.7	14.8	12.7	6.5	4.3
	Dinoseb	23.5	13.6	10.2	5.4	3.6
31619	Pyridine	-14.8	-13.6	-12.8	-11.7	-11.1
	N-Nitrosodiphenylamine	-13.6	-13.0	-12.4	-11.2	-10.4
	Aniline	-5.4	-5.5	-5.4	-5.7	-5.7
	N-Nitrosodi-n-propylamine	-2.7	-3.7	-3.9	-4.6	-4.8
	4-Chloroaniline	4.3	2.6	1.8	-0.6	-1.6
	3-Nitroaniline	14.3	9.0	7.2	3.2	1.8
	2-Nitroaniline	17.9	11.1	8.7	4.3	2.7
	Diphenylamine	20.2	12.3	9.6	5.0	3.2
	4-Nitroaniline	21.1	13.3	10.6	5.8	3.9
	Benzidine	32.6	20.9	17.0	9.8	6.9
	3,3'-Dichlorobenzidine	36.9	23.3	19.0	10.9	8.1
30451	n-Hexane	-18.1	-17.2	-16.7	-15.3	-14.5
	Methyl tert-butyl ether	-19.5	-18.5	-17.8	-16.3	-15.4
	Benzene	-17.8	-16.5	-15.8	-14.3	-13.6
	n-Octane	-17.5	-16.2	-15.5	-14.0	-13.2
	Toluene	-16.8	-14.9	-14.1	-12.6	-12.0
	Ethylbenzene	-14.3	-12.5	-11.9	-10.7	-10.1
	p-Xylene	-14.5	-12.4	-11.6	-10.5	-10.0
	m-Xylene	-14.5	-12.4	-11.6	-10.5	-10.0
	n-Decane	-13.7	-11.8	-11.2	-10.3	-10.0
	o-Xylene	-13.0	-11.3	-10.7	-9.7	-9.3
	1,2,3-Trimethylbenzene	-7.7	-6.6	-6.5	-6.5	-6.5
	n-Dodecane	-5.4	-5.9	-6.0	-6.2	-6.2
	Naphthalene	2.7	1.0	0.2	-1.5	-2.2
	1-Methylnaphthalene	8.0	4.9	3.6	0.8	-0.3
31064	n-Decane	-12.6	-11.6	-11.2	-10.3	-9.9
	n-Dodecane	-6.0	-5.5	-5.7	-6.1	-6.4
	n-Tetradecane	3.4	-0.1	-1.1	-2.6	-3.1
	n-Hexadecane	9.7	4.4	2.8	0.2	-0.9
	n-Octadecane	15.1	7.8	5.7	2.2	0.9
	n-Eicosane	19.1	10.7	8.1	3.8	2.2

Table 4.8 Absolute error for all analytes across 5 temperature programs on rxi®17ms column (30 m × 0.25 mm × 0.25 µm).

		Absolute Error in Prediction				
Mixture #	Compound Name	5 °C·Min^{-1}	8 °C·Min^{-1}	10 °C·Min^{-1}	16 °C·Min^{-1}	20 °C·Min^{-1}
	n-Docosane	20.6	13.0	10.4	5.1	2.9
	n-Tetracosane	24.2	14.8	11.7	6.1	3.9
	n-Hexacosane	26.7	16.4	12.9	6.8	4.5
	n-Octacosane	29.2	17.6	13.9	7.5	5.1
35249	Methyl myristate	14.3	7.9	5.8	2.3	1.0
	Methyl myristoleate	14.8	8.8	6.5	2.7	1.1
	Methyl palmitate	16.7	9.8	7.5	3.4	1.8
	Methyl palmitoleate	17.8	10.6	8.2	3.8	2.1
	Methyl stearate	24.1	12.8	8.7	4.4	3.1
	Methyl oleate	24.8	12.6	9.6	5.0	3.4
	Methyl octadecenoate	24.5	12.7	9.6	5.0	3.5
	Methyl linoleate	25.2	13.3	10.1	5.4	3.8
	Methyl linolenate	25.8	13.9	10.7	5.8	4.1
	Methyl arachidate	25.3	14.6	9.8	5.6	4.2
	Methyl eicosenoate	26.9	14.3	10.9	6.0	4.3
	Methyl eicosadienoate	27.5	14.8	11.4	6.4	4.6
	Methyl arachidonate	27.9	15.5	12.0	6.6	4.7
	Methyl eicosatrienoate	27.0	14.6	11.4	6.5	4.7
	Methyl eicosapentaenoate	27.6	15.5	11.9	6.6	4.7
	Methyl behenate	27.7	16.0	12.4	6.9	4.9
	Methyl erucate	28.2	16.4	12.8	7.0	4.9
	Methyl docosahexaenoate	28.8	17.0	13.3	7.4	5.1
	Methyl lignocerate	30.8	17.5	13.6	7.5	5.4
	Methyl nervonate	30.7	17.8	14.0	7.8	5.6
31011	Naphthalene	3.7	1.2	0.3	-1.4	-2.0
	Acenaphthylene	15.2	9.4	7.5	3.5	1.9
	Acenaphthene	15.9	10.0	8.0	3.8	2.1
	Fluorene	19.2	11.9	9.4	4.8	3.1
	Phenanthrene	26.1	16.2	13.0	7.2	5.1
	Anthracene	25.7	16.4	13.2	7.3	5.0
	Fluoranthene	32.0	20.5	16.5	9.5	6.9
	Pyrene	35.6	21.5	17.2	10.1	7.7
	Benz[a]anthracene	40.1	24.0	19.0	11.3	8.6
	Chrysene	39.8	24.4	19.4	11.4	8.6
	Benzo[b]fluoranthene	43.8	26.1	20.9	15.5	14.1
	Benzo[k]fluoranthene	44.1	26.1	20.9	15.7	14.4
	Benzo[a]pyrene	45.4	26.6	21.7	19.4	18.3
	Indeno[1,2,3-cd]pyrene	40.7	34.9	34.4	32.8	32.3
	Dibenz[a,h]anthracene	42.5	36.6	35.9	34.1	33.4

It is readily apparent that a point exists when the model switches from overestimating the predicted retention time to underestimating the retention time. Analysis of the data reveals that this point corresponds to the approximate average

retention time of the Grob standard mixture on the column. The implication of this being that any analyte that elutes before this time will have its retention overestimated and any compound that elutes after the average retention time of the Grob standard mixture will be underestimated. The absolute error in prediction also increases the farther away from this point the analyte elutes. This appears to be a fundamental problem with the manner in which the phase ratio is estimated from the Grob standard mixture. Unfortunately, this was not noticed in the intra-lab study due to the fact that the test probes eluted directly in the middle of the Grob test mixture's elution. The observed pattern potentially suggests that later eluting analytes experience a different apparent film thickness than early eluting compounds, or an as of yet unexplained physical phenomenon is occurring. One potential solution to this that has not yet been attempted is to individually calculate β for each analyte in the Grob test mixture and plot these with respect to elution temperature. It is possible that the increase in β that is observed will follow a trend, linear or otherwise that can be extrapolated and used to remove the bias from the predictions. Despite the fact that the current calibration method is introducing bias into the predicted values, on average the method is able to predict retention times with a relatively high degree of accuracy across laboratories. So long as the retention times of the target analytes remains close to that of the Grob standard mixture the errors encountered are minimal. While the result is not perfect, the use of the current calibration method is able to predict retention times much more accurately than if no method was used at all.

4.4 Conclusions

The problem of data transfer between individual columns presents a significant challenge for thermodynamics based prediction models. Several individual methods to account for this variability were attempted throughout the course of the research. While earlier methods were simplistic in their approaches they did not provide satisfactory results for inter-lab use. The nonlinear approach, built upon the lessons learned from earlier attempts resulted in a more robust approach to column normalization which permits thermodynamic-based models of retention to account for changes in column inner diameter and film thickness, including variability during the manufacturing process and degradation of stationary phase that occurs as a column ages. This allows for thermodynamic parameters collected on one column to be translated to another column of the same stationary phase chemistry and used to produce accurate predictions of retention time. This method ensures the calibration of a new column is reasonably fast, and requires inexpensive calibration standards. The round robin studies while exhibiting slightly higher errors than those observed for our intralab studies, illustrate the validity of using thermodynamic information for GC separations on a global scale. At the same time the biases observed in the predictions, and the errors in the predicted retention times that are distant from the retention of the Grob standard compounds show that there is work left to be done if column-to-column data transfer is to be accurate and without biases. Even so, the ability to use thermodynamic data on multiple columns, instruments, and laboratories

represents an important step forward in the development of predictive thermodynamic models and should help in increasing the usage of such models.

Chapter 5: Application of Thermodynamics to GC×GC[5]

5.1 Introduction

The preceding chapters have outlined a series of tools that increase both the speed of data collection and allow for the accurate transfer and application of thermodynamic data from column-to-column. In this chapter the application of various thermodynamic methods to the prediction of GC×GC separations shall be presented. As previously discussed, predictive models of chromatographic behavior have many potential uses, from aiding in the optimization of separation conditions,[64] to helping identify unknown peaks in a chromatogram.[100] With the proliferation of GC×GC instrumentation, there is an urgent need for an accurate and precise modelling of two-dimensional gas chromatographic retention. In a GC×GC separation, the two separation dimensions are coupled by a modulator, and not truly independent; for any change to the conditions used for one column will influence the conditions of the separation on the other column.[101] Consequently, optimization of the instrumental conditions and column geometry/chemistry for the two dimensions is exponentially more difficult than for a conventional one-dimensional (1D) GC separation. The second use for a predictive model would be to allow researchers to automatically access the information that remains locked inside of the structured retention patterns observed in GC×GC. Such a model could work in conjunction with a mass spectrometric detector, potentially allowing positive identification of unknown

[5] Sections of this chapter have been previously published as T.M. McGinitie, J.J. Harynuk. *J. Chromatogr. A*. 1255 (2012) 184-189.

compounds in a sample. This would be particularly useful in distinguishing structural isomers which are often difficult (or impossible) to distinguish by mass spectrometry alone. When a GC×GC chromatogram may contain thousands (or even tens of thousands) of unknown peaks,[102] the need for such a model is obvious.

Given the large increase in papers that discuss GC×GC and its applications to various real world samples, there is no question that GC×GC is gaining popularity. However, until recently there has been very little research focused on modeling retention in GC×GC. One of the first examples was the prediction of analytes' retention times based on calculated vapor pressures and linear retention indices.[103] Retention indices have been a recurring theme in the modeling of GC×GC separations. The models generally rely on relating retention index data to the analytes' partition coefficients which are then used to predict retention behavior in GC×GC separations.[104] Variations of this approach have been used to model the retention of hydrocarbons in petroleum samples.[49,105] QSRR models for the prediction of polychlorinated biphenyl (PCB) retention times have also been developed.[106,107] Seeley et al. used molecular descriptors of the solute and stationary phase to predict retention times in GC×GC based on solvation parameters.[108] Models based upon thermodynamic calculations have also been previously studied. Zhu et al. used thermodynamics predicted from isovolatility curves to predict the retention indices of alcohols,[109] while Lu et al. estimated enthalpic and entropic parameters to predict retention times for a variety of pyridines.[110] Finally Dorman et al. also used a two-parameter thermodynamic

model based on the van't Hoff equation to predict the retention times of select components within the Grob mixture.[81]

Previous chapters presented the development of techniques used in the collection and standardization of thermodynamic data for use in the prediction of GC retention times. Predictions made using these thermodynamic methods have until this point been presented only for the purpose of validation. This chapter presents the application of the previously discussed thermodynamic models in the prediction of retention times for GC×GC. While making predictions for GC×GC is in itself important, using GC×GC within this research offered several other benefits. Using data collected via traditional one-dimensional separations to generate analyte retention times in GC×GC allowed for a 'true' prediction rather than just an extrapolation. As well GC×GC separations offer in the second-dimension an extreme set of conditions with which to stress-test predictions. If one is able to demonstrate that thermodynamic models can be easily transferred from traditional GC to GC×GC, the applicability of the model is increased as a singular solution can be used for all manner of GC separations.

This chapter is arranged in a semi-chronological manner to illustrate the results of the predictive models as both the thermodynamic collection methods and normalization methods discussed in previous chapters evolved. While many of the earlier predictions presented here were later replicated and improved upon by data generated using different techniques developed over the course of the research, the predictions made by earlier methods are still of significance and worthy of discussion by themselves as well as to provide context to the results

achieved using later techniques.

5.2 Experimental

A 7890A gas chromatograph (Agilent Technologies, Mississauga, ON) equipped with a split/splitless injector, flame ionization detector, and a capillary flow technology (CFT) GC×GC modulator was used for all experiments. Injections were performed in split mode with a split ratio of 50:1 and an inlet temperature of 280 °C. The flame ionization detector was maintained at a temperature of 250 °C with a data sampling rate of 200 Hz. 99.999% Hydrogen (Praxair, Edmonton, AB) was used as a carrier gas. The modulation period was set at 1.5 s with a flush time of 0.15 s. Wraparound determination experiments used a modulation period of 1.6 s.

For all experiments raw data files were exported from Chemstation (Agilent) as text files and then converted using a custom script written in MATLAB 7.10.0 (The Mathworks, Natick, MA) into a format that was then imported into ChromaTOF 4.33 (Leco Corporation, St. Joseph, MI) for GC×GC data processing.

5.2.1 Constant Pressure Experiments

The primary column for constant pressure experiments was an HP-5 (15 m × 0.1 mm × 0.1 μm) (5% phenyl substituted polydimethylsiloxane). The secondary column was a Supelcowax (3 m × 0.25 mm × 0.25 μm) (polyethylene glycol) purchased from Supelco (Oakville, ON). All separations were performed under constant pressure conditions to simplify the modeling of the separation. The

inlet pressure was set at 43 psi (gauge) and the modulator pressure was set at 11.6 psi (gauge). These pressures were selected to provide a flow rate of 0.6 $mL \cdot min^{-1}$ in the primary column and 20 $mL \cdot min^{-1}$ in the secondary column at the initial temperature of 50 °C. The separations were initiated at 50 °C, and temperature programmed at ramp rates of 3, 8, and 15 $°C \cdot min^{-1}$ to 200 °C, with a hold time of 1 min at the beginning and end of the run. A more complicated ramp program consisting of 50 °C (1 min hold) followed by a 15 $°C \cdot min^{-1}$ ramp to 90 °C (4 min hold) and an 8 $°C \cdot min^{-1}$ ramp to a final temperature of 200 °C was also used.

A single standard mixture comprised of alkanes, alcohols and ketones was used in all experiments. Undecane, dodecane, tridecane, tetradecane, pentadecane, hexadecane, and heptadecane (Sigma-Aldrich, Oakville, ON) were used as alkane standards. 2-Undecanone, 2-dodecanone, and 2-tridecanone (Alfa-Aesar, Ward Hill, MA) were selected as ketone standards. Finally the alcohol standards included were 1-undecanol, 1-dodecanol, and 1-tridecanol (Sigma-Aldrich). All standard compounds were 1000 ppm in toluene (Sigma-Aldrich). Methane (Praxair, Edmonton Alberta) was used as a dead time marker for the columns.

5.2.3 Constant Flow Experiments

Constant flow experiments used the same instrumentation settings; however the primary column used was a Supelco SLB5ms (15 m × 0.1 mm × 0.1 μm). The second dimension column was a Supelco IL-61 (1,12-di(tripropylphosphonium)dodecane-bis(trifluoromethylsulfonyl)imide trifluoromethylsulfonate) (3 m × 0.25 mm i.d. × 0.25 μm) column. A flow of 0.6

$mL \cdot min^{-1}$ in the primary dimension and 20 $mL \cdot min^{-1}$ in the secondary dimension was set throughout the run. Separations were initiated at 50 °C, with temperature programmed ramp rates of 3, 8, and 15 $°C \cdot min^{-1}$ to 200 °C, with a hold time of 1 min at the beginning and end of the run.

The standards used were, ethylbenzene, propylbenzene, butylbenzene, naphthalene, 2-methylnaphthalene, 1-methylnaphthalene, 2-ethylnaphthalene, 1-ethylnaphthalene, anthracene, 2-methylanthracene, 9-methylanthracene, 2-ethylanthracene, which were obtained from Sigma Aldrich (Sigma-Aldrich, Oakville, Ontario). Additional standards of 1-propylnaphthalene, 2-propylnaphthalene, 2-butylnaphthalene, 1-methylanthracene, 2,7-dimethylanthracene, 1,3-dimethylanthracene, 1,4-dimethylanthracene, 1,5-dimethylanthracene, 2,3-dimethylanthracene, 1,2-dimethylanthracene were obtained from Chiron (Trondheim, Norway). Standards were prepared at a concentration of 100 ppm.

5.2.4 Temperature-programmed Thermodynamic Experiments

Standards for the temperature programmed thermodynamic studies were the same as in the earlier constant pressure studies (alkanes, ketones, alcohols). A Supelco SLB5ms (15 m × 0.1 mm; 0.1 μm) was again used in the primary dimension and a Supelcowax (3 m × 0.25 mm; 0.25 μm) column in the second dimension. All separations were performed under constant-flow conditions. In GC×GC, flows of 0.6 $mL \cdot min^{-1}$ and 21.3 mL $mL \cdot min^{-1}$ were set for the primary and secondary columns, respectively. The separations were initialized at 30 °C,

with the oven temperature programmed at ramp rates of 3, 5, 8, 10, 12, 16, and 20 °C·min^{-1} to 230 °C, with a hold time of one minute at the beginning and end of the run.

5.2.5 Thermally Modulated

The experimentation for this set of experiments was carried out at Universidade Federal do Rio de Janeiro, Brazil. An Agilent 6890 GC with a Leco GC×GC dual-jet cryogenic modulator was used. The modulator temperature was +45 °C offset from the oven temperature. Helium was used as a carrier gas, and the inlet was a split/splitless injector set at 280 °C with a split ratio of 10:1. The detector was a TOFMS in EI mode at 70 eV and 230 °C with a data collection rate of 50 Hz. The transfer line was held at 280 °C. Injections were performed using pulsed pressure (50 psi, for 45 s). The temperature program initialized at 140 °C with a 0.2 min hold, the temperature ramped at 40 °C·min^{-1} to 180 °C, the ramp then decreased to 3 °C·min^{-1} to a temperature of 280 °C. The secondary column oven was offset by +20 °C for the entire run. An Agilent Ultra-1 100% dimethylpolysiloxane (17 m × 0.20 mm × 0.11 μm) column was used in the primary dimension and an OV1701 (14%) Cyanopropylphenyl (86%) dimethylpolysiloxane (1 m × 0.11 mm × 0.1 μm) column was used in the secondary dimension. A (0.5 m × 0.25 mm) deactivated fused silica capillary was used as a transfer line at the end of the second dimension column. Pressures were determined directly from the Agilent software used for the instrument.

5.3 Results

When evaluating the accuracy of retention times in GC×GC, the secondary dimension retention time ${}^{2}t_r$ must first be accurately determined before the determination of the first dimension retention time ${}^{1}t_r$. This is due to the potential for analytes in the second dimension to "wrap-around" the secondary dimension separation space. For example, if an analyte takes longer than the modulation period to traverse the second dimension column, it will have an apparent ${}^{1}t_r$ that is longer than the true ${}^{1}t_r$ time as the secondary retention time in the chromatogram remains fixed to the length of the modulation period, thus displaying a later apparent ${}^{1}t_r$. The predictive model however calculates only the absolute retention times for both ${}^{1}t_r$ and ${}^{2}t_r$. Consequently, the predicted ${}^{1}t_r$ must be increased, and the predicted ${}^{2}t_r$ must be decreased to match with the predicted values. As an example, with a modulation period of 1.5 s and a predicted ${}^{2}t_r$ of 13.86 s, the peak would be plotted 13.86 ÷ 1.5 = 9.24 modulation periods after injection. Thus the predicted ${}^{1}t_r$ would be increased by 9 × 1.5 s = 13.5 s, and the predicted ${}^{2}t_r$ would be 0.24 × 1.5 s = 0.36 s. Alternately, one could calculate the unwrapped experimental retention coordinates of peaks that had wrapped around by following a similar process in reverse, if the number of times that a peak has wrapped around is known. This would provide a peak table with true values for the retention coordinates of the peaks.

In order to determine the number of times that an analyte had wrapped around under experimental conditions, the method developed by Micyus et al. was used.[111] In this method, the experiment is performed twice with the modulation

period changed slightly in the two analyses (in this case, Run 1 was 1.5 s and Run 2 was 1.6 s). Peaks that do not wrap around will not experience a shift in ^2t_r between the two runs. Peaks that do wrap around will experience a shift in ^2t_r that corresponds to the number of times that they have wrapped around. In our case, the difference between modulation periods was 0.1 s. Thus, analytes which wrapped around once would have ^2t_r values 0.1 s shorter in Run 2 than in Run 1, those which wrapped around twice would have ^2t_r values 0.2 s shorter in Run 2 than in Run 1, etc.

5.3.1 Constant Pressure Results

The first GC×GC predictions made within this research were performed in constant pressure mode. This was done to ensure a simplified set of conditions with which to investigate if isothermally collected thermodynamics could be used to make predictions in GC×GC. In this set of experiments the primary column was of a different manufacture than the original column; the original column used to collect thermodynamic information was a Supelco-5ms, and the column in the GC×GC was a HP-5 (Agilent). It was assumed that the phase (5% phenyl substituted dimethylpolysiloxane) should be chemically similar in both cases. For the secondary column a section of the original wax column that thermodynamic data were collected on was used. Although several GC×GC systems were available on which to study thermodynamics, a GC×GC equipped with a pneumatic modulator was chosen. This modulator has two distinct chromatographic zones, unlike thermal-based modulators which create a complex zone of chromatographic behaviour at the end of the primary dimension that

would be more difficult to model.

The retention times in GC×GC mode were predicted for all compounds using the nominal column dimensions provided by the manufacturer. There were slight, predictable biases observed between the predicted and measured retention times. These were attributed to slight differences between the nominal and actual inner diameters, and stationary phase film thicknesses in the columns. At this stage in the research, the previously discussed calibration methods had not been investigated. As such the inner diameter and stationary phase thickness were estimated using undecane and undecanol as marker compounds. Using the 8 °C·min^{-1} experimental results, the column inner diameter was adjusted while keeping film thickness constant until the predicted ${}^{1}t_{r}$ for undecane matched closely with its actual ${}^{1}t_{r}$. Undecane was chosen as a probe as it was the least retained analyte in the sample and was assumed that most of the discrepancy in retention was due to differences in the column flow. Next the stationary film thickness was adjusted while keeping column diameter constant until the predicted ${}^{1}t_{r}$ for undecanol was in line with experimentation. Undecanol was chosen as the film thickness probe as being a more retained species in the test mixture the interaction it was assumed the stationary phase film thickness would contribute more to the difference in retention than column flow. The procedure was then repeated for the second-dimension column. The estimated values for the primary and secondary column diameters and film thicknesses were 95 μm and 0.1 μm and 265 μm and 0.258 μm, respectively. All other analyte retention times were then predicted using these estimated column dimensions. This internal

calibration made the assumption that the probe was affected only by either the column inner diameter or film thickness which is not accurate. While this was a very rudimentary method it was rapid and was able to correct for much of the systematic bias that was observed. The use of this method was however subjective as it depended on the user manually adjusting the column inner diameter and film thickness in an attempt to minimize the error between experimental and predicted retention of the probe molecule. This was a time consuming process as the entire method was applied through trial and error.

Comparisons of prediction accuracy were performed on the basis of these true, "unwrapped" ${}^{2}t_r$ values (Table 5.1). Figures 5.1, 5.2 and 5.3 depict the predicted peak apexes overlaid on the collected chromatograms for the 3, 8, and 15 °C·min^{-1} temperature ramps. The predicted values for all three temperature ramp profiles show a high level of agreement with the experimental values for ${}^{1}t_r$. Although the difference between predicted and experimental values appears to be greater in the 3 °C·min^{-1} run, given the length of the separation the relative percent error between predicted and actual values is comparable with the other two temperature programs, with the maximum relative percent error for any temperature ramp being 0.83%. The average error for ${}^{1}t_r$ across all compounds tested was only 0.64%. The accuracy of the model for ${}^{2}t_r$ predictions was on

Table 5.1. Experimental values for primary and secondary retention times for constant pressure separations, along with the thermodynamically predicted values for each temperature program.

Ramp Rate	Compound	Primary Retention Time (min)	Estimated Retention Time (min)	Difference (s)	Secondary Retention Time (s)	Estimated Retention Time (s)	Difference (s)
15 °C·min^{-1}	Undecane	5.000	4.923	4.6	0.8	0.9	0.0
	Dodecane	6.050	6.007	2.6	0.9	0.9	0.0
	Tridecane	7.075	7.018	3.4	0.9	1.0	0.0
	Tetradecane	8.025	7.970	3.3	1.0	1.0	0.0
	Undecanol	7.775	7.770	0.3	3.0	3.1	0.1
	Dodecanol	8.700	8.696	0.2	2.8	2.9	0.1
	Tridecanol	9.600	9.570	1.8	2.6	2.7	0.0
	Undecanone	7.025	6.936	5.3	1.8	1.9	0.1
	Dodecanone	8.000	7.905	5.7	1.8	1.9	0.1
	Tridecanone	8.900	8.818	4.9	1.8	1.9	0.0
8 °C·min^{-1}	Undecane	6.500	6.458	2.5	1.0	1.0	0.1
	Dodecane	8.350	8.353	0.2	1.0	1.1	0.0
	Tridecane	10.150	10.167	1.0	1.1	1.1	0.0
	Tetradecane	11.875	11.892	1.0	1.1	1.2	0.0
	Undecanol	11.425	11.482	3.4	5.4	5.4	0.0
	Dodecanol	13.100	13.167	4.0	5.0	5.0	0.0
	Tridecanol	14.700	14.764	3.8	4.7	4.5	0.2
	Undecanone	10.050	10.005	2.7	2.8	2.9	0.1
	Dodecanone	11.800	11.761	2.4	2.8	2.9	0.0
	Tridecanone	13.450	13.423	1.6	2.8	2.9	0.1
3 °C·min^{-1}	Undecane	9.550	9.563	0.8	1.2	1.3	0.0
	Dodecane	13.675	13.890	12.9	1.4	1.4	0.0
	Tridecane	18.050	18.317	16.0	1.5	1.6	0.0
	Tetradecane	22.400	22.662	15.7	1.6	1.7	0.0
	Undecanol	21.300	21.472	10.3	13.9	13.7	0.2
	Dodecanol	25.550	25.754	12.2	12.6	12.5	0.2
	Tridecanol	29.625	29.854	13.7	11.6	11.0	0.6
	Undecanone	17.775	17.871	5.7	5.9	5.9	0.0
	Dodecanone	22.175	22.285	6.6	5.8	5.9	0.1
	Tridecanone	26.400	26.527	7.6	5.8	5.8	0.0

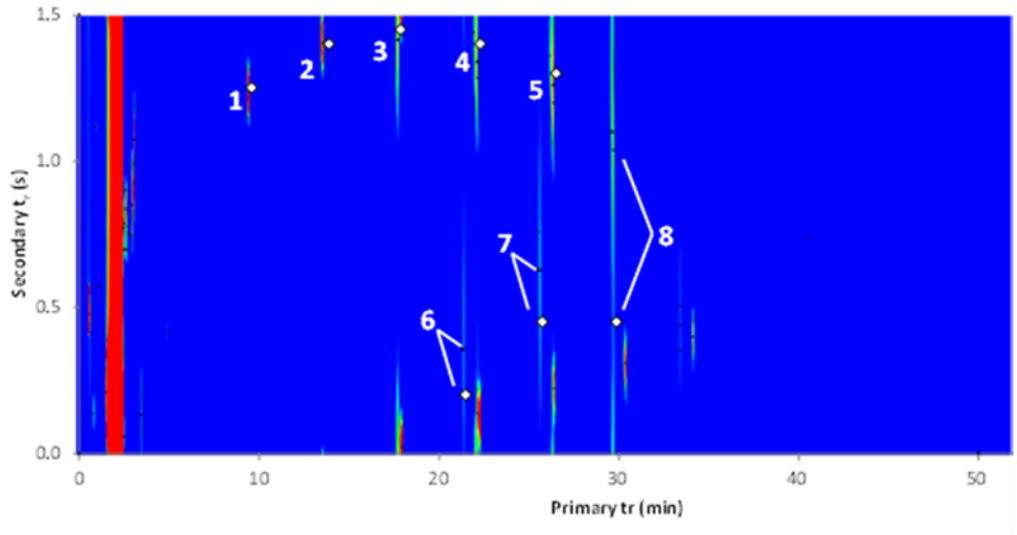

Figure 5.1 Chromatogram of 3 °C•min^{-1} temperature ramp white squares depict predicted peak apex. 1-4 undecane, dodecane, tridecane, tetradecane. 5 tridecanone. 6-8 undecanol, dodecanol, tridecanol (note undecanone and dodecanone not shown due to visual limitation imposed by chromatogram)

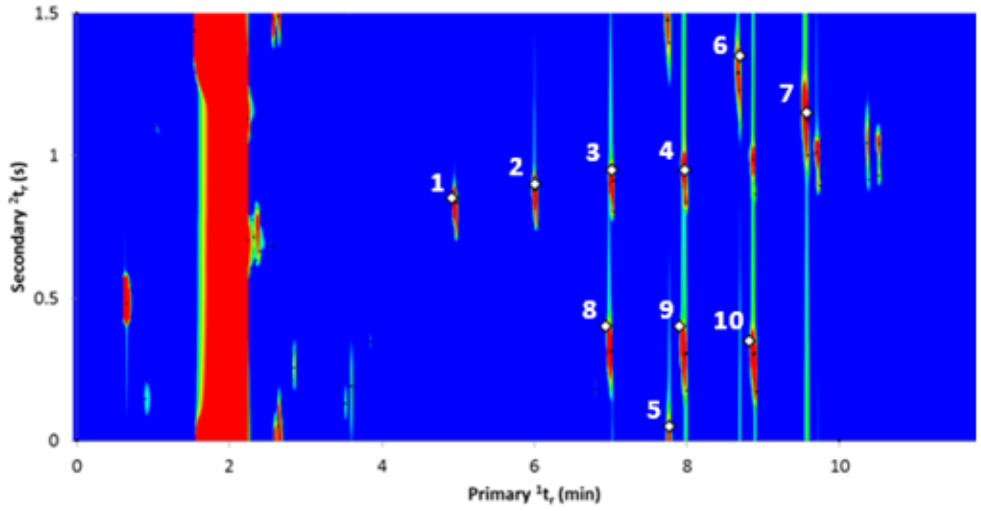

Figure 5.2 Chromatogram of 8 °C·min^{-1} temperature ramp white squares depict predicted peak apex. 1-4 undecane, dodecane, tridecane, tetradecane. 5-7 undecanol, dodecanol, tridecanol. 8-10 undecanone, dodecanone, tridecanone.

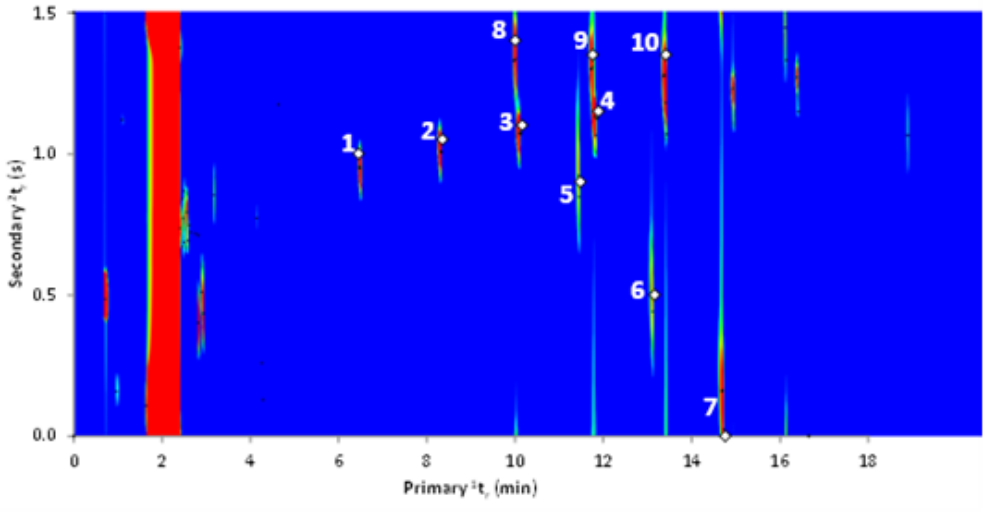

Figure 5.3 Chromatogram of 15 °C·min^{-1} temperature ramp white squares depict predicted peak apex. 1-4 undecane, dodecane, tridecane, tetradecane. 5-7 undecanol, dodecanol, tridecanol. 8-10 undecanone, dodecanone, tridecanone.

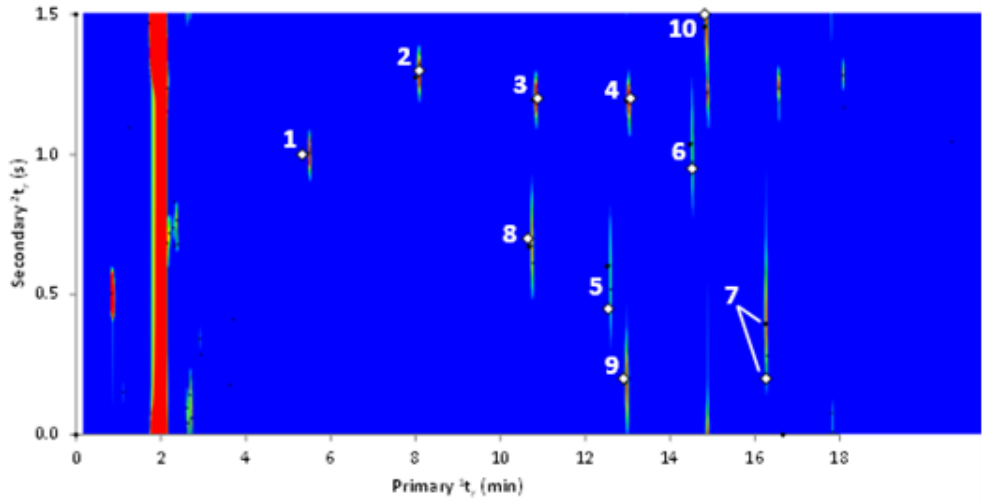

Figure 5.4 Chromatogram of a two-step temperature ramp 15 °C·min^{-1} followed by 8 °C·min^{-1} white squares depict predicted peak apex. 1-4 undecane, dodecane, tridecane, tetradecane. 5-7 undecanol, dodecanol, tridecanol. 8-10 undecanone, dodecanone, tridecanone.

average 2.22% across all compounds. This equates to an average error of 5.2 s in the primary dimension and 0.07 s in the second dimension. Apparent within the data is the fact that the calibration method used, created bias within the predictions. Analytes that were closer to the probe had smaller errors in the predicted retention times, with molecules that fell farthest from the probes having the highest error. The error in the prediction of K based on the errors in the regression used to determine the thermodynamic parameters was propagated through to the prediction of the retention times. This was achieved by estimating the %RSD for both ${}^{1}K$ and ${}^{2}K$. Then, to estimate the worst-case scenario, the calculation of retention coordinates was performed using ${}^{1}K + {}^{1}\sigma$ and ${}^{2}K - {}^{2}\sigma$ or vice versa. In this way, the errors were both forcing ${}^{2}t_r$ in the same direction.

For example, if ${}^{1}K$ was increased slightly, this would increase ${}^{1}t_r$ and increase the elution temperature, decreasing ${}^{2}t_r$. Thus, decreasing ${}^{2}K$ simultaneously would magnify the error in this dimension. Even with this worst-case scenario, the predicted error was found to be negligible in comparison to the absolute error between predicted and actual values (typical errors in ${}^{1}t_r$ were ~1–2 s and ~50 ms for ${}^{2}t_r$ (the time increment used in the model)). As a test of the robustness of the model, a more complicated ramp profile was used to separate the test mixture. This program contained two different linear ramps with an isothermal hold between them. As can be seen from Figure 5.4, even with the complicated ramp the thermodynamic-based predictions were in excellent agreement with the experimental results with an average relative error of 0.61% for ${}^{1}t_r$ and 1.38% for ${}^{2}t_r$. This study provided the initial proof that the

thermodynamic models used for traditional one dimensional GC could provide acceptable predictions in GC×GC. It also highlighted the need for the calibration methods developed in Chapter 4 to properly translate the thermodynamic data from column-to-column. Furthermore, it demonstrated that with calibration, columns of differing geometries could be used without recalculating the thermodynamic parameters for each analyte.

5.3.2 Constant Flow Predictions

Although the previous experiment was a success, the separation was carried out using constant pressure to simplify the equations used in the predictions. Using constant flow conditions is non-ideal in a GC separation as due to the increase in carrier gas viscosity with temperature, the column flow slows down resulting in broad peaks and poor chromatographic resolution. The model was therefore expanded upon to predict separations that use a constant flow of carrier gas. In constant flow mode the inlet pressure and modulator pressures increase with temperature to maintain a constant flow of carrier gas through the column. To account for this change, both the inlet and modulator pressure must be calculated as a function of time. Equation 5.1 is used to obtain the ratio of inlet/modulator, or modulator/outlet pressures *P*. In the case of the first dimension, P_o would be the modulator pressure, rather than outlet pressure.

$$u_o = \frac{{d_c}^2}{32}\frac{P^2-1}{2\eta L}P_o \qquad (5.1)$$

By accounting for the changing pressures in the inlet and modulator it is possible to model constant flow conditions in GC×GC. To test the constant flow

model, isothermal thermodynamic data for a series of 23 polyaromatic hydrocarbons collected via the automated method discussed in Chapter 2 were used in conjunction with GC×GC. This data were first adjusted for use with manual injections as per the methods described in Chapter 2. All analytes had their thermodynamic parameters estimated previously on the two columns used in the separation using the nominal dimensions for each column. After which the data were used to predict GC×GC retention times for a constant flow separation. The separation conditions were otherwise kept identical to those used in the previous constant pressure experiments. Given the success of the isothermal calibration method discussed in Chapter 4, the method was applied to calibrate the inner diameter and film thickness for both the primary and secondary columns. Since resources were not available to study the column set used in the GC×GC experiment via SEM, the nominal method was used instead. To calibrate the dimensions of the column set, 2-methylanthracene was chosen as a probe. The 2-methylanthracene was injected with gaseous methane to determine 2-Methylanthracene's retention factor k on both the primary and secondary columns. The separation was carried out isothermally at 200°C which was chosen to provide suitable retention. As discussed to predict retention accurately the exact length, inner diameter, and film thickness of the columns must be known. In the case of the primary column the exact length was unknown and so was estimated using a measurement of the circumference of the column cage and the number of coils around the cage. This method provides a decent measure for length (±10 cm) so the column inner diameter could be estimated via flow

calculations. In the second dimension the length of the column was known so it was possible to determine the column inner diameter using flow calculations and the void time. The retention time of methane was used along with HP Flowcalc software to estimate the inner diameters of both the primary and secondary dimension columns. This was the first instance within this GC×GC research of methane's retention in the primary and secondary dimension being used to calibrate the internal diameter. The retention time of methane and 2-methylanthracene were then used to determine k. The previously determined isothermal thermodynamics for 2-methylanthracene were then used along with the determined k to determine β. Using the estimated value of β and the estimated inner diameter it is then possible to solve for the film thickness. 2-methylanthracene was chosen as the probe due to it being situated in the middle of the separation plane which was assumed would provide an average value for the film thickness experienced by all analytes in the sample for both the primary and secondary dimensions. The estimated length, column diameter and film thickness were then used along with the estimated thermodynamics for the remaining 22 PAHs to predict the first and second dimension retention times. Table 5.2 compares the experimental and predicted retention times for the 8°C·min^{-1} temperature ramp (additional ramps in Appendix A). Figure 5.5 shows a peak apex plot for the predicted and experimental values of the PAHs in the 8 °C·min^{-1} separation. This method provided a novel way in which a single probe, used in a single isothermal run could be used to calibrate the inner diameter and film thickness of both columns simultaneously. Despite the relatively high success of

the method, bias is present and the errors between the predicted and experimental retention times increase

Table 5.2 Experimental values for primary and secondary retention times for 8°C·min^{-1} constant flow separation, along with the thermodynamically predicted values for each temperature program.

Compound	Primary Retention Time (min)	Estimated Retention Time (min)	Difference (s)	Secondary Retention Time (s)	Estimated Retention Time (s)	Difference (s)
ethylbenzene	2.747	2.440	18.4	1.2	1.3	-0.1
propylbenzene	3.920	3.705	12.9	1.3	1.4	-0.1
butylbenzene	5.547	5.403	8.6	1.3	1.4	-0.1
naphthylene	7.683	7.700	-1.0	4.0	4.1	-0.1
2-methylnaphthylene	9.577	9.610	-2.0	3.7	3.6	0.0
1-methylnaphthylene	9.843	9.905	-3.7	3.5	3.5	0.0
2-ethylnaphthylene	11.202	11.223	-1.3	3.0	3.0	0.0
1-ethylnaphthylene	11.255	11.250	0.3	2.8	2.9	-0.1
1-propylnaphthylene	12.642	12.610	1.9	2.5	2.6	-0.1
2-propylnaphthylene	12.668	12.702	-2.0	2.6	2.6	0.0
2-butylnaphthylene	14.268	14.312	-2.6	2.3	2.3	0.0
anthracene	16.807	16.982	-10.5	6.2	6.0	0.2
2-methylanthracene	18.352	18.448	-5.8	5.6	5.5	0.1
1-methylanthracene	18.512	18.632	-7.2	5.2	5.1	0.1
9-methylanthracene	18.938	19.082	-8.6	5.3	5.2	0.1
2-ethylanthracene	19.605	19.775	-10.2	4.6	4.6	0.0
2,7-dimethylanthracene	19.765	19.920	-9.3	5.1	5.1	0.0
1,3-dimethylanthracene	19.872	19.998	-7.6	4.7	4.8	-0.1
1,4-dimethylanthracene	20.030	20.143	-6.8	4.4	4.4	0.0
1,5-dimethylanthracene	20.057	20.167	-6.6	4.5	4.5	0.0
2,3-dimethylanthracene	20.298	20.435	-8.2	5.4	5.5	-0.1
1,2-dimethylanthracene	20.352	20.457	-6.3	4.9	5.1	-0.2

away from the probe. This is contrary to what was previously seen when using two probes where the error was largest in the center of the separation plane and minimal near the extremes where the probe molecules were located.

The practice of using methane as a means to calibrate column inner diameter was established as a viable option from this set of experiments. This practice was incorporated into the nonlinear calibration method discussed in Chapter 4. Despite the lack of a direct comparison the use of a single probe in the middle of the run was able to provide comparable results to the previous two probe approach.

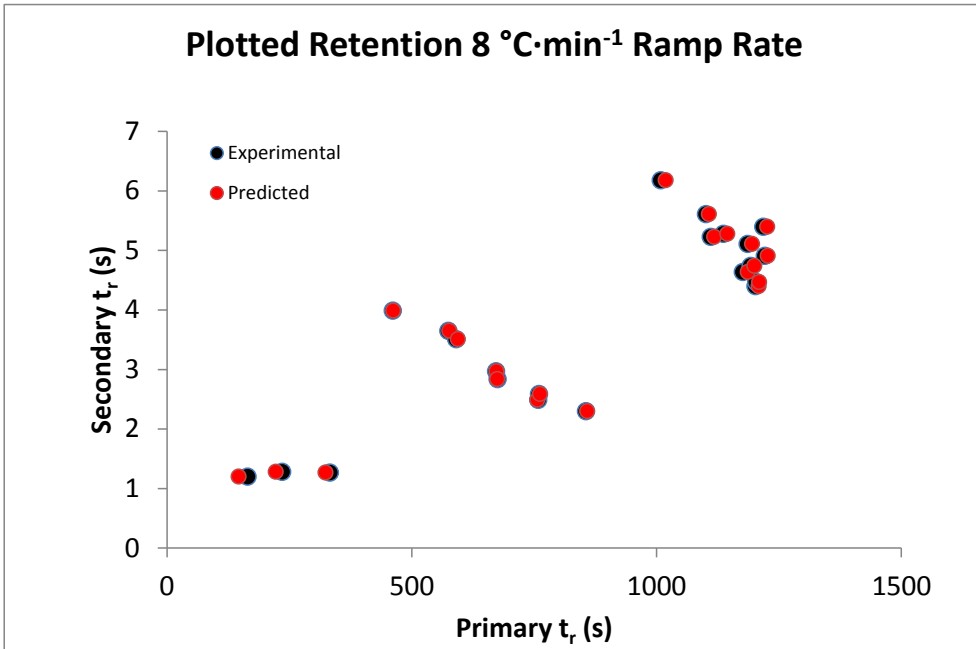

Figure 5.3 Peak apex plot showing experimental and predicted separation of 22 PAHs using constant flow conditions at 8°C·min^{-1}.

One can argue that it was able to provide more accurate predictions as a much larger separation space was predicted in the case of the PAH study over the smaller separation space predicted in the original alkane, ketone, alcohol investigation. The single probe approach use in this method was however far more

subjective as it did not require trial and error methods in the determination of column inner diameter and stationary phase film thickness.

5.4.3 Temperature Programmed Thermodynamics in GC×GC

After the development of the rapid thermodynamic collection method described in Chapter 3, it was necessary to investigate the validity of applying temperature-programmed thermodynamic data to GC×GC separations. Before predictions were made the exact column length was measured, and methane was used as a void time marker to estimate for the average column inner diameter. Three isothermal separations carried out at 50, 100, and 150 °C were used to estimate the column inner diameter. A custom script was written that employed the Poiseuille equation to calculate the average column inner diameter for both the primary and secondary dimension. In these separations the average film thickness of each column was estimated as in the previous constant flow experiment, i.e. undecanol acted as the probe molecule used to determine β. The column inner dimensions for the primary and secondary columns were 102.5 µm and 262.5 µm respectively. The film thicknesses for the primary and secondary columns were 0.101 µm and 0.290 µm. To compare the predicted and experimentally determined second-dimension retention times the wraparound of the analytes eluting from the second-dimension column were again determined using the method developed by Micyus et al.[111]

Table 5.3 lists the experimental and predicted values for all compounds in both the primary and secondary dimensions across the three temperature ramps.

Table 5.3 Predicted and experimental retention times for primary and second dimension separations for three ramp rates and associated absolute error.

Temperature Ramp °C·min^{-1}	Compound	Primary Retention Time (min)	Estimated Retention Time (min)	Difference (s)	Secondary Retention Time (s)	Estimated Retention Time (s)	Difference (s)
3	Undecane	944	933	-10.3	1.0	1.0	0.0
	Dodecane	1220	1215	-4.3	1.0	1.0	0.0
	Tridecane	1487	1488	1.9	1.1	1.0	0.0
	Tetradecane	1740	1745	4.8	1.1	1.1	0.0
	Undecanone	1473	1467	-6.5	4.1	4.1	0.0
	Dodecanone	1730	1728	-1.4	4.0	3.9	-0.1
	Tridecanone	1973	1975	2.9	3.8	3.8	0.0
	Undecanol	1682	1678	-3.2	9.5	9.4	-0.1
	Dodecanol	1925	1929	4.8	8.6	8.4	-0.2
	Tridecanol	2157	2172	14.6	7.8	7.5	-0.3
	Tetradenol	2376	2394	18.5	7.2	6.9	-0.3
8	Undecane	543	537	-6.0	0.7	0.7	0.0
	Dodecane	653	649	-3.2	0.7	0.7	0.0
	Tridecane	756	756	0.0	0.7	0.7	0.0
	Tetradecane	855	856	0.9	0.7	0.7	0.0
	Undecanone	752	748	-3.5	1.9	1.9	0.0
	Dodecanone	851	850	-0.9	1.8	1.8	0.0
	Tridecanone	945	945	-0.1	1.8	1.8	0.0
	Undecanol	831	829	-1.7	3.6	3.6	0.0
	Dodecanol	926	926	0.7	3.3	3.3	0.0
	Tridecanol	1016	1019	4.0	3.0	3.0	0.0
	Tetradenol	1100	1106	6.1	2.9	2.8	-0.1
16	Undecane	369	365	-3.8	0.5	0.5	0.0
	Dodecane	426	423	-2.8	0.5	0.5	0.0
	Tridecane	480	478	-2.0	0.5	0.5	0.0
	Tetradecane	530	529	-0.5	0.5	0.6	0.0
	Undecanone	477	474	-2.8	1.1	1.1	0.0
	Dodecanone	528	526	-1.8	1.1	1.1	0.0
	Tridecanone	576	575	-1.2	1.0	1.1	0.0
	Undecanol	518	516	-2.0	1.8	1.8	0.1
	Dodecanol	566	565	-0.5	1.7	1.7	0.0
	Tridecanol	612	613	0.7	1.5	1.6	0.0
	Tetradecnol	654	657	2.6	1.5	1.5	0.0

The predicted ${}^{1}t_r$ retention times were in excellent agreement with the experimentally determined values with an average relative error of 0.37 %. The second-dimension average relative error in the prediction of ${}^{2}t_r$ was slightly higher at 2.09 %. The worst estimates for the predicted retention times in both ${}^{1}t_r$ and ${}^{2}t_r$ were found to be from the 3 °C·min^{-1}, however while the absolute error was the highest in these cases the relative error was in line with the predictions made for all other temperature ramps.

Figures 5.6 shows an example of the predicted peak apexes overlaid with the actual chromatogram and illustrates the high accuracy with which these predictions are made. The accuracy of the predictions is on par with those from data obtained from isothermal runs, with the previous constant pressure study having an average relative error in ${}^{1}t_r$ of 0.64 % and 2.22 % for ${}^{2}t_r$.

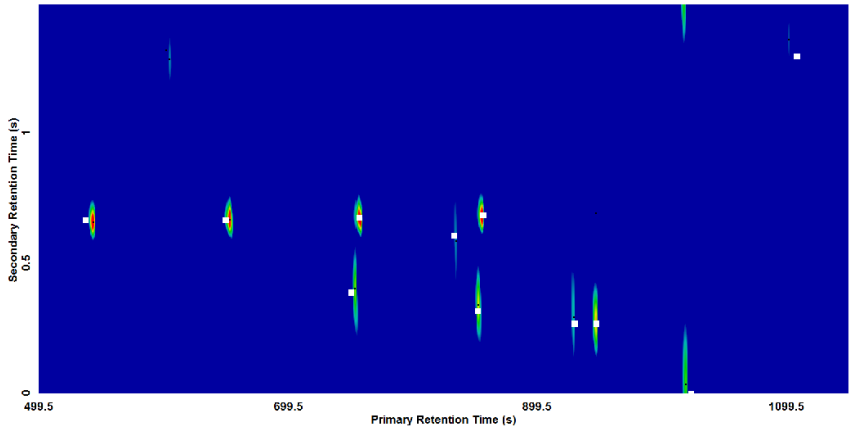

Figure 5.4 Chromatogram of 8°C·min^{-1} temperature ramp white squares depict predicted peak apex. 1-4 undecane, dodecane, tridecane, tetradecane. 5-7 undecanone, dodecanone, and tridecanone. 8-11 undecanol, dodecanol, tridecanol, and tetradecanol.

This equates to an average error of 3.6 s in the primary dimension and only 0.05 s in the second dimension. Again there is a slight bias present in the primary dimension as the distance from the β probe increases. Predictions made in the second dimension however have near perfect agreement and exhibit no bias.

5.3.3 Thermal Modulated GC×GC Predictions

As mentioned in the thesis introduction, thermally modulated GC×GC instrumentation is currently more popular in the field of multidimensional gas chromatography. The work presented here was a collaborative project where the only available instrumentation was a thermally modulated GC×GC. Thermodynamic parameters were collected for a set of O-TMS (trimethylsilated hydroxyl) and MO-TMS (methoxime-trimethylsilated) derivatized steroid standards using the methods outlined in Chapter 4. The data were collected on columns of the same phase and dimensions (excluding length) as the column set used in the GC×GC. The standards were then separated using the conditions listed above in the experimental section. Given the complexity of the sample, several assumptions were made to simplify the separation conditions. The first is that the pressure pulsed injection had zero impact on the separation. This assumption is reasonable as the initial temperature was low compared to the remainder of the separation and so, even with the pressure pulse the steroids will remain absorbed to the stationary phase at the head of the column until the initial temperature ramp commences. Another assumption was that the segment of transfer line column had no effect on the separation. This was due to the inability to calculate a pressure value at the head of the transfer line segment as the vacuum from the mass spec

extended past the inlet of this segment of column. This takes into account the fact that the linear velocity at that point in the column is nearly 500 $cm \cdot s^{-1}$, and with zero retention all analytes should traverse the length of the transfer line in less than 0.1 s. Finally any retention occurring in the modulator was ignored.

Initial predictions showed significant errors between the experimental and predicted values. The cause of this was a discrepancy in the length of the second dimension column, while the total column length was 100 cm only 87 cm of this length was present after the modulator. Thus the analytes would elute from the primary column and quickly transfer to the modulator box, effectively shortening the total column length. Once this length was accounted for the retention times for all analytes were then predicted using the same methods as previously discussed. The predicted and experimental times for O-TMS modified steroids are listed in Table 5.4, and MO-TMS modified results are shown in Table 5.5.

Primary dimension retention times show a high level of agreement between the experimental and predicted results. MO- modified androsterone and epitestosterone have significant deviations. The collaborative nature of the work means that at this time it is unclear as to whether these deviations were real or the result of a transcription error in either the retention times used to generate the thermodynamics or experimental retention times.

Table 5.4 Experimental and predicted $^{1}t_r$ and $^{2}t_r$ retention times for O-TMS derivatized steroids on a thermally modulated GC×GC.

O-TMS Modified Steriods	Experimental $^{1}t_r$ (min)	Predicted $^{1}t_r$ (min)	Error (s)	Experimental $^{2}t_r$ (s)	Predicted $^{2}t_r$ (s)	Error (s)
5α-Androstanediol	13.800	13.798	0.1	2.7	2.7	0.0
5β-Androstanediol	14.000	13.940	3.6	2.7	2.8	-0.1
Androsterone	13.400	13.392	0.5	2.7	2.8	-0.1
11-keto etiocholanolone	14.900	14.965	-3.9	2.7	2.3	0.4
11βOHAndrosterone	16.500	16.637	-8.2	2.7	2.8	-0.1
DHEA	14.900	14.873	1.6	2.9	3.0	-0.1
Testosterone	16.300	16.305	-0.3	3.1	3.3	-0.2
Methyltestosterone	18.100	18.202	-6.1	3.3	3.5	-0.2
Pregnanediol	18.600	18.686	-5.1	3.0	3.2	-0.1
Pregnanetriol	19.200	19.273	-4.4	2.9	3.1	-0.2
Pregnanolone	18.000	18.043	-2.6	3.0	3.1	-0.2

Table 5.5 Experimental and predicted $^{1}t_r$ and $^{2}t_r$ retention times for MO-TMS derivatized steroids on a thermally modulated GC×GC.

MO-TMS Modified Steriods	Experimental $^{1}t_r$ (min)	Predicted $^{1}t_r$ (min)	Error (s)	Experimental $^{2}t_r$ (s)	Predicted $^{2}t_r$ (s)	Error (s)
Androsterone	13.900	13.429	28.3	3.3	3.3	0.0
11-keto etiocholanolone	15.700	15.611	5.3	4.0	4.4	-0.4
11βOHAndrosterone	17.300	17.317	-1.0	3.3	3.2	0.1
DHEA	14.800	14.717	5.0	3.4	3.6	-0.2
EpiTestosterone	15.300	16.233	-56.0	3.6	3.4	0.1
Testosterone	16.200	16.361	-9.6	3.6	3.8	-0.2
Methyltestosterone	18.200	18.131	4.1	3.9	4.1	-0.2
Pregnanolone	17.600	17.588	0.7	3.4	3.6	-0.2

Given that the majority of compounds show a high level of agreement the latter is more likely. The predicted second-dimension retention times also show a high level of agreement with the experimentally determined values. However, it is apparent that all predicted retention times in the second dimension lag behind the experimental values. Unfortunately at this time it is unclear as to the origin of this discrepancy. It could be a result of the added segment of transfer line capillary, a

slight discrepancy in the flow of the system, or a discrepancy between the set and actual value of the secondary column oven. It is also hypothesised that this discrepancy could be the result of the hot jet on the modulator system causing the analyte to experience a higher temperature in the second column than would be expected. This would reduce the time the analyte is retained. Given that such discrepancies were not seen in the pneumatically modulated experiments, this may be the true cause. However, the significant differences between the two systems warrants further experimentation before the exact cause of the discrepancy can be determined. Despite the discrepancies in the second dimension this experiment demonstrates that thermodynamic models can be used in conjunction with thermally modulated systems to provide accurate predictions, albeit with some slight modifications to the calculations to account for the modulator.

5.4 Conclusions

The predictions in this chapter, while simplistic in terms of the sample mixtures used, highlight the ability to use thermodynamic data for the prediction of retention times. Both isothermally collected data and temperature programmed data accurately predicted both $^{1}t_r$ and $^{2}t_r$ for a range of separation conditions. Key to these predictions is the calibration of the column set dimensions to the dimensions of the column set used to generate the data. The work performed here lays the foundation for others to use these tools to in actual applications.

Chapter 6: Conclusions and Future Work

6.1 Conclusions

This work began with the sole intent of adapting the three parameter thermodynamic model previously singled out by our research group for use in the prediction of GC×GC separations. During the development of these GC×GC predictive models, techniques for the automation, rapid estimation, and inter-lab transfer of thermodynamic parameters were also created. Ultimately the focus of this work fell on increasing the accessibility of thermodynamic data for use in the prediction of gas chromatographic retention times. The goal of any predictive model is to reduce the experimentation necessary to obtain an ideal solution to a chromatographic problem. And while previous thermodynamic models provided superior accuracy when making predictions compared to traditional methods such as retention indices, this advantage was nullified by the extensive experimentation required to obtain the necessary data to make predictions. In a sense this work attempted to take the best aspects of thermodynamic based predictions and predictions based upon retention indices and combine them to create a system with the advantages of both.

As stated, the original goal of the thesis was to develop models for the prediction of GC×GC retention times. The experimentation required to obtain thermodynamic data to make these predictions was however extensive, and required constant operator supervision to complete. Without another method to collect the data the obvious solution was to implement the automation of the

technique so that while extensive experimentation was still required little operator input was necessary. The immediate advantage was that data could be collected 24 hours a day rather than the 8 – 10 hours with an operator, effectively tripling the output. Furthermore, outside of academia very few research labs have the resources to commit an individual to the sole purpose of data collection and so the creation of an automated system for thermodynamic data collection immediately increases the potential for such a system to be adapted. Automation in this case was achieved by solvating methane into the sample so that co-injection of methane was still possible when using an autosampler attachment. An alternative method was also used where a simple calibration curve was developed which related the retention of methane to that of the solvent peak on a particular column removing the need for methane to be solvated in the sample, while being far from revolutionary these two methods helped to increase the practicality of thermodynamic data collection. At the same time work was done to ensure that these new automated methods were both forwards and backwards compatible with the previous manual data collection methods. While initially there were discrepancies, again the simple application of a calibration curve allowed for the transfer of data between manually collected and autosampler collected thermodynamics. Although the automation of thermodynamic data collection was successful in increasing the throughput of thermodynamic data it did nothing to reduce the actual experimentation required to generate that data. It was at this point that it became apparent that in order to truly increase the applicability of thermodynamic methods an entirely new form of data collection was required.

The need for isothermal runs to determine thermodynamic parameters restricts the rate at which data can be collected. Analytes in the sample must have similar retention otherwise the separation becomes prohibitively long or analytes elute too rapidly which affects the determined thermodynamics. At the same time analytes that are closely retained often will co-elute at one or more points across the temperature range studied. In the development of a new thermodynamic data collection method, the simplest way to decrease the experimentation was to use a temperature programmed method which allowed for analytes with a wide range of partition coefficients to be examined within a single mixture. The ability to separate a wide range of compounds simultaneously meant that potentially hundreds of isothermal separations could be avoided, saving a considerable amount of time. While thermodynamic data collection had been previously demonstrated using temperature programmed separations, these experiments required the use of a two parameter thermodynamic model which had been shown to be less accurate than three parameter models. A new method was created to determine thermodynamic parameters for a three parameter model using temperature programmed separations. Due to the three parameter model being non-linear an unconstrained non-linear optimization method was used to solve $\Delta S(T_0)$, $\Delta H(T_0)$, and ΔC_P for each analyte. The method requires retention times from only three temperature programmed separations to find a solution through the use of the Nelder-Mead simplex, dramatically reducing the experimentation required to obtain accurate thermodynamic values. As well the method demonstrated the successful simultaneous collection of thermodynamic

parameters from a set of analytes which would have been otherwise impossible using isothermal methods. The thermodynamic parameters determined using this method fell close to those obtained using the previous isothermal method. However given the huge reduction in experimental time using the new temperature programmed method and the accuracy of the predictions made using data generated from the method, it is the opinion of the author that it is unlikely that the isothermal method will be used in the future. The temperature programmed method also provides the advantage of not requiring the void time of the column and should also account for intersystem variance which the isothermal method is unable to do, again showing a clear advantage to the new method's adoption. Prior to the creation of the temperature programmed method of data collection thermodynamic predictive models had little hope of competing against already established LRI predictive models. The time requirement was simply to vast to warrant its use. Now however with vastly reduced experimental requirements thermodynamic methods are near equal to LRI in the experimentation required to collect data, and are superior in their predictive abilities. Furthermore thermodynamic methods are to date the forerunner in GC×GC predictive models in terms of practicality and accuracy of predictions.

The nonlinear optimization method also allowed for the development of a new method that allows for the calibration of the column stationary phase film thickness through the use of a Grob standard mixture. This along with the development of a standardized method for determining the column length and inner diameter has allowed for a simple and universal way for individual

laboratories to calibrate a column for use with existing thermodynamic libraries. Besides the new rapid collection method this is one of the most important tools developed during this research. Without a proper method to standardize thermodynamic information between columns the creation of a large library of compounds would be impossible, not to mention irrelevant as it would only be useful on a singular column. This method demonstrated that thermodynamic parameters collected on one column could be used to accurately predict retention times on any column regardless of dimension or stationary phase condition so long as the phase chemistry remained the same. As well the research demonstrated that thermodynamic information collected in one laboratory could be used to accurately predict retention times in another so long as the column was calibrated using the methods developed here. Unfortunately at this time biases are still found in the predicted retention times and so further work is required to account for these errors. Providing evidence of intra and inter lab transfer of data has helped to further validate the use of thermodynamics for use in gas chromatographic retention time predictions. While validation of these methods is still ongoing, the work done here provides promising initial evidence for the success of the method.

The significant developments presented above are an indirect result of models developed to predict retention times in GC×GC. Without the high success of these predictive models the nonlinear optimization method would not be accurate or consistent in its determining of thermodynamic parameters. The work here has demonstrated the use of this predictive model in both GC and GC×GC

for a variety of column and flow conditions. A key lesson learnt from making these predictions is that the calibration of the column set is critical to the accuracy of any prediction made, this discovery lead to the extensive work to develop a standardized calibration method for use in GC and GC×GC. Thermodynamics present an ideal tool for predicting GC×GC separations as they lack the limitations and difficulties associated with retention index methods. There is no need for retention markers of any kind and so predictions can be made quickly and accurately for any stationary phase where thermodynamic information has been previously collected.

Before this research thermodynamic predictive models, while more accurate than other models in their predictions, were likely to remain within the realm of academic curiosity. The extensive experimentation required for accurate thermodynamic values meant that only a handful of molecules could be investigated which limited the applicability of the method for predictive research. For thermodynamics to replace LRI as the go to method for predictive models it needs to meet two criteria; first it must be more accurate in its predictions and secondly it must have an equal or greater amount of compound information available. While the first criteria was already established using a three parameter model, by creating a new method that enables the rapid collection of the relevant thermodynamic parameters the second criteria has a chance to be fulfilled. Whether or not this will occur is yet to be seen. However demonstrating to the academic community that thermodynamic data can be rapidly acquired and accurately transferred between labs is the first step. The ability to use

thermodynamics to obtain accurate GC×GC predictions provides a concrete reason for such a model to exist as to date no other model has been able to match its accuracy.

6.2 Future Projects

While many improvements have been made to both the collection and use of thermodynamics for GC predictions much work still remains to be done. First and foremost is the finishing of the inter-lab validation of the new thermodynamic collection and calibration methods. Due to time constraints and the nature of collaborative projects this work was unable to be completed in full at the time of this thesis. However, final thermodynamic values across every column are required from all labs for the 91 compounds used in the study. Only then can proper calculations for the precision of the determined thermodynamics and accuracy of cross lab retention time predictions be made. The increase in the average error across all predictions made in the inter-lab study suggests that there may be an as of yet undetermined factor that effects the model. The bias present in the preliminary data points to the current method for determining β as the problem. Upon completion of the round robin study work should be conducted to investigate if a new method can be implemented to determine β thus improving the accuracy. It has been suggested already that perhaps a different simplex algorithm may function better than the Nelder-Mead simplex for use in the nonlinear optimization, which would help to correct for the bias observed near the edges of the separation space. Another aspect that should be investigated through the continued use of the round robin data is both how many iterations are required

within the simplex to generate accurate and reproducible thermodynamic values and can the leave-one-out methodology be replaced with the entire data set to estimate the thermodynamic parameters. Currently these calculations are computationally intensive and the reduction of iterations and leave-one-out methodology could save a significant amount of time.

Secondly, the current calibration method which uses non-linear fitting and the Grob standard mixture should be expanded for use in GC×GC. Currently the model does not allow for the solving of the second dimension film thickness as each analyte experiences a different set of instrument conditions, the adaptation of the code to support this is a significant amount of work. However the benefit of increased accuracy in the film thickness of the second dimension is important enough to warrant it.

Several other projects should also be attempted. First preliminary work not discussed in this thesis showed that it is possible to gather thermodynamic parameters from GC×GC separations. The advantage of this is that potentially thousands of compounds could be investigated on two phases simultaneously, or at the very least the resolving power of GC×GC separations could allow for an increase in the thermodynamics collected from the first dimension separation. This was not included at this time due to a lack of research into whether the collected thermodynamics were reproducible and able to make accurate predictions. Another project that was not discussed in this thesis is the adaptation of the temperature programmed thermodynamic method in conjunction with a QSRR model. This model was able to take the thermodynamic parameters from

the method described in Chapter 3 and use that data along with calculated descriptors consisting of constitutional, topological, electronic, thermodynamic, and geometric descriptors to link class specific structures to the thermodynamic parameters of $\Delta S(T_0)$, $\Delta H(T_0)$, and ΔC_P. These were then used to predict the retention times of 39 molecules that had their thermodynamic parameters estimated via the above method. The results showed high accuracy in the RMSEP, and so further work into the use of QSRR and thermodynamic modelling of retention times should be conducted.

Finally significant work should be devoted to the study of thermodynamic predictions with the use of thermal modulators. The collaborative work in this thesis that used thermal modulation provided a proof of concept for thermodynamics with non-pneumatic modulation. However the project did not allow for the tight controlling of factors that would allow for the specific identification of problems. Work should be performed that investigates the various parameters associated with thermal modulators i.e. jet temperature, secondary oven temperature, modulation period, and transfer line temperature to ensure the changing of these factors does not alter the success of predictions made. Given the widespread use of thermal modulators the study of these factors may be one of the more important aspects in increasing the applicability of thermodynamic methods in modern GC×GC.

Bibliography

[1] M. Tsvet. Ber Deutsch Bot Ges. 24 (1906) 316

[2] A.T. James, A.J.P. Martin. *Analyst.* 77 (1952) 921 p.915

[3] S.T. Teng, A.D. Williams, K. Urdal. *J. High Resol. Chromatogr*. 17 (1994), p. 469

[4] ASTM D 6733-01: Annual Book of ASTM Standard, vol. 05.03, 2006

[5] J.C. Giddings, *J. High Resol. Chromatogr*. 10 (1987) 319

[6] L. Blumberg, M.S. Klee, *J. Chromatogr. A*. 1217 (2010) 99

[7] P.J. Schoenmakers, P. Marriott, J. Beens, *LC–GC Eur*. 16 (2003) 335

[8] J.C. Giddings, *J. Chromatogr. A* 703 (1995) 3

[9] J.C. Giddings, *Anal. Chem*. 56 (1984) 1258A

[10] Z. Liu, J.B. Phillips, *J. Chromatogr. Sci*. 29 (1991) 227

[11] R. Grob, E.F. Barry. *Modern Practice of Gas Chromatography 4th edition.* Wiley 2004

[12] Gross, Jürgen H. M*ass spectrometry: a textbook*. 2010. n.p.: Berlin ; London : Springer

[13] K. Grob and G. Grob *J.Chromatogr.* 244 (1982) 197-208

[14] R.E. Murphy, M.R. Schure, J.P. Foley. *Anal. Chem*. 70 (1998) 8 p.1585-1594

[15] W. Khummueng, J. Harynuk, P.J. Marriott. *Anal. Chem.*78 (2006) 13, p.4578-4587

[16] M. Edwards, A. Mostafa, T. Gorecki. *Anal. Bioanal. Chem.* 401 (2011) 8 p.2335-2349

[17] Deans, D. R. *J. Chromatogr*. 1965, 18, 477−481.

[18] Deans, D. R. *J. Chromatogr.* 1981, 203, 19−28.

[19] P.A. Bueno, J.V. Seeley. *J. Chromatogr A*. 1027 (2004) p.3-10

[20] J.V. Seeley, N.J. Micyus, J.D. McCurry, S.K. Seeley. *Am. Lab*. 38 (2006) 9, p. 24

[21] B.D. Quimby, J.D. McCurry, W.M. Norman. *LCGC The Peak*. (2007) p.7-15

[22] http://www.sge.com/products/silflow-stainless-steel-micro-fluidic-platform - accessed April, 2014.

[23] P. McA. Harvey, R.A. Shellie, P.R. Haddad. *J. Chromatogr Sci*. 48 (2010) p.245-250

[24] T. Gerbino, G. Castello, G. D'Amato. *J. Chromatogr.* 609 (1992) 289

[25] J. Perez-Parajon, J. Santiuste, J. Takacs. *Chromatographia*. 60 (2004) 199

[26] K. Heberger, T. Kowalska. *J. Chromatogr. A*. 845 (1999) 13

[27] K. Heberger, T. Kowalska. *Chromatographia*. 44 (1997) 179

[28] T. Gerbino, G. Castello. *J. High. Resolut. Chromatogr*. 19 (1996) 377

[29] K. Bouharis, M.L. Souici, D. Messadi. *Asian J .of Chemistry*. 23 (2011) 1044-1048

[30] A. Antonio D'Archivio, A. Giannitto, M.A. Maggi. *J. Chromatogr A.* 1298 (2013) p.118-131

[31] M.H. Fatemi, M. Elyasi. *Acta Chromatographica.* 25 (2013) 3 P. 411-422

[32] L.T. Qin, S.S. Liu, F. Chen, Q.F. Xiao, Q.S. Wu. *Chemosphere*. 90 (2013) 300-305

[33] N.E. Moustafa, K.E.F. Mahmoud. *Chromatographia*. 72 (2010) 905-912

[34] R. Ghavami, S. Faham. *Chromatographia*. 72 (2010) 893-903

[35] N.E. Moustafa. *Chromatographia*. 67 (2008) 1-2 p. 85-91

[36] H. Noorizadeh, M. Noorizadeh. *Medicinal Chemistry Research*. 21, (2012) 8, p. 1997-2005

[37] V.K. Gupta et al. *Talanta*. 83 (2010) 3 p. 1014-1022

[38] R. Kaliszan. *Chem. Rev*. 107 (2007) 3212

[39] K. Heberger. *J. Chromatogr. A*. 1158 (2007) 273

[40] Kovats, E. *Helv. Chim. Acta*. 41, (1958) 7, p.1915–32

[41] H. van Den Dool, P. Kratz. *J. Chromatogr. A*. 11 (1963) 463-471

[42] C. von Mühlen, P.J. Marriott. *Anal. And Bioanal. Chem*. 401 (2011) 2351-2360

[43] http://www.nist.gov/srd/nist1a.cfm. Accessed April, 2014.

[44] B. Zellner, C. Bicchi, P. Dugo, P Rubiolo, G. Dugo, L. Mondello. *J. Flavour Fragr.* 23 (2008) 297-314

[45] J. Zhang, I. Koo, B. Waang, Q. Gao, C. Zheng, X. Zhang. *J Chromatogr A*. 1251 (2012) p. 188-193

[46] http://webbook.nist.gov/chemistry/gc-ri/. Accessed April, 2014.

[47] S. Bieri, P.J. Marriott. *Anal. Chem.* 80 (2008) 760-768

[48] J. Dimandja, T. Leavell, F.L. Dorman, D.W. Armstrong *Characterization of GC×GC column sets with bidimensional retention normalization* Presented at Pacifichem 2010, International Chemical Congress of Pacific Basin Societies, Honolulu, HI, United States, December 15-20, 2010 (2010), ANYL-142.

[49]J.V. Seeley, S.K. Seeley. *J. Chromatogr. A*. 1172 (2007) 72-83

[50] Y.P. Zhao et al. *J. Chromatogr. A* 1218 (2011) 2577-2583

[51] M. Gorgenyi, K. Heberger. J. Sep. Sci. 28 (2005) 506

[52] B. Karolat. *Predicting Gas Chromatographic Retention Times using Thermodynamics*. University of Alberta, 2010

[53] E. Clarke, D. Glew. *Trans. Faraday Soc*. 62 (1966) 539

[54] R. Castells, E. Arancibia, A. Nardillo. *J. Chromatogr.* 504 (1990) 45-53

[55] K. Ciazynska-Halarewicz, T. Kowalska. J. *Chromatogr. Sci*. 40 (2002) 421

[56] K. Ciazynska-Halarewicz, T. Kowalska. *Acta Chromatogr*. 13 (2003) 81

[57] K. Ciazynska-Halarewicz, T. Kowalska. *J. Chromatogr. Sci*. 41 (2003) 467

[58] K. Ciazynska-Halarewicz, M. Helbin, P. Korzenecki, T. Kowalska. *J. Chromatogr. Sci*. 45 (2007) 492

[59] E. Dose. *Anal Chem.* 59 (1987) 2414-2419

[60] J. Dolan, R. Snyder, D. Bautz. *J. Chromatogr.* 541 (1991) 21

[61] G. Castello, S. Vezzani, R Moretti. *J. Chromatogr A*. 742 (1996) 151-160

[62] S. Vezzani, P. Moretti, G. Castello. *J. Chromatogr. A*. 667 (1994) 331

[63] S. Vezzani, P. Moretti, G. Castello *J. Chromatogr A*. 767 (1997) 115-125

[64] F. Aldaeus, Y. Thewalim, A. Colmsjo. *Anal. Bioanal. Chem*. 389 (2007) 941

[65] Y. Thewalim, F. Aldaeus, A. Colmsjo. *Anal. Bioanal. Chem*. 393 (2009) 327

[66] Y. Thewalim, I. Sadiktsis, A. Colmsjö. *J. Chromatogr A*. 1218 (2011) 31 p.5305– 5310

[67] F. Aldaeus, Y. Thewalim, A. Colmsjo. *J. Chromatogr. A.* 1216 (2009) 134

[68] C. Freissineta, A. Bucha, C. Szopac, R. Sternberg. *J. Chromatogr A*. 1306 (2013) 59– 71

[69] J. Randona, L. Mareta, C. Ferronato. *Analytica Chimica Acta*. 812 (2014) 258– 264

[70] B. Karolat, J. Harynuk. *J. Chromatogr A*. 1217 (2010) 4862–4867

[71] B.M. Weber, J.J. Harynuk. *J Chromatogr A*. 1271 (2013) 170– 175

[72] S. Vezzani, P.Moretti, M. Mazzi, G. Castello. *J. Chromatogr*. 1055 (2004) 151

[73] S. Vezzani, G. Castello, D. Pierani. *J. Chromatogr. A*. 811 (1998) 85

[74] R. Lebrón-Aguilar, J.E. Quintanilla-López, J.A. Garcia-Domínguez. *J. Chromatogr A*, 760 (1997) p. 219-226

[75] J.E. Quintanilla-Lopez, R. Lebron-Aguilar, J.A. Garcia-Domínguez, *J. Chromatogr. A*. 1997, 767, 127-136.

[76] F. Gonzalez. *J. Chromatogr. A*. 873 (2000) 209

[77] M. McGuigan, R Sacks. *Anal. Chem*.73 (2001) 3112–3118

[78] H. Snijders, H.G. Janssen, C. Cramers. *J. Chromatogr A*. 718 (1995) 339-355

[79] Y. Thewalim, O. Bruno, A. Colmsjo. *Anal. Bioanal. Chem*. 399 (2011) 3, p. 1335-1345

[80] G. Castello, R. Moretti, and S. Vezzani *J. Chromatography A*, 1216 (2009) p. 1607–1623

[81] F.L. Dorman, P.D. Schettler, L.A. Vogt, J.W. Cochran. *J. Chromatogr. A*. 1186 (2008) 196-201

[82] P. Boswell, P.W. Carr, J.D. Cohen, A.D. Hegeman. J. Chromatogr A. 1263 (2012) P. 179-188

[83] B.B. Barnes et al. *Analytical Chemistry*. 85 (2013) 23, p. 11650-11657

[84] Lagarias, J. C., J. A. Reeds, M. H. Wright, and P. E. Wright. "Convergence Properties of the Nelder-Mead Simplex Method in Low Dimensions." SIAM Journal of Optimization, Vol. 9, Number 1, 1998, pp. 112–147

[85] Comprehensive Chemometrics Vol.1 pp. 555

[86] T.M. McGinitie, J.J. Harynuk. *J. Chromatogr A*. 1255 (2012) p. 184-189

[87] F.L. Dorman, P. Dawes. *Gas Chromatography: Chapter 3*. Elsevier (2012)

[88] L.L. Blyler, F.V. DiMarcello. *Proceedings of the IEEE*. 68 (1980) 10 p.1194-1198

[89] D. H. Smithgall, L. S. Watkins, R. E. Frazee. *Appl. Opt*. 16 (1977) p.2395

[90] K. Grob, *Making and manipulating capillary columns for gas chromatography*, Huethig, Basel, Heidelberg, New York, 1986.

[91] J. Macomber, P. Nico, G. Nelson. *LC GC North America*. June 2004. S71

[92] http://imagej.nih.gov/ij/. Accessed April, 2014

[93] S.S Stafford, Editor. *Electronic Pressure Control in Gas Chromatography, Hewlett-Packard Company*. Wilmington, DE, (1993) p. 25-42.

[94] R.C. Weast, M.J. Astle, W.H. Beyer, (1988) CRC Handbook of Chemistry and Physics, 69th edn, CRC Press, Boca Raton, FL.

[95] J.J. Harynuk, T.M. M^{c}Ginitie, J.R. Witty. *Practical considerations for the prediction of gc retention times based on thermodynamic data*. 94th Canadian Society of Chemistry Conference, Montreal (2011). AN-2, 23.

[96] K. Grob, Jr. G. Grob, K. Grob. *J Chromatogr*. 156 (1978) 1-20.

[97] T.M. McGinitie, H. Ebrahimi-Najafabadi, J.J. Harynuk. *J. Chromatogr. A*. 1325 (2014) p. 204-212

[98] L. Moio, P. Etievant, D. Langlois, J. Dekimpe, F. Addeo. *J. Dairy Research*. 61 (1994) 385-394

[99] S. Lee, C. Macku, T. Shibamoto. *J. Agric. Food Chem*. 39 (1991) 1972-1975

[100] Y.F. Guan, Z. Peng, L.M. Zhou. *J. High Res. Chromatogr.* Vol. 15 (1992) p. 18-23

[101] J. Harynuk. T Gorecki. *American Laboratory*. Vol. 39, Issue 4 (2007) p. 36-39

[102] J. Dalluge et al. *J. Chromatogr. A*. 974. (2002) p. 169-184

[103] J. Beens, R. Tijssen, J. Blomberg. *J. Chromatogr. A*. 822 (1998) 233-251

[104] C. Vendeuvre, F. Bertoncini, D. Thiebaut, M. Martin, M. Hennion. *J. Sep. Sci*. 28 (2005) 1129-1136

[105] J.S. Arey, R.K. Nelson, L. Xu, C.M. Reddy. *Anal. Chem*. 77 (2005) 7172-7182

[106] Y. Ren, H. Liu, X. Yao, M. Liu, *Anal. Bioanal. Chem*. 388 (2007) 165-172

[107] A.A. D'Archivio, A. Incani, F. Ruggieri. *Anal. Bioanal. Chem*. 399 (2011) 903-913

[108] J.V. Seeley, E.M. Libby, K.A. Hill Edwards, S.K. Seeley. *J. Chromatogr. A*. 1216 (2009) 1650-1657

[109] S. Zhu, X. Lu, Y. Qiu, T. Pang, H. Kong, C. Wu, G. Xu. *J. Chromatogr. A*. 1150 (2007) 28-36

[110] X. Lu, H. Kong, H. Li, C. Ma, J. Tian, G. Xu. *J. Chromatogr. A*. 1086 (2005) 175-184

[111] N.J. Micyus, S.K. Seeley, J.V. Seeley. *J. Chromatogr. A*, 1086 (2005), p. 171

Appendix A

Appendix Table 1. Supplemental PAH Thermodynamic information for five column types.

Compound	Thermodynamic Parameter	5% Phenyl	50% Phenyl	IL-61	IL-76	IL-111
Toluene	ΔH T(o) KJ·mol-1	-31.69	-31.79	-31.50	-32.81	-32.51
	ΔS T(o) J·mol-1·K-1	-51.83	-47.40	-47.80	-54.12	-53.75
	ΔCp J·mol-1·K-1	22.34	63.97	-21.31	5.69	26.42
Ethylbenzene	ΔH T(o) KJ·mol-1	-34.82	-33.57	-36.16	-36.78	-35.96
	ΔS T(o) J·mol-1·K-1	-54.18	-49.03	-56.71	-61.44	-60.22
	ΔCp J·mol-1·K-1	35.62	-32.71	-2.01	14.04	56.28
Propylbenzene	ΔH T(o) KJ·mol-1	-38.03	-36.63	-39.19	-39.53	-38.36
	ΔS T(o) J·mol-1·K-1	-57.36	-52.23	-60.85	-65.36	-64.12
	ΔCp J·mol-1·K-1	42.43	-39.32	6.65	27.93	63.57
Butylbenzene	ΔH T(o) KJ·mol-1	-41.96	-40.22	-42.80	-40.62	-41.58
	ΔS T(o) J·mol-1·K-1	-62.21	-56.46	-67.84	-65.96	-71.36
	ΔCp J·mol-1·K-1	34.50	-27.98	13.52	168.44	67.78
Naphthalene	ΔH T(o) KJ·mol-1	-44.71	-46.55	-49.51	-50.54	-50.58
	ΔS T(o) J·mol-1·K-1	-62.30	-61.72	-64.72	-70.03	-70.79
	ΔCp J·mol-1·K-1	55.03	57.43	51.69	61.22	79.39
1-Methylnaphthalene	ΔH T(o) KJ·mol-1	-49.71	-50.70	-54.49	data not available	-54.35
	ΔS T(o) J·mol-1·K-1	-69.32	-66.49	-74.45	data not available	-77.87
	ΔCp J·mol-1·K-1	57.99	60.09	68.90	data not available	73.73
2-Methylnaphthalene	ΔH T(o) KJ·mol-1	-48.78	-50.74	-54.80	-55.00	-54.35
	ΔS T(o) J·mol-1·K-1	-67.65	-67.91	-75.71	-79.26	-78.32
	ΔCp J·mol-1·K-1	60.17	67.59	71.63	71.95	71.95
1-Ethylnaphthalene	ΔH T(o) KJ·mol-1	-52.57	-53.54	-57.43	data not available	-56.57

Appendix Table 1. Supplemental PAH Thermodynamic information for five column types.						
Compound	Thermodynamic Parameter	5% Phenyl	50% Phenyl	IL-61	IL-76	IL-111
	ΔS T(o) J·mol-1·K-1	-72.90	-70.86	-79.84	data not available	-82.43
	ΔCp J·mol-1·K-1	68.76	62.11	76.42	data not available	79.28
2-Ethylnaphthalene	ΔH T(o) KJ·mol-1	-52.22	-53.69	-57.83	-58.20	-57.05
	ΔS T(o) J·mol-1·K-1	-72.05	-71.19	-80.56	-84.89	-83.38
	ΔCp J·mol-1·K-1	58.70	63.55	76.14	78.76	79.11
1-Propylnaphthalene	ΔH T(o) KJ·mol-1	-55.62	-53.86	-60.17	data not available	-59.13
	ΔS T(o) J·mol-1·K-1	-76.85	-70.92	-82.38	data not available	-85.57
	ΔCp J·mol-1·K-1	67.39	62.26	78.62	data not available	84.00
2-Propylnaphthalene	ΔH T(o) KJ·mol-1	-55.99	-56.88	-60.89	-64.43	-59.47
	ΔS T(o) J·mol-1·K-1	-77.52	-75.56	-83.59	-96.49	-85.93
	ΔCp J·mol-1·K-1	68.31	67.01	80.92	146.86	84.01
Anthracene	ΔH T(o) KJ·mol-1	-66.26	-63.24	-71.62	-73.73	-71.35
	ΔS T(o) J·mol-1·K-1	-90.83	-76.29	-88.58	-96.70	-92.29
	ΔCp J·mol-1·K-1	105.41	53.14	77.95	91.93	85.75
1-Methylanthracene	ΔH T(o) KJ·mol-1	-69.05	-69.39	-77.78	-77.85	-74.52
	ΔS T(o) J·mol-1·K-1	-92.75	-86.71	-101.58	-105.15	-99.22
	ΔCp J·mol-1·K-1	96.51	76.20	97.66	99.04	84.81
2-Methylanthracene	ΔH T(o) KJ·mol-1	-69.84	-69.27	-75.17	-77.40	-74.58
	ΔS T(o) J·mol-1·K-1	-95.19	-87.03	-93.38	-102.06	-97.13
	ΔCp J·mol-1·K-1	104.95	76.97	79.40	93.48	86.95
2-Ethylanthracene	ΔH T(o) KJ·mol-1	-72.79	-74.24	-78.51	-80.42	-77.44
	ΔS T(o) J·mol-1·K-1	-98.35	-95.70	-99.00	-107.30	-102.55
	ΔCp J·mol-1·K-1	102.73	97.99	85.40	98.89	94.11
9-Methylanthracene	ΔH T(o) KJ·mol-1	-67.89	-72.67	-76.62	-78.66	-75.88

Appendix Table 1. Supplemental PAH Thermodynamic information for five column types.						
Compound	Thermodynamic Parameter	5% Phenyl	50% Phenyl	IL-61	IL-76	IL-111
	ΔS T(o) J·mol-1·K-1	-88.77	-92.50	-95.58	-103.83	-98.86
	ΔCp J·mol-1·K-1	78.08	97.89	84.82	101.29	90.92
1,2-Dimethylanthracene	ΔH T(o) KJ·mol-1	-71.70	-75.63	-81.52	-82.10	-78.24
	ΔS T(o) J·mol-1·K-1	-93.82	-95.94	-102.95	-108.26	-101.18
	ΔCp J·mol-1·K-1	81.41	93.43	94.51	99.52	82.71
1,3-Dimethylanthracene	ΔH T(o) KJ·mol-1	-73.44	-73.89	-80.73	-81.78	-77.35
	ΔS T(o) J·mol-1·K-1	-99.42	-93.58	-103.00	-109.31	-100.99
	ΔCp J·mol-1·K-1	105.71	83.91	92.41	102.60	83.43
1,4-Dimethylanthracene	ΔH T(o) KJ·mol-1	-71.20	-74.63	-79.44	-80.85	-78.16
	ΔS T(o) J·mol-1·K-1	-93.47	-94.77	-100.44	-107.54	-103.24
	ΔCp J·mol-1·K-1	79.23	89.50	86.73	98.16	90.07
1,5-Dimethylanthracene	ΔH T(o) KJ·mol-1	-70.40	-73.89	-79.64	-82.46	-79.56
	ΔS T(o) J·mol-1·K-1	-91.45	-92.88	-100.67	-111.07	-106.42
	ΔCp J·mol-1·K-1	71.05	81.96	86.97	109.69	101.94
2,3-Dimethylanthracene	ΔH T(o) KJ·mol-1	-71.19	-77.28	-83.26	-82.42	-77.20
	ΔS T(o) J·mol-1·K-1	-92.60	-100.30	-106.15	-108.06	-98.44
	ΔCp J·mol-1·K-1	75.67	107.71	99.96	95.91	73.19
2,7-Dimethylanthracene	ΔH T(o) KJ·mol-1	-73.78	-81.49	-80.20	-82.76	-80.56
	ΔS T(o) J·mol-1·K-1	-100.54	-111.86	-101.35	-111.17	-108.68
	ΔCp J·mol-1·K-1	112.63	142.42	87.27	107.35	111.57

Appendix Table 2. Supplemental LOO results for rapid thermodynamic determination method.

Compound		LOO Ramp	Estimated $\Delta H(T_o)$ (kJ·Mol-1)	Estimated $\Delta S(T_o)$ (J·K-1·Mol-1)	Estimated ΔCp (J·K-1·Mol-1)	Experimental Retention Time (min)	Predicted Retention Time (min)	Error (s)
Undecane	5 % Phenyl Column (SLB5ms)	3	-47.29	-74.09	78.17	20.349	20.347	0.1
		5	-47.29	-74.11	89.52	14.874	14.870	0.2
		12	-47.30	-74.12	79.02	8.784	8.785	0.0
		20	-47.30	-74.11	78.91	6.592	6.593	-0.1
		Average Value	-47.30	-74.11	81.41			
	50 % Phenyl Column (SPB50)	3	-39.44	-55.20	108.61	11.700	11.705	-0.3
		5	-38.76	-53.46	175.17	9.572	9.570	0.1
		12	-38.72	-53.39	186.24	6.647	6.648	-0.1
		20	-38.72	-53.40	187.73	5.399	5.400	-0.1
		Average Value	-38.73	-53.42	183.05			
	Wax Column (Supelco Wax)	3	-38.01	-62.44	67.87	9.342	9.357	-0.9
		5	-37.78	-61.77	71.73	7.827	7.818	0.5
		12	-37.78	-61.78	72.79	5.605	5.602	0.2
		20	-37.62	-61.23	68.93	4.613	4.623	-0.6
		Average Value	-37.80	-61.81	70.33			
dodecane	5 % Phenyl Column (SLB5ms)	3	-51.59	-80.15	87.45	25.039	25.043	-0.3
		5	-51.56	-80.07	86.80	17.748	17.745	0.2
		12	-51.56	-80.05	87.86	10.014	10.015	-0.1
		20	-51.56	-80.05	87.86	7.337	7.338	-0.1
		Average Value	-51.57	-80.08	87.49			
	50 % Phenyl Column (SPB50)	3	-44.31	-63.81	199.88	21.780	21.792	-0.7
		5	-44.28	-63.73	195.71	15.873	15.867	0.4
		12	-44.26	-63.65	197.56	9.362	9.363	-0.1
		20	-44.27	-63.69	195.43	7.033	7.033	0.0
		Average Value	-44.28	-63.72	197.14			
	Wax Column (Supelco Wax)	3	-42.34	-69.22	32.02	13.231	13.230	0.1
		5	-42.36	-69.25	31.23	10.405	10.407	-0.1
		12	-42.36	-69.26	31.96	6.812	6.808	0.2
		20	-41.90	-67.96	49.16	5.371	5.377	-0.3
		Average Value	-42.24	-68.93	36.09			
tridecane	5 % Phenyl Column	3	-55.73	-85.77	91.90	29.536	29.537	0.0

Appendix Table 2. Supplemental LOO results for rapid thermodynamic determination method.

Compound		LOO Ramp	Estimated $\Delta H(T_o)$ (kJ·Mol-1)	Estimated $\Delta S(T_o)$ (J·K-1·Mol-1)	Estimated ΔCp (J·K-1·Mol-1)	Experimental Retention Time (min)	Predicted Retention Time (min)	Error (s)
	(SLB5ms)	5	-55.73	-85.77	91.90	20.487	20.487	0.0
		12	-55.73	-85.77	91.90	11.180	11.180	0.0
		20	-55.73	-85.77	91.90	8.042	8.042	0.0
		Average Value	-55.73	-85.77	91.90			
	50 % Phenyl Column (SPB50)	3	-49.85	-73.84	203.47	26.235	26.252	-1.0
		5	-48.64	-70.43	135.32	18.599	18.623	-1.5
		12	-49.84	-73.86	208.73	10.524	10.525	-0.1
		20	-49.82	-73.80	207.77	7.736	7.737	0.0
		Average Value	-49.54	-72.98	188.82			
	Wax Column (Supelco Wax)	3	-45.35	-72.29	32.63	17.388	17.380	0.5
		5	-45.51	-72.71	24.94	13.040	13.047	-0.4
		12	-45.39	-72.40	34.77	7.982	7.983	-0.1
		20	-45.40	-72.43	35.35	6.092	6.093	-0.1
		Average Value	-45.41	-72.46	31.92			
tetradecane	5 % Phenyl Column (SLB5ms)	3	-59.31	-90.36	102.56	33.485	33.482	0.2
		5	-59.29	-90.29	101.45	22.899	22.900	-0.1
		12	-59.32	-90.36	102.10	12.215	12.215	0.0
		20	-59.30	-90.32	100.96	8.673	8.672	0.1
		Average Value	-59.31	-90.33	101.77			
	50 % Phenyl Column (SPB50)	3	-53.66	-78.51	163.38	30.980	30.948	1.9
		5	-53.65	-78.44	155.61	21.506	21.522	-0.9
		12	-53.77	-78.77	162.84	11.776	11.785	-0.5
		20	-53.80	-78.85	153.26	8.499	8.477	1.3
		Average Value	-53.72	-78.64	158.77			
	Wax Column (Supelco Wax)	3	-48.57	-76.14	72.07	21.541	21.557	-0.9
		5	-48.49	-75.93	63.29	15.613	15.608	0.3
		12	-48.50	-75.94	62.62	9.098	9.095	0.2
		20	-48.36	-75.54	57.73	6.773	6.778	-0.3
		Average Value	-48.48	-75.89	63.92			
2-undecone	5 % Phenyl Column (SLB5ms)	3	-55.29	-85.03	102.00	29.188	29.190	-0.1
		5	-55.20	-84.78	98.56	20.285	20.285	0.0

Appendix Table 2. Supplemental LOO results for rapid thermodynamic determination method.

Compound		LOO Ramp	Estimated $\Delta H(T_o)$ (kJ·Mol-1)	Estimated $\Delta S(T_o)$ (J·K-1·Mol-1)	Estimated ΔCp (J·K-1·Mol-1)	Experimental Retention Time (min)	Predicted Retention Time (min)	Error (s)
		12	-55.24	-84.89	100.06	11.104	11.103	0.0
		20	-55.20	-84.78	98.56	8.001	8.002	0.0
		Average Value	-55.24	-84.87	99.80			
	50 % Phenyl Column (SPB50)	3	-53.87	-79.65	167.91	30.486	30.465	1.3
		5	-53.90	-79.72	166.31	21.186	21.197	-0.6
		12	-53.97	-79.91	171.00	11.621	11.632	-0.6
		20	-54.16	-80.43	168.71	8.398	8.383	0.9
		Average Value	-53.98	-79.93	168.48			
	Wax Column (Supelco Wax)	3	-51.49	-74.25	36.77	29.481	29.475	0.4
		5	-51.64	-74.64	42.77	20.571	20.572	0.0
		12	-51.64	-74.65	41.44	11.295	11.293	0.1
		20	-51.72	-74.87	46.34	8.134	8.137	-0.2
		Average Value	-51.62	-74.60	41.83			
2-dodecone	5 % Phenyl Column (SLB5ms)	3	-59.34	-90.05	84.94	33.761	33.750	0.7
		5	-59.33	-90.00	83.13	23.053	23.062	-0.5
		12	-59.37	-90.13	83.63	12.268	12.268	0.0
		20	-59.38	-90.15	82.80	8.700	8.695	0.3
		Average Value	-59.36	-90.08	83.62			
	50 % Phenyl Column (SPB50)	3	-58.50	-86.52	170.57	35.056	35.030	1.6
		5	-58.49	-86.43	166.89	23.982	23.997	-0.9
		12	-58.61	-86.76	171.27	12.827	12.835	-0.5
		20	-58.65	-86.88	168.07	9.133	9.118	0.9
		Average Value	-58.56	-86.65	169.20			
	Wax Column (Supelco Wax)	3	-54.63	-78.03	47.07	33.366	33.362	0.3
		5	-54.93	-78.83	55.07	22.936	22.935	0.1
		12	-54.95	-78.89	54.96	12.304	12.302	0.1
		20	-55.00	-79.02	57.89	8.745	8.748	-0.2
		Average Value	-54.88	-78.69	53.75			
2-tridecone	5 % Phenyl Column (SLB5ms)	3	-63.58	-96.43	110.22	37.530	37.527	0.2
		5	-63.65	-96.58	111.16	25.354	25.353	0.0
		12	-63.65	-96.58	111.16	13.256	13.257	0.0

Appendix Table 2. Supplemental LOO results for rapid thermodynamic determination method.

Compound		LOO Ramp	Estimated $\Delta H(T_o)$ (kJ·Mol-1)	Estimated $\Delta S(T_o)$ (J·K-1·Mol-1)	Estimated ΔCp (J·K-1·Mol-1)	Experimental Retention Time (min)	Predicted Retention Time (min)	Error (s)
		20	-63.65	-96.58	111.16	9.302	9.302	0.0
		Average Value	-63.63	-96.55	110.93			
	50 % Phenyl Column (SPB50)	3	-61.72	-90.26	152.17	38.930	38.870	3.6
		5	-61.72	-90.17	145.99	26.334	26.362	-1.7
		12	-62.22	-91.48	153.11	13.823	13.827	-0.2
		20	-62.26	-91.57	150.06	9.734	9.708	1.5
		Average Value	-61.98	-90.87	150.33			
	Wax Column (Supelco Wax)	3	-57.43	-80.99	48.64	37.073	37.062	0.7
		5	-57.42	-80.95	47.09	25.191	25.197	-0.3
		12	-58.14	-82.84	61.80	13.263	13.262	0.1
		20	-58.08	-82.70	61.84	9.326	9.330	-0.2
		Average Value	-57.77	-81.87	54.84			
1-undecanol	5 % Phenyl Column (SLB5ms)	3	-58.45	-89.13	93.49	32.642	32.623	1.1
		5	-59.34	-91.50	116.95	22.371	22.370	0.1
		12	-59.20	-91.13	112.40	11.983	11.982	0.1
		20	-59.21	-91.16	112.96	8.530	8.532	-0.1
		Average Value	-59.05	-90.73	108.95			
	50 % Phenyl Column (SPB50)	3	-58.13	-87.04	198.06	33.810	33.813	-0.2
		5	-58.12	-87.01	198.44	23.232	23.230	0.1
		12	-58.14	-87.09	200.64	12.515	12.520	-0.3
		20	-58.12	-87.02	197.49	8.948	8.943	0.3
		Average Value	-58.13	-87.04	198.66			
	Wax Column (Supelco Wax)	3	-61.22	-88.33	49.80	39.049	39.028	1.2
		5	-61.85	-89.95	59.21	26.311	26.315	-0.2
		12	-62.52	-91.71	71.20	13.676	13.673	0.2
		20	-62.44	-91.51	71.48	9.552	9.555	-0.2
		Average Value	-62.01	-90.38	62.92			
1-dodecanol	5 % Phenyl Column (SLB5ms)	3	-63.88	-98.21	126.12	36.743	36.752	-0.5
		5	-62.14	-93.63	89.83	24.865	24.877	-0.7
		12	-63.90	-98.26	128.02	13.043	13.042	0.1
		20	-63.89	-98.26	129.38	9.172	9.175	-0.2
		Average Value	-63.45	-97.09	118.34			
	50 % Phenyl Column (SPB50)	3	-61.90	-92.13	180.80	37.777	37.757	1.2
		5	-59.41	-85.55	129.07	25.642	25.678	-2.2
		12	-62.23	-92.95	183.88	13.537	13.538	-0.1

Appendix Table 2. Supplemental LOO results for rapid thermodynamic determination method.

Compound		LOO Ramp	Estimated $\Delta H(T_o)$ (kJ·Mol-1)	Estimated $\Delta S(T_o)$ (J·K-1·Mol-1)	Estimated ΔCp (J·K-1·Mol-1)	Experimental Retention Time (min)	Predicted Retention Time (min)	Error (s)
		20	-62.27	-93.07	183.24	9.565	9.553	0.7
		Average Value	-61.45	-90.93	169.25			
	Wax Column (Supelco Wax)	3	-65.12	-94.19	70.15	42.413	42.403	0.6
		5	-65.30	-94.64	71.98	28.357	28.360	-0.2
		12	-65.38	-94.84	72.74	14.548	14.547	0.1
		20	-65.86	-96.10	81.38	10.082	10.083	-0.1
		Average Value	-65.41	-94.94	74.06			
1-tridecanol	5 % Phenyl Column (SLB5ms)	3	-68.25	-104.39	133.05	40.708	40.713	-0.3
		5	-68.21	-104.30	132.98	27.275	27.273	0.1
		12	-68.18	-104.22	132.66	14.068	14.067	0.1
		20	-68.23	-104.37	134.55	9.792	9.797	-0.3
		Average Value	-68.22	-104.32	133.31			
	50 % Phenyl Column (SPB50)	3	-66.86	-100.32	189.28	41.552	41.532	1.2
		5	-66.82	-100.16	187.12	27.932	27.943	-0.7
		12	-66.82	-100.19	187.61	14.507	14.513	-0.4
		20	-66.87	-100.29	184.86	10.151	10.137	0.9
		Average Value	-66.84	-100.24	187.22			
	Wax Column (Supelco Wax)	3	-68.40	-98.46	78.30	45.642	45.635	0.4
		5	-68.45	-98.59	78.63	30.321	30.325	-0.2
		12	-68.49	-98.69	78.37	15.385	15.383	0.1
		20	-69.16	-100.38	88.52	10.590	10.592	-0.1
		Average Value	-68.62	-99.03	80.96			
1-tetradecanol	5 % Phenyl Column (SLB5ms)	3	-71.96	-109.05	130.99	44.375	44.372	0.2
		5	-71.91	-108.93	129.94	29.500	29.502	-0.1
		12	-71.98	-109.12	131.04	15.011	15.012	-0.1
		20	-71.92	-108.94	129.30	10.363	10.360	0.2
		Average Value	-71.94	-109.01	130.32			
	50 % Phenyl Column (SPB50)	3	-72.27	-109.57	203.98	45.144	45.128	0.9
		5	-72.25	-109.49	202.00	30.110	30.115	-0.3
		12	-72.29	-109.62	203.46	15.429	15.435	-0.4
		20	-72.32	-109.66	201.54	10.707	10.697	0.6
		Average Value	-72.28	-109.59	202.74			
	Wax Column (Supelco Wax)	3	-71.14	-101.46	80.00	48.735	48.722	0.8
		5	-71.68	-102.79	85.71	32.202	32.205	-0.2
		12	-71.98	-103.54	88.97	16.186	16.185	0.1

Appendix Table 2. Supplemental LOO results for rapid thermodynamic determination method.

Compound		LOO Ramp	Estimated $\Delta H(T_o)$ (kJ·Mol-1)	Estimated $\Delta S(T_o)$ (J·K-1·Mol-1)	Estimated ΔCp (J·K-1·Mol-1)	Experimental Retention Time (min)	Predicted Retention Time (min)	Error (s)
		20	-72.81	-105.64	100.32	11.076	11.080	-0.2
		Average Value	-71.90	-103.36	88.75			

Appendix Table 3. Additional retention time predictions for rapid thermodynamic collection method.

Compund	Column	Temperature Ramp °C·min^{-1}	Experimental tr (min)	Predicted tr (min)	Difference (s)
undecane	5 % Phenyl Column (SLB5ms)	3	20.349	20.348	0.0
		5	14.874	14.872	0.1
		12	8.784	8.785	0.0
		20	6.592	6.593	-0.1
		8	11.172	11.170	0.1
		10	9.777	9.777	0.0
		16	7.453	7.453	0.0
	50 % Phenyl Column (SPB50)	3	17.179	17.175	0.2
		5	13.022	13.022	0.0
		12	8.130	8.133	-0.2
		20	6.284	6.283	0.0
		8	10.085	10.088	-0.2
		10	8.950	8.952	-0.1
		16	7.016	7.017	0.0
	Wax Column (Supelco Wax)	3	9.342	9.347	-0.3
		5	7.827	7.822	0.3
		12	5.605	5.603	0.1
		20	4.613	4.618	-0.3
		8	6.552	6.553	-0.1
		10	5.947	6.013	-4.0
		16	5.017	5.020	-0.2
dodecane	5 % Phenyl Column (SLB5ms)	3	25.039	25.040	-0.1
		5	17.748	17.747	0.1
		12	10.014	10.013	0.0
		20	7.337	7.337	0.0
		8	12.997	12.995	0.1
		10	11.246	11.245	0.1
		16	8.381	8.382	0.0
	50 % Phenyl Column (SPB50)	3	21.780	21.783	-0.2
		5	15.873	15.868	0.3
		12	9.362	9.363	-0.1
		20	7.033	7.033	0.0
		8	11.907	11.905	0.1
		10	10.419	10.420	-0.1
		16	7.947	7.948	-0.1
	Wax Column (Supelco Wax)	3	13.231	13.232	0.0
		5	10.405	10.405	0.0
		12	6.812	6.810	0.1

Appendix Table 3. Additional retention time predictions for rapid thermodynamic collection method.

Compund	Column	Temperature Ramp °C·min^{-1}	Experimental tr (min)	Predicted tr (min)	Difference (s)
		20	5.371	5.372	0.0
		8	8.280	8.283	-0.2
		10	7.402	7.433	-1.9
		16	5.948	5.947	0.1
tridecane	5 % Phenyl Column (SLB5ms)	3	29.536	29.537	0.0
		5	20.487	20.487	0.0
		12	11.180	11.180	0.0
		20	8.042	8.042	0.0
		8	14.729	14.728	0.1
		10	12.640	12.638	0.1
		16	9.260	9.258	0.1
	50 % Phenyl Column (SPB50)	3	26.235	26.242	-0.4
		5	18.599	18.602	-0.2
		12	10.524	10.528	-0.3
		20	7.736	7.733	0.2
		8	13.635	13.638	-0.2
		10	11.808	11.813	-0.3
		16	8.823	8.823	0.0
	Wax Column (Supelco Wax)	3	17.388	17.387	0.1
		5	13.040	13.043	-0.2
		12	7.982	7.982	0.0
		20	6.092	6.093	-0.1
		8	9.992	9.997	-0.3
		10	8.815	8.825	-0.6
		16	6.840	6.840	0.0
tetradecane	5 % Phenyl Column (SLB5ms)	3	33.485	33.485	0.0
		5	22.899	22.898	0.0
		12	12.215	12.215	0.0
		20	8.673	8.673	0.0
		8	16.261	16.262	0.0
		10	13.874	13.873	0.1
		16	10.043	10.043	0.0
	50 % Phenyl Column (SPB50)	3	30.980	30.970	0.6

Appendix Table 3. Additional retention time predictions for rapid thermodynamic collection method.

Compund	Column	Temperature Ramp °C·min^{-1}	Experimental tr (min)	Predicted tr (min)	Difference (s)
undecanone	Wax Column (Supelco Wax)	5	21.506	21.515	-0.5
		12	11.776	11.780	-0.2
		20	8.499	8.488	0.6
		8	15.485	15.495	-0.6
		10	13.301	13.308	-0.4
		16	9.771	9.767	0.3
	5 % Phenyl Column (SLB5ms)	3	21.541	21.547	-0.3
		5	15.613	15.612	0.1
		12	9.098	9.097	0.1
		20	6.773	6.777	-0.2
		8	11.639	11.638	0.0
		10	10.154	10.152	0.1
		16	7.684	7.687	-0.2
	50 % Phenyl Column (SPB50)	3	29.188	29.188	0.0
		5	20.285	20.285	0.0
		12	11.104	11.103	0.0
		20	8.001	8.002	0.0
		8	14.609	14.608	0.1
		10	12.547	12.545	0.1
		16	9.206	9.207	0.0
	Wax Column (Supelco Wax)	3	30.486	30.478	0.5
		5	21.186	21.192	-0.3
		12	11.621	11.627	-0.3
		20	8.398	8.390	0.5
		8	15.269	15.278	-0.6
		10	13.122	13.128	-0.4
		16	9.649	9.647	0.1
		3	29.481	29.480	0.1
		5	20.571	20.572	0.0
		12	11.295	11.295	0.0
		20	8.134	8.135	-0.1
		8	14.844	14.848	-0.3

Appendix Table 3. Additional retention time predictions for rapid thermodynamic collection method.

Compund	Column	Temperature Ramp °C·min^{-1}	Experimental tr (min)	Predicted tr (min)	Difference (s)
		10	12.762	12.758	0.2
		16	9.363	9.363	0.0
dodecanone	5 % Phenyl Column (SLB5ms)	3	33.761	33.757	0.3
		5	23.053	23.057	-0.2
		12	12.268	12.268	0.0
		20	8.700	8.697	0.2
		8	16.350	16.352	-0.1
		10	13.942	13.943	-0.1
		16	10.080	10.078	0.1
	50 % Phenyl Column (SPB50)	3	35.056	35.047	0.6
		5	23.982	23.992	-0.6
		12	12.827	12.832	-0.3
		20	9.133	9.125	0.5
		8	17.048	17.060	-0.7
		10	14.557	14.567	-0.6
		16	10.562	10.560	0.1
	Wax Column (Supelco Wax)	3	33.366	33.365	0.1
		5	22.936	22.935	0.1
		12	12.304	12.303	0.0
		20	8.745	8.747	-0.1
		8	16.342	16.343	-0.1
		10	13.967	13.962	0.3
		16	10.123	10.125	-0.1
tridecanone	5 % Phenyl Column (SLB5ms)	3	37.530	37.528	0.1
		5	25.354	25.353	0.0
		12	13.256	13.257	0.0
		20	9.302	9.302	0.0
		8	17.812	17.810	0.1
		10	15.120	15.118	0.1
		16	10.828	10.828	0.0
	50 % Phenyl Column (SPB50)	3	38.930	38.923	0.4
		5	26.334	26.350	-1.0
		12	13.823	13.827	-0.2
		20	9.734	9.718	0.9
		8	18.532	18.547	-0.9
		10	15.749	15.758	-0.6
		16	11.312	11.305	0.4
	Wax Column	3	37.073	37.070	0.2

Appendix Table 3. Additional retention time predictions for rapid thermodynamic collection method.

Compund	Column	Temperature Ramp °C·min^{-1}	Experimental tr (min)	Predicted tr (min)	Difference (s)
	(Supelco Wax)	5	25.191	25.192	0.0
		12	13.263	13.263	0.0
		20	9.326	9.327	0.0
		8	17.768	17.772	-0.2
		10	15.115	15.110	0.3
		16	10.847	10.848	-0.1
undecanol	5 % Phenyl Column (SLB5ms)	3	32.642	32.637	0.3
		5	22.371	22.372	0.0
		12	11.983	11.983	0.0
		20	8.530	8.532	-0.1
		8	15.922	15.920	0.1
		10	13.599	13.598	0.0
		16	9.867	9.867	0.0
	50 % Phenyl Column (SPB50)	3	33.810	33.812	-0.1
		5	23.232	23.232	0.0
		12	12.515	12.517	-0.1
		20	8.948	8.945	0.2
		8	16.580	16.582	-0.1
		10	14.183	14.185	-0.1
		16	10.330	10.328	0.1
	Wax Column (Supelco Wax)	3	39.049	39.043	0.3
		5	26.311	26.312	0.0
		12	13.676	13.677	0.0
		20	9.552	9.553	-0.1
		8	18.426	18.430	-0.2
		10	15.625	15.620	0.3
		16	11.142	11.143	-0.1
dodecanol	5 % Phenyl Column (SLB5ms)	3	36.743	36.747	-0.2
		5	24.865	24.867	-0.1
		12	13.043	13.043	0.0
		20	9.172	9.172	0.0
		8	17.498	17.498	0.0
		10	14.866	14.867	0.0
		16	10.666	10.667	-0.1
	50 % Phenyl Column (SPB50)	3	37.777	37.770	0.4
		5	25.642	25.653	-0.7
		12	13.537	13.542	-0.3
		20	9.565	9.555	0.6

Appendix Table 3. Additional retention time predictions for rapid thermodynamic collection method.

Compund	Column	Temperature Ramp °C·min^{-1}	Experimental tr (min)	Predicted tr (min)	Difference (s)
		8	18.101	18.113	-0.7
		10	15.405	15.415	-0.6
		16	11.099	11.097	0.1
	Wax Column (Supelco Wax)	3	42.413	42.410	0.2
		5	28.357	28.358	-0.1
		12	14.548	14.548	0.0
		20	10.082	10.082	0.0
		8	19.721	19.725	-0.2
		10	16.667	16.662	0.3
		16	11.801	11.802	0.0
tridecanol	5 % Phenyl Column (SLB5ms)	3	40.708	40.710	-0.1
		5	27.275	27.273	0.1
		12	14.068	14.067	0.1
		20	9.792	9.795	-0.2
		8	19.023	19.018	0.3
		10	16.092	16.090	0.1
		16	11.439	11.440	-0.1
	50 % Phenyl Column (SPB50)	3	41.552	41.545	0.4
		5	27.932	27.937	-0.3
		12	14.507	14.510	-0.2
		20	10.151	10.142	0.6
		8	19.546	19.553	-0.4
		10	16.566	16.572	-0.3
		16	11.830	11.827	0.2
	Wax Column (Supelco Wax)	3	45.642	45.640	0.1
		5	30.321	30.322	0.0
		12	15.385	15.385	0.0
		20	10.590	10.590	0.0
		8	20.964	20.967	-0.2
		10	17.668	17.662	0.4
		16	12.433	12.433	0.0
tetradecanol	5 % Phenyl Column (SLB5ms)	3	44.375	44.373	0.1
		5	29.500	29.500	0.0
		12	15.011	15.010	0.0
		20	10.363	10.362	0.1
		8	20.427	20.425	0.1
		10	17.219	17.218	0.1
		16	12.150	12.148	0.1

Appendix Table 3. Additional retention time predictions for rapid thermodynamic collection method.

Compund	Column	Temperature Ramp °C·min^{-1}	Experimental tr (min)	Predicted tr (min)	Difference (s)
	50 % Phenyl Column (SPB50)		45.144	45.138	0.3
			30.110	30.113	-0.2
			15.429	15.432	-0.2
			10.707	10.702	0.3
			20.920	20.925	-0.3
			17.669	17.673	-0.3
			12.523	12.522	0.1
	Wax Column (Supelco Wax)	3	48.735	48.732	0.2
		5	32.202	32.202	0.0
		12	16.186	16.187	0.0
		20	11.076	11.077	0.0
		8	22.153	22.157	-0.2
		10	18.624	18.618	0.3
		16	13.038	13.038	0.0